UiT Norges arktiske universitet

Faculty of Science and Technology, Department of Geoscience

Investigating limitations of RAMMS:Debrisflow as a slushflow simulation tool

Using numerical modelling as a tool to predict slushflow runouts

Vilde Edvardsen Hansen

Master's Thesis in Geology, GEO-3900, May 2024

Abstract

Slushflows are defined as rapid mass movement and occur when water-saturated snow (slush), rapidly moves downslope as a flowlike process. The high-water content of the flow results in high density and mobility flow that poses a significant danger to everything in its path. To predict how slushflows navigates the terrain, numerical modelling is a valuable tool. The output of the simulations would provide valuable information for spatial planning, construction of mitigation measures and for identifying areas that requires early warning.

A gravitational mass runout simulation tool used for hazard assessments of the slushflow danger is RAMMS:Debrisflow. To calibrate the model to simulate slushflow runouts with statistic confident, an already established parameter was attempted validated. To be able to extent the dataset and back-calculate slushflow events, they need to be well documented. Four events from three field sites occurring winter/spring 2023 in Northern Norway, were digitised based of field observations.

The calibrated parameters would generally represent the slushflow runout for starting conditions in slopes over 10° angle. Because of assumption in the model, it is not possible to replicate starting conditions in gentler slope. This limitation excludes slushflows traveling over low slope gradient terrain from this method, and a method for assessing this hazard must be developed. However, for other events the shortcoming can be overcome by defining the release area in steeper part of the slushflow path. The uncertainties related to this solution investigated by analysing the sensitivity of defining these release areas (location and volume). These input variables were too sensitive to truly test the capability of RAMMS:Debrisflow to simulate slushflows, and guidelines must be created to standardise the method to define these release areas.

Acknowledgments

Firstly, a large thank you to my supervisors Christopher D'Amboise and Louise Vick, for giving me guidance, by sharing their knowledge and experience through constructive feedback. I have especially appreciated their positive attitude and all the opportunities they have provided during the period of this thesis work.

I have also appreciated all the people that have shared videos and documentation of slushflows during this thesis work, Trond Jøran Nilsen from TFFK, has been especially helpful in this work by sharing drone photos and videos from events happening in Finnmark winter/spring 2023. He also made the field work unforgettable by letting us join the helicopter ride to document a slushflow event in Kvænangen. I will also state my gratitude towards Graziella Devoli and Monica Sund from NVE for helping with understanding the slushflow database and giving me an understanding of the forecast system today.

For the simulation work I would like to thank Kalle Kronholm from Skred AS, for providing the polygons used for their simulation, that was helpful in the work of replicating their events. He also provided good advice from their work establishing the parameter set, that was useful to limit the uncertainties in the process of extending the dataset for validation the calibration of the parameter set. I would also like to thank SLF for providing a RAMMS: Debrisflow student license for the thesis work, to make this possible.

I have also appreciated all geology master students in the 2022-2024 class, in the Blue Barracks. Everyone has contributed to a good learning environment, with good advice, motivation, lots of coffee breaks and smiles in stressful times, but most of all for being helpful and provided critical feedback.

Table of Contents

1. Introduction

In Norway all types of rapid mass movements must be considered in hazard assessments. This includes the slushflow danger (Hestnes & Lied, 1980). Slushflows are gravitational mass flows, that initiates when water saturates the snowpack. A slushflow event occurs when the snowpack losses its cohesion and rapidly moves downslope like a fluid (Jaedicke et al., 2022). The high-density water-snow mixture have the potential to entrain debris and organic material along the path (Hestnes & Jaedicke, 2018). This factor combined with a long runout results in a large damage potential to everything in their path (Jaedicke et al., 2022; Washburn & Goldthwait, 1958). To make communities better prepared to prevent unnecessary damage and mitigate the areas prone to this hazard, it is important to connect the science of slushflows to their social and economic impact (Relf et al., 2015).

Slushflow hazards occurs on a global scale in areas with a seasonal snow cover (Onesti & Hestnes, 1989). In Japan, a single slushflow event in 1945 resulted in 88 fatalities (Kobayashi et al., 1994). This hazard type also poses a significant hazard in Norway (Onesti & Hestnes, 1989; Sund et al., 2023). In the winter seasons of 2010 and 2011, 11 fatalities were registered in Norway (Hestnes et al., 2012). Since these flows often release in gentler terrain that is normally not prone to avalanches (Jaedicke et al., 2022), an important question when it comes to slushflows is their predictability (Scherer et al., 1998). Slushflow events are rare, however, when they occur, they are often massive (Hestnes, 1985).

Numerical modelling is a tool that is widely used for spatial planning and the construction of mitigation measures both concerning the debris flow and snow avalanches danger (Christen, Kowalski, et al., 2010). As of yet, no model is developed to exclusively simulate slushflow runouts (Jaedicke et al., 2022). However, one software that has been used as a tool in hazard assessments to simulate this flow process is RAMMS:Debrisflow. To cover the complexity of different debris flow scenarios, the software allows a wide range of different inputs values and friction parameter calibration (Christen et al., 2012). This allows the model to be calibrated to simulate the high-water content flow, although a good dataset is needed for statistical confidence of this calibration (Christen et al., 2012). The friction parameter set used to simulate these runouts in the RAMMS:Debrisflow model is only based on a few well

documented events, and needs to be further validated by other high quality documented events (Kronholm, 2021).

Since slushflows pose a significant danger to humans, constructions, and infrastructure, the limitation of the methods used in the numerical modelling of slushflow runouts, needs to be evaluated, to reduce the risk in future spatial planning. This would not only affect spatial planning but also limit areas for early warning and strengthen the foundation in the process of developing mitigation measures.

1.1 Objectives:

The aim of this project is to investigate the limitations of simulating slushflow runouts using RAMMS:Debrisflow and validate an already calibrated friction parameter set for this purpose. This will be done by evaluating the credibility of the established parameter set (Kronholm, 2021). This leads to these objectives:

Investigate the limitations of using RAMMS:Debrisflow to simulate slushflow runouts.

- Validate the credibility of the model through replicating events.
- Study how different input variables effect the simulation output.
- Investigate calibrated parameterisation for slushflow runouts using this software.

2. Study area

This investigation focusses on slushflows in Northern Norway and this section will first present the setting where slushflows can occur. Slushflows have been documented in all regions in the world that experience a seasonal snow cover (Onesti & Hestnes, 1989). Particularly, slushflows have posed a danger to maritime mountainous communities worldwide for centuries, including the Pacific Northwest of the United States, New Zealand, and Scandinavia (Relf et al., 2015). The atmospheric and hydraulic boundary conditions in the polar and sub-polar regions, fulfil the conditions for slush flow initiation and make slushflows relatively common (Scherer et al., 1998). Most slushflow events are identified above 50°N, and have been observed occurring in all parts of Norway (Figure 1) (Hestnes, 1996; Onesti & Hestnes, 1989). The settlement of Longyearbyen in Western Spitsbergen (78 °N) is also exposed to this hazard (Hestnes, 1996). From these presented statements, it is clear that slushflow hazards are a well-known problem that threaten properties, infrastructure and human life in the mountainous areas in the Artic (Hestnes, 1985). In light of this, and considering the impacts that slushflow hazards have on the inhabitants in Northern Norway (Hestnes, 1996), it is both a suitable and interesting study area to select for the purpose of this project.

2.1 National rapid mass movement database (NSDB)

All the historical data of rapid mass movements in Norway is registered in NSDB (www.skredregistreringer.no). The database include necessary information needed for hazard and risk analysis (Devoli et al., 2020). All the registered slushflow events downloaded from the database in July 2023 is spread all over Norway (Figure 1). The events are either registered as polygons and points, or just a point registered. Slushflows are registered occurring all over Norway. However, they are most often observed in the mountainous areas along the coast.

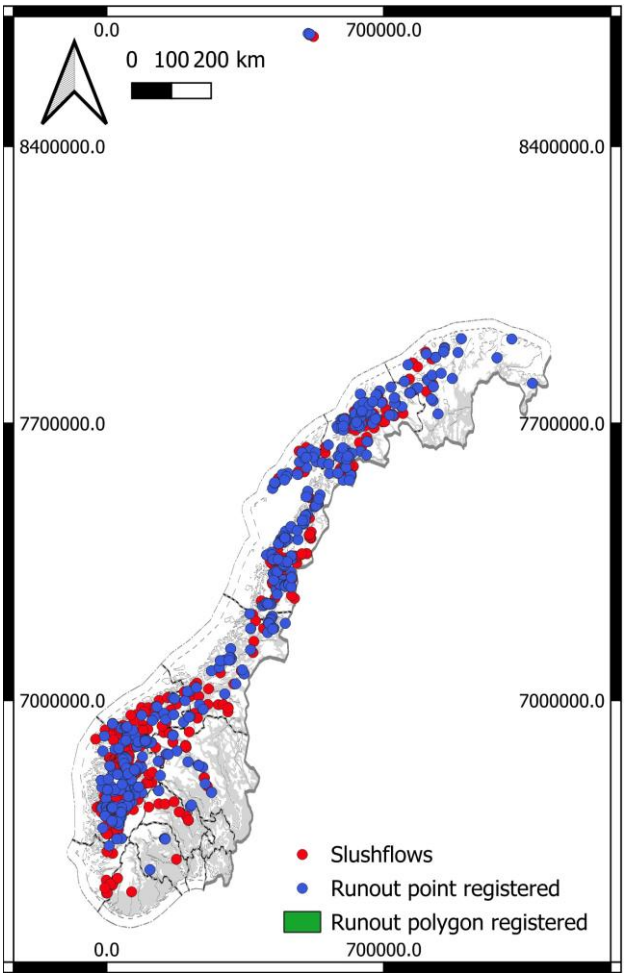

Figure 1: The distribution of registered slush flow events in NSDB Norway. The red dots are point registered slush flow events. The blue dots are events where the runout is registered as points. The green polygons are polygon registered events. The events are downloaded from NVE's database skredregisteringer.no in July. Background map "Topografisk norgeskart gråtoner" from Kartverket.

There are several challenges in the collection of slushflow data, underreporting also one of the main problems (Sund et al., 2024). One large insecurity with the database is the classification of the rapid mass movement type. Slushflow events are often miss categorized as snow avalanches or debris flow (Jaedicke et al., 2022; Sund et al., 2024). Since the deposit always contains snow and ice it is possible to classify them if the slushflow deposition is fresh. However, it is not easy to divide old slush flow deposition from debris flow deposition (Jaedicke et al., 2022). Historical and media documented events are mostly related to damage of property and infrastructure, which do not represent the frequency of slushflows (Hestnes, 1996).

The quality of the data registered for the events varies a lot. Many registrations of the events lack important information about the location and time of the event. This has led to a quality classification of the different events, when the events is classified in the range A-D, where A is defined when the location and time is documented with a high accuracy. (Devoli et al., 2020). To be able to back-calculate events for calibration and validation of parameterisation the location of the event needs to be exact (Christen, Bartelt, et al., 2010). Of all the registered slushflow events this would mean that only 5.3 % of the event could be used for this purpose (Figure 2), which would be a total amount of 30 well documented events in Norway (Figure 3) (NVE, 2023). Since, there is registered quality A events with only points indicating the "accurate" location of slushflows, would this mean that even a lower amount of these events could be used for this purpose (NVE, 2023).

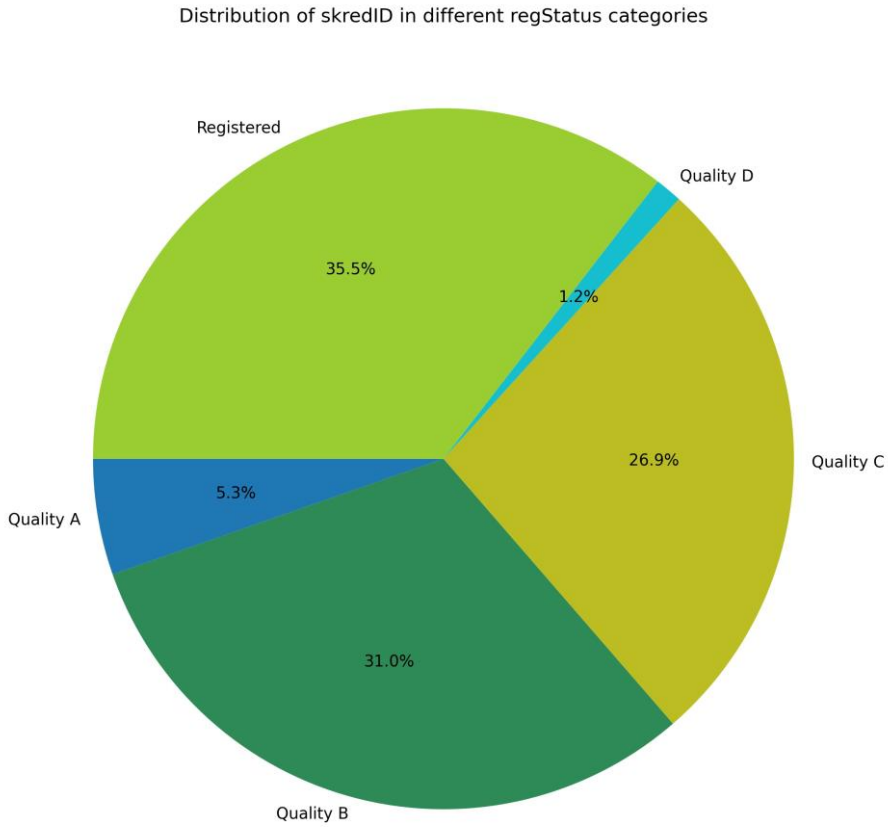

Figure 2: The distribution of the documentation quality of the registered events in the database. The dataset is downloaded from NVE's database skredregistreinger.no in July 2023.

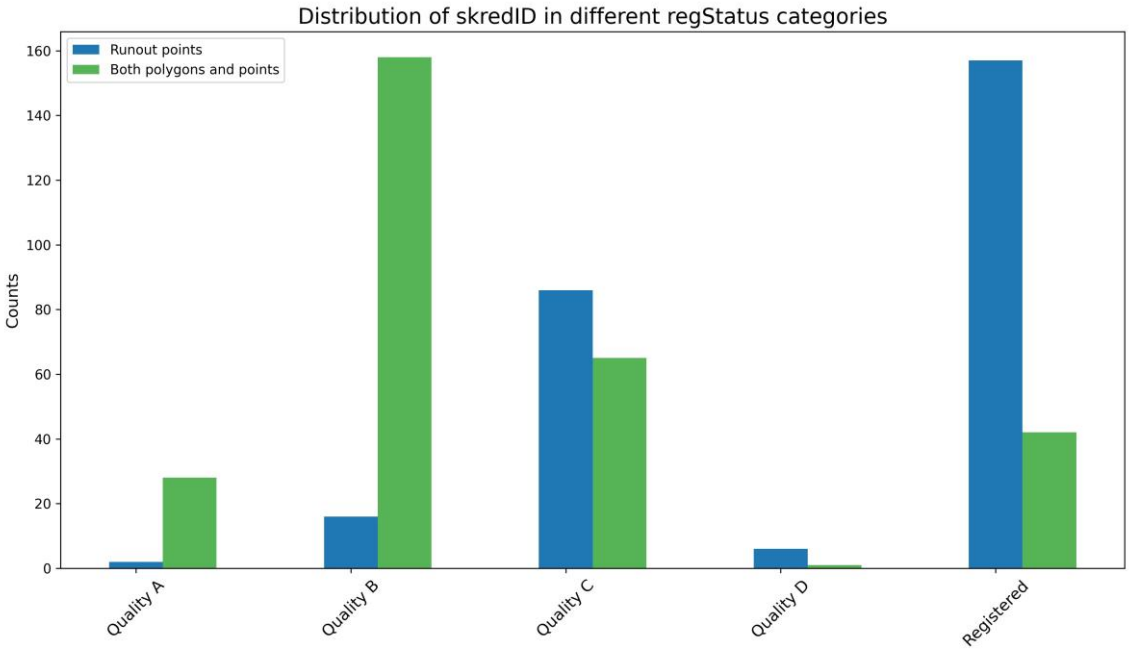

Figure 3: The distribution of the polygon and point registered events for each quality. Most of the quality A and B events are registered with polygons outlining the slush flow event to some extent.

2.3 Location

The events that are studied in this project occurred in Finnmark in Northern Norway during winter/spring 2023. The location of the events used to establish the friction parameter set that is used in this project is in the southern part of Norway (Figure 4). The difference in latitude would cause some variation in regional influences such as weather patterns, that affects the cause of initiation (Relf et al., 2015). Slushflows in higher-latitude continental climate typically occur in the late spring/early summer such as in May, June, or July (Onesti & Hestnes, 1989). For western maritime climates, slushflows most often occur during winter months when warm fronts intrusions cause heavy rainfall (Stimberis & Rubin, 2011).

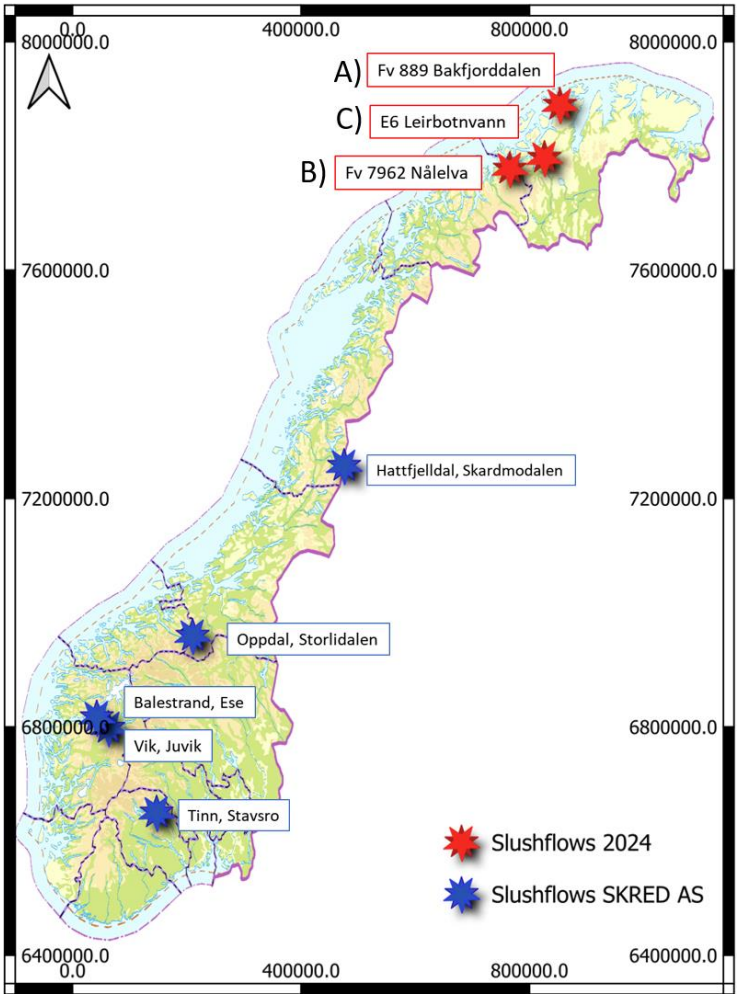

Figure 4: Location of the Skred As events with blue stars, and the location of the events in the extended dataset marked with red stars. The background map is "Topografisk Norgeskart" from Kartverket.

2.3.1 Field sites

According to the database it was no observation of historical slushflow events in either of the three field sites (NVE, 2023). The three slushflows in these locations initiated in different terrain features and geomorphological settings (Figure 5, 6). The one terrain features all the field sites had in common was channel or in sinks. The slope angle in the investigated areas would vary from initiating slushflow in an angle as high as 34° (Figure 6A) to a slope angle as gentle 1.3° angle (Figure 6C). All the terrain profiles of the flows variated for the locations. From initiating in steeper part of the path and depositing in the gentler part of the slope (Figure 5A), initiating in the gentler part of the slope roll over into steeper terrain (Figure 6B), or initiating and travel in a low angle slope gradient terrain (Figure 6C).

Both the Bakfjorddalen and Nålelva events initiated on exposed bedrock, that is favourable for water saturation of the snowpack (Figure 5A-B). The difference in geomorphology between these events, is that the slushflow path at the Nålelva event would flow over to mapped moraine material. In this transition it could be expected that the slushflow potentially can entrain sediments along the way. The last event located in Leirbotn, the slushflow follows the river valley covered in moraine material, depositing on glaciofluvial material (Figure 5C).

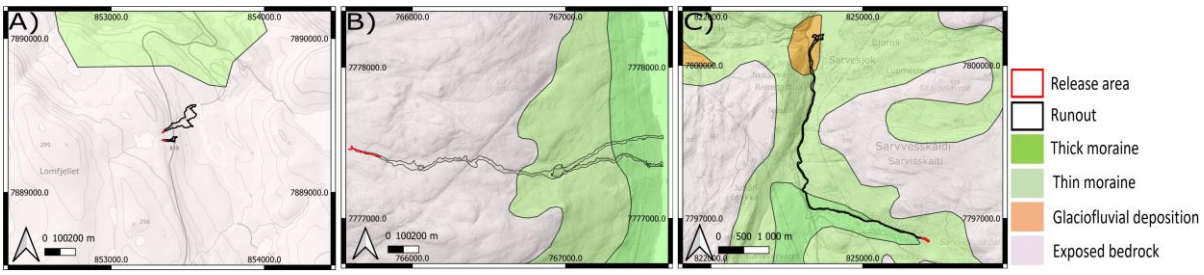

Figure 5: Geomorphological map for the three investigated field sites (NGU, 2024). A) Bakfjorddalen event releasing and traveling on exposed bedrock) Nålelva event releasing on exposed bedrock. C) Leirbotn event initial slushflow release on moraine materials.

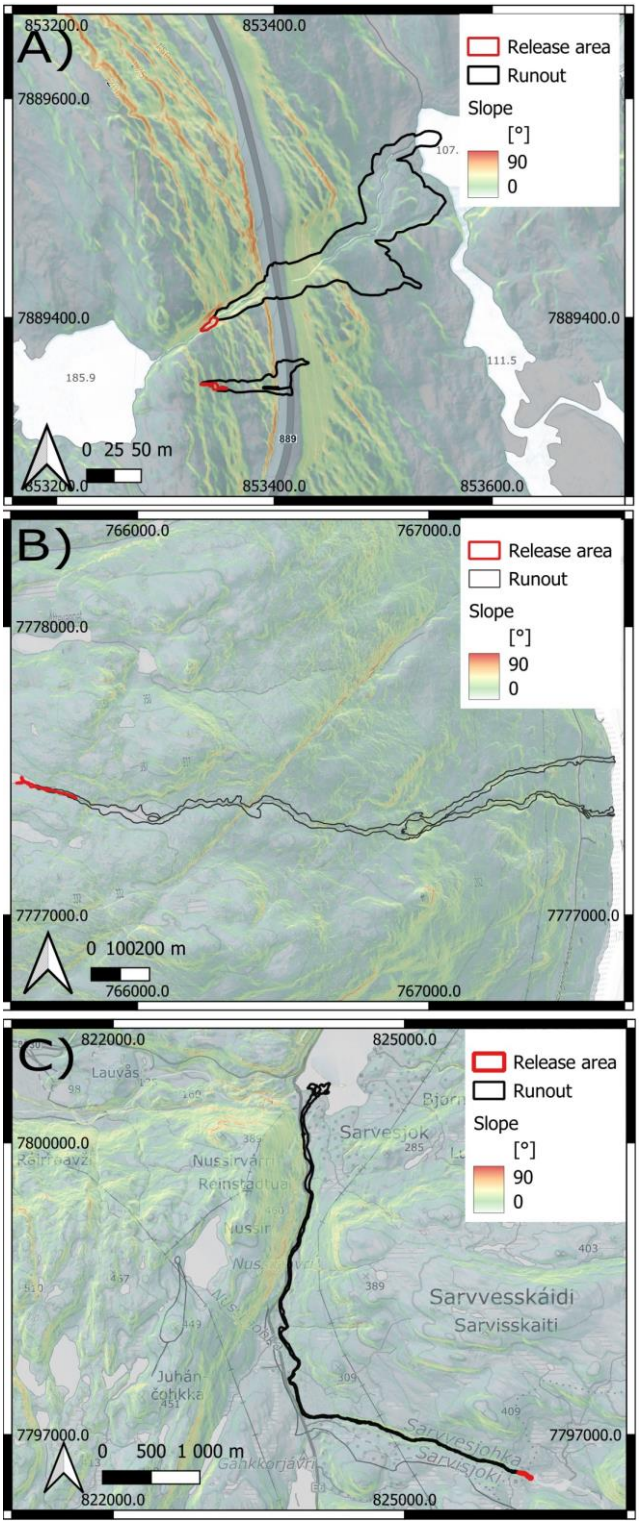

Figure 6: The terrain features and slope map for the three field sites, investigated in this project. A) Bakfjorddalen events, the largest event is in one steeper channel, with initial staring conditions with a 34° slope angle. While the smaller event follows an in sink in the bedrock, with an initial releasing area of 21°. B) Nålelva event, releasing in a gentle slope 3.5° and rolls into steeper terrain downslope. C) Leibotn event follow a river valley until depositing one a horizontal Lake. Initial starting condition 1.3° and travel over a low slope gradient terrain. Slope map generated based on

3. Background

3.1 Slushflows definitions

Hestnes et al. (2017) created a classification system for slushflows (Figure 7). This classification system of rapid mass movement events explains the variations of slushflow events based of the material mixture in the flow. Slushflow events result from a complex interaction between snow, water, terrain, and weather and any variation of the these factor in an event would result in a broad range of ultimately unique slushflows (Jaedicke et al., 2022).

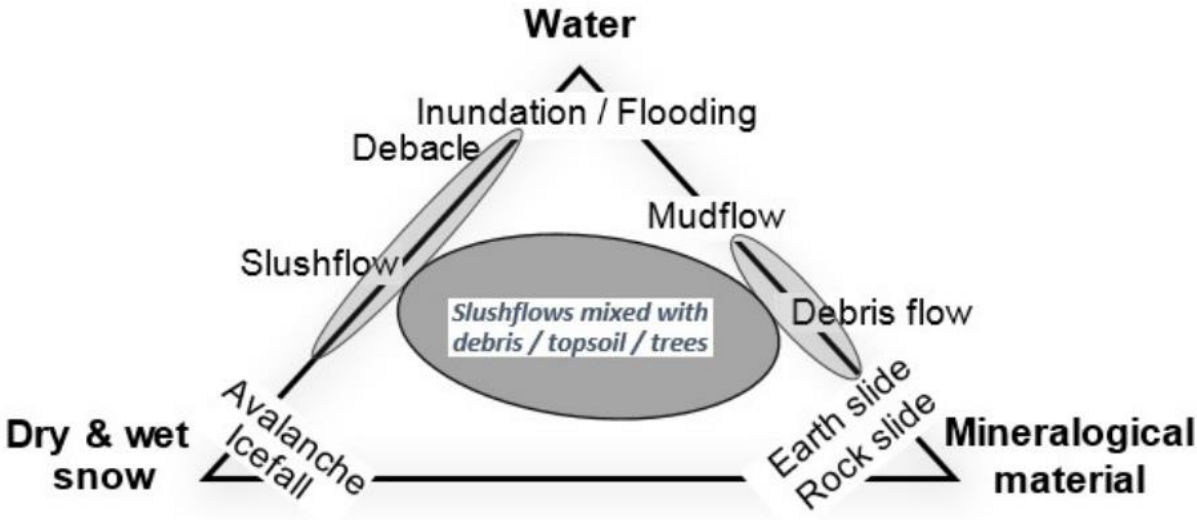

Figure 5: Classification of the rapid mass movements processes including with slushflows (Hestnes et al., 2017).

Slush is defined as snow with a water content above 15%. When the crystals are surrounded by water, the crystals loose the direct contact with each other (Fierz et al., 2009). This is because when the water level rise in the snowpack the bindings between the crystals weaken until they eventually disappear. When this happens the snow becomes cohesionless and starts to act like a fluid (Jaedicke et al., 2022). A slushflow is defined as the process when the slush starts rapidly moving downslope (Nobles, 1966; Washburn & Goldthwait, 1958). On the way downslope large amount of debris and organic materials can become entrained within the slushflow masses. This results in slushflow deposition often being mistakenly classified as debris flow deposition (Hestnes & Jaedicke, 2018). The saturated snow has a high-density

ρ. 800 to 1000 kg/m^3 (Hestnes, 1985; Jaedicke et al., 2022). The high-density flow poses a significant danger to human life and infrastructure (Hestnes, 1985).

The occurrence of slushflows depends on complex interactions between geomorphic features, snowpack properties and the rate of water supply (Hestnes et al., 2017). Slushflow are triggered when the snow cover becomes saturated and the slush starts moving downslope (Jaedicke et al., 2022). Slushflows are often observed to initiate in relatively flat terrain, where meltwater inflow is higher than outflow. Meltwater is not the only factor causing water pooling (Scherer et al., 1998). Another crucial factor for slushflow development is the drainage from the channels. The saturated snow would not release if the snowpack drained the water before the cohesion between the snow crystals is overcome (Jaedicke et al., 2022). Slushflows generally release when the water discharge rate is lower than the water recharge rate (Gude & Scherer, 1998). Water-saturation of snow cover is often indicated by the appearance of a blue-grey colour on the snow surface (Hestnes, 1985). The observations of accumulation of water indicate saturated snow, with a low shear strength. Relatively few cases of this observation lead to a slushflow release. Other conditions that must be evaluated when considering the slushflow danger aside from the drainage output are the acceleration rate of water input to the snowpack; the slope in the starting zone; and free water sources (Onesti, 1987).

3.1.1 Static variable

Slushflows pose a danger to communities located in mountainous areas, effected by the maritime climate (Relf et al., 2015). In contrast to other type of geohazards occurring in mountainous terrain such as snow avalanches, landslides and debris flow, slushflows can be released in gentle slopes (Vegvesen, 2014). Studies have shown that slushflows tend to initially start in depressions as well as gentler slopes (Nobles, 1966). This is because these terrain features hold the potential for the water to accumulate leading to enhances saturation of the snowpack (Scherer et al., 1998).

To identify slushflow terrain it is important to evaluate the processes that lead to these events. As mentioned, one of the key features of slushflow formation is the extent to which the snowpack is subject to saturation from water (Jaedicke et al., 2022). Terrain types that

enhance snowpack saturation are open slopes, bog, or flat areas as water added to the snowpack within these tends to stay within it rather than drain away (Figure 8) (Hestnes, 1996). Because large snow avalanche runouts can block channels and reduce the drainage the snow easier can saturate and result in slushflow release. This scenario would increase the susceptibility of slushflow initiations in runout zones for snow avalanches (Jaedicke et al., 2022).

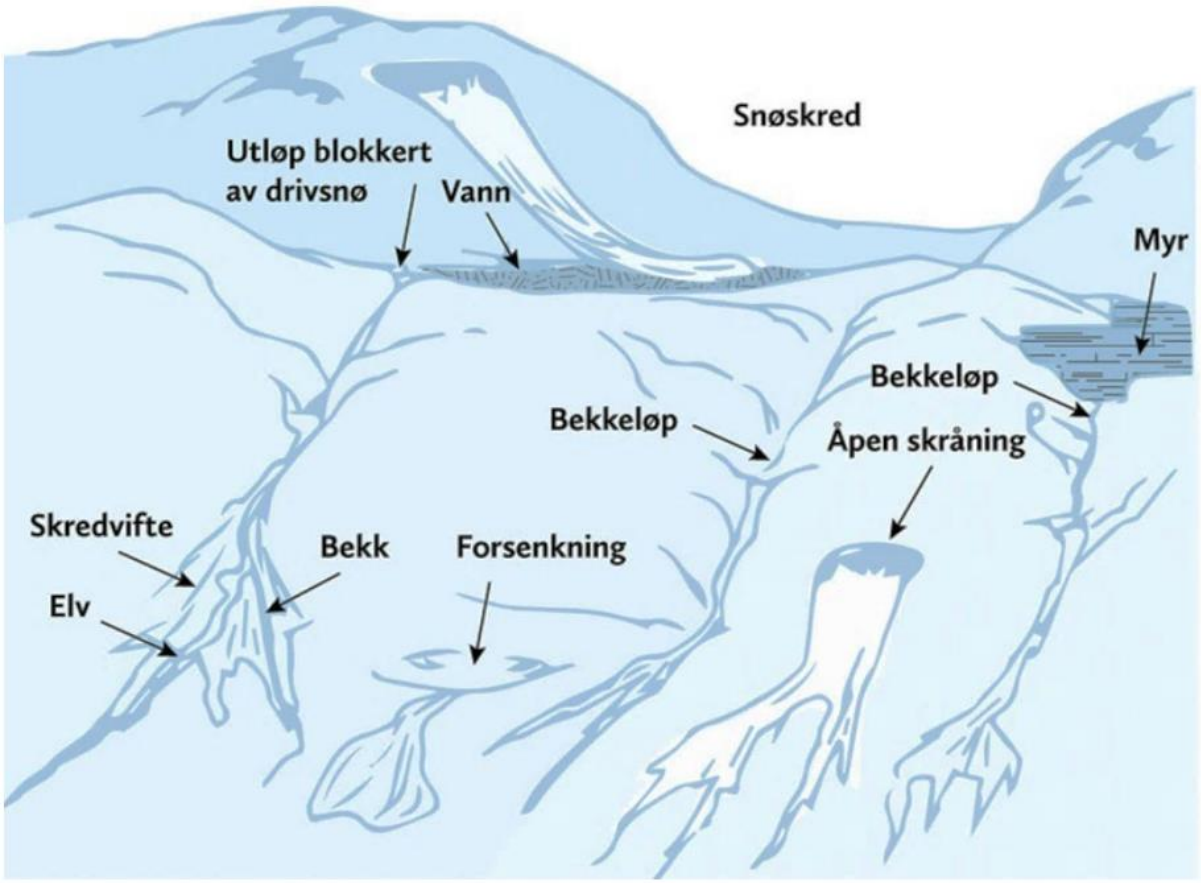

Figure 6: Classification of slushflow release from modified from (Hestnes, 1996). Illustrates the different observation of slushflow initiation from (Jaedicke et al., 2022). To the left hand-side slushflow events caused by snow avalanche are releasing onto a lake. The lower middle event on the left-hand side represents events starting under small geomorphic depressions. The middle event towards the right indicates a slushflow events starting in the small streams. Further to the right hand-side a slushflow event released in an open area is illustrated, and all the way to the right hand-side a slushflow released under a flatter bog.

One primary characteristic for the terrain types susceptible to slushflow release is the presence of downhill transport of water to the area (Scherer et al., 1998). When the water input is excessive, the capacity of drainage tunnels may be overwhelmed. The most obvious areas for water saturation of snow are topographic features such as streams, channels,

depressions or bogs (Elder & Kattelmann, 1993). Terrain features where water flowing from large catchments where the channels narrows into a bottle neck, are typical areas where the snow more easily reaches the necessary saturation to trigger a slushflow (Scherer et al., 1998). Another factor needed for the snowpack to reach the required level of saturation for slushflows to release is mechanisms that will work against the drainage. Favourable features to look out for in the terrain are impermeable substrates, bedrock, and frozen ground like permafrost or seasonally frozen soil (Scherer et al., 1998). These features prevent the water from percolating into the ground, and thus enhance water saturation in the snow (Relf et al., 2015).

The slope angle of the terrain is another interesting static variable for slushflow occurrence as there is a large variability in the angle of slopes described where slushflows release. Sund et al. (2020) and Elder and Kattelmann (1993) state that the easiest way to distinguish slushflow and wet snow avalanche releases is the slope angle. If the slope gradient is under 30° the event should be classified as wet snow avalanche. Observations from other slushflow studies confirm this trend with gentle slushflow release areas. There have been observations of slushflow release in 6° slopes, with an average mean slope of 3° (Elder & Kattelmann, 1993; Nyberg, 1985). A study based on 75 measured slushflow paths in Northern Swedish Lapland, identified an average starting zone for the slushflows being a 19° slope angle (Nyberg, 1985). In a recent study by Jaedicke et al., (2022) they state that slushflows studies has shown can start on terrain with slopes of 0 to 40°. Additionally, slushflows can start as a wet slab avalanches that immediately transitions into a slushflow (Hestnes et al., 1994).

Not all observations follow the same trends as these observations. There is a well-known slushflow path at Mt. Fuji in Japan. The stratovolcano is 3776 m a.s.l., and would normally be covered in snow from 2000 m a.s.l from mid-winter to early spring (Anma, 1988; Pérez-Guillén et al., 2019). The upper part of the volcano over 2900 m a.s.l., has a slope angle of around 35°, and transitions into 25° slopes at mid elevations, and 10° for the lower elevations under 17000 m a.s.l. On the 5th of March 2018 a slushflow release from the steeper parts of the Mt. Fuji was documented. This event entrained water and sediments along its path, and turned into a highly water-saturated debris flow (Pérez-Guillén et al., 2019).

3.1.2 Identifying slushflow release areas

The predictability of the slushflow initiation is one of the main challenges of identifying potential slushflow release areas (Scherer et al., 1998). Challenges connected to the research of slushflows release is that they could in theory release almost everywhere and this would lead to an overestimate of the slushflow danger (Jaedicke & Sandersen, 2021). To identify slushflow release areas, the understanding of the slushflow initiation mechanisms is an important consideration to make (Jaedicke et al., 2022). A video from a slushflow event in the Kärkerieppe cirque clearly demonstrates the dominant role of meltwater accumulation in slushflow initiation (Elder & Kattelmann, 1993). Even though the accumulation of meltwater plays a crucial role in the formation of slushflows, relatively few cases where water saturated snow is observed, actually end up releasing a slushflow (Onesti & Hestnes, 1989). There are still some uncertainties when it comes to the basic mechanics of slush stability and strength (Elder & Kattelmann, 1993). This leads to uncertainties of defining potential release areas for numerical models.

Hestnes (1985) conducted a study identifying trends in slushflow starting zones. This resulted in observations of the most frequent starting zones located in small streams. The study also identified three main type of release area (Figure 9). The release areas were divided into:

1) Sudden release from crown surface drainage of snow-embanked
2) Water-saturated snowfields through narrow outlets
3) Rapid head ward growth from first point of release (Hestnes, 1985).

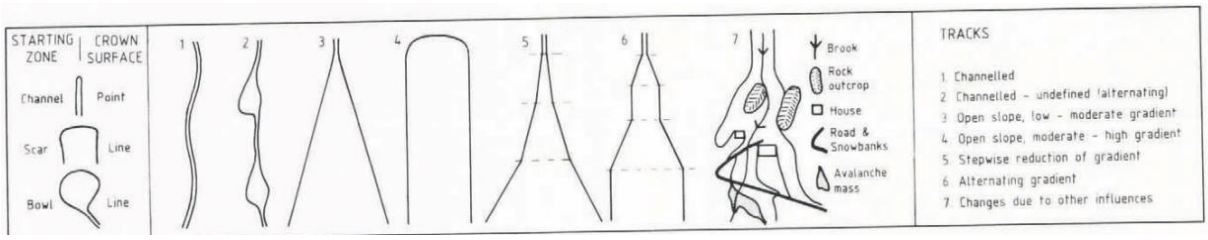

Figure 9: The different types of slushflow starting zone illustrated to the left. The observation of different track types in the middle, with the descriptions to the right. The figure is sourced from (Hestnes, 1985).

Other initiation mechanisms that can lead to slushflow release are physical barriers, like avalanche deposits and ice jams, that hinder the water to flow, and block channels. This block could eventually lead to damming of water, and could eventually result in a slushflow release (Rapp, 1960).

3.1.3 Slushflow dynamics

The initiation mechanism and flow dynamics is similar to debris flows (Vegvesen, 2014). Due to the high-water content, slushflows usually have long runouts and could transform into debris flows (Sund et al., 2023). Slushflow flow paths are characterized by long distances up to several kilometres. There is recorded a slushflow on Mt. Fuji Japan, with an estimated runout distance from 3.9 $\pm$ 0,4 km (Pérez-Guillén et al., 2019).

In snow avalanches a diverse array of particle interaction produces a wide range of flow behaviours depending on particle properties and terrain characteristics, controlling the particle interaction with the snow cover and the ground (Bartelt et al., 2012). When the snowpack becomes water saturated and the pore pressure increases, which leads to weaking of the bonds between individual crystals are weakened and the snowpack becomes more unstable. The increased pore pressure due to the increased water content also contributes to the weakening of the snowpack (Jaedicke et al., 2008). Since the snow particles start to behave separate from one another, the slushflow events can mobilise like a fluid and move past obstacles that results in rapid, long runout (Jaedicke et al., 2022).

A noticeable feature of slushflows is the fact that the ground is the gliding surface, in the starting zone as well parts of the track. Entertainment of organic and mineralogic material is therefore common and results in slushflow deposit are often dark, dirty and contain sediment. Slushflows often grow because of added water and slush downslope, which can be enhanced through a thawing snowpack and rain, especially in especially river valleys (Hestnes, 1996). This could be the reason why slushflows often behaves in pulses (Jaedicke et al., 2022).

Slushflows often flow with a velocity between 15m/s and 30 m/s, because of its high density and erosional effect on the vegetation the damage potential of a potential event is high (Jaedicke et al., 2022).

3.2 Numerical modelling

Numerical modelling is one tool used to simulates and replicate natural hazards events. The model uses equations to describe the parameters that operates in the real world and is a way to simulate the observation from the nature. The results of the mathematical models describes the deposition processes, and often include flow depth, velocity, and impact forces (Simoni et al., 2012). Since these simulations potentially provides realistic results, numerical models are used to estimate the hazard in use in hazard assessments (Christen, Kowalski, et al., 2010; Sampl & Zwinger, 2004).

At present, there is no existing numerical models specifically developed for slushflows runouts (Kronholm, 2021). However, there are models developed to simulate the dynamic of debris flows. Debris flows are rapid mass movement flows that can occurs in steep channels with significant entrainment of material and water (Hungr et al., 2014). These types of events can move with a speed as high as 16 m/s, which is the lower speed observed for slushflows. There are observed debris flow runouts in slopes as gentle as 4° (Shieh et al., 1996). Since both debris flows and slushflow dynamic are mainly caused by rapid flowing mixture of water and debris/slush, it could be possible to calibrate the debris flow model by changing the parametrisation to simulate the slushflow runout. The software used to simulate gravitational mass flow process in this project is RAMMS:Debrisflow. RAMMS stands for Rapid Mass Movement Simulation, and is a two-dimensional simulation program (Christen, Kowalski, et al., 2010; Kronholm, 2021). The software allows a wide range of different input variables, to fit different hazard scenarios. This is to represent both the complexity of debris flow events, but also to meet different requirements from hazard assessment guidelines. To investigate hazard scenarios specific release conditions must be provides as inputs to the model. Due to the wide spectre of starting conditions this is challenging, the variety of input parameters also provide the freedom to calibrate the parameterisation to fit slushflow runouts (Christen et al., 2012).

To construct hazard scenarios specification of the release properties is necessary. This includes release area location and spatial extent. Other necessary input variables includes friction parameters describing the flow dynamic (Christen, Kowalski, et al., 2010). To

calibrate these parameters the use of historical events is required (Meyrat et al., 2022). The quality of the result is determined by the input values. The initial conditions of the hazard scenario, combined with the reaction of the numerical model to accurately simulate the flow in the three-dimensional terrain will affect the credibility of the results (Christen, Kowalski, et al., 2010).

Challenges around accurately quantifying the initial starting and entrainment of masses are a well-known problem in numerical simulations of debris flow (Meyrat et al., 2022). The differences in flow material also leads to some uncertainties. As mentioned, the model is based on debris flow releases. To initiate a debris flow the release area has to be located in slopes greater than 14,8º (Armanini & Michiue, 1997). This would differ from the observed release areas for slushflow, that often are observed to release in more gentle slopes then this threshold value (Elder & Kattelmann, 1993; Nyberg, 1985). Due to the difference in material, the slushflow release area would in some cases be placed in a steeper part than the initial release area is either observed or predicted to occur. This is recommended to be steeper than 10 º (Kronholm, 2021). The quality of the result is determined by the input values, so by changing the initial conditions of the hazard scenario, the credibility of the results will be affected (Christen, Kowalski, et al., 2010). To generate appropriate scenarios, the experience of the user who is generating the runout in the models contributes towards how realistic the hazard scenario is (Graf et al., 2019).

To be able to conduct a numeric simulation in three-dimensional terrain, a digital elevation model (DEM) needs to be added (Christen, Bartelt, & Kowalski, 2010). The cell sizes of the DEM will affect the simulation results (Majid & MOTAMEDI, 2024). If the resolution of the DEM is low, this would potentially lead to loss of important terrain information. However, a too high train resolution also lead to inaccurate simulation results (Christen et al., 2012). Since the snows cover some of the terrain features a lower resolution model with 5 m cell size is used similarly to snow avalanche simulations (Bartelt et al., 2012). However, in the establishment of the slushflow friction parameter set a 2 m cell size was used (Kronholm, 2021).

3.2.1 Friction parameter calibration

One of the challenges linked to numerical modelling of natural hazards is parameter validation. To be able to create a parameter set with statistic confidence, a high quality dataset is required (Christen et al., 2012). The friction parameters in RAMMS:Debrisflow can be modified to account for variations of water content, sediment size, and channel roughness to fit the properties of the area of interest (Graf et al., 2019). Since slushflows have a significantly different mobility compared with debris flows, it requires a calibration of the friction parameters (Kronholm, 2021).

Equation 1: Total friction in Voellmy-Slam model

$$S = \mu N + \frac{\rho g u^2}{\xi}, with\ N = \rho h g cos(\phi)$$

The software used in this project, RAMMS:Debrisflow, uses the two-parameters, Voellmy-Slam friction model (Zhang, 2019). This two model splits into the total basal friction (coefficient μ [-]) and a velocity depended "viscous" or "turbulent" friction (ξ [m/s^2]) (Salm, 1993). The basal friction (μ) is more pronounced in the deposition phase, when the slushflow starts losing velocity. The internal friction (ξ) represents the viscosity and the turbulent forces inside the slushflow, this parameter decides the maximum velocity of the event. The friction forces are also affected by the slope angle (ϕ) and the density of the moving material (ρ). The total friction resistance in the Voellmy-Slam model (S), Equation 1, is directly proportional with Coulomb-friction μ, and inversely proportional of the friction ξ (Kronholm, 2021).

Table 1: Friction parameters established for slushflow simulations in RAMMS:Debrisflow

Frequency	**Erosion**	μ **(-)**	ξ **(m/s^2)**
1/100	No	0,08	2000
	Yes	0,08	3000
1/1000	No	0,05	3000
	Yes	0,05	4000
1/5000	No	0,04	4000
	Yes	0,04	5000

The calibration of the parameters resulted in a combination of the ground and the internal friction that matched the extent of the event. Because of a lack of data it was not possible to determine value for each parameter, only the combination (Kronholm, 2021).

3.3 Hazard and risk

Since slushflows poses a significant danger to everything in its path is it important to predict where this flow release and how it will travel in the terrain. This will contribute to the work of reducing the slushflow danger. In Norway all types of rapid mass movements have to be considered in hazard assessments (Hestnes & Lied, 1980). NGI started an own research program for slushflows after extensive damages and deaths from slushflow events occurring in the last week of march in 1979 in the Western part of Norway (Domaas & Lied, 1979) and January in the Northern part of Norway, between 65° and 69° (Hestnes & Sandersen, 1987). The specific purpose of this program was to develop objective criteria to enable identification

of slushflow hazard and methods for slushflow prediction and control (Hestnes, 1985; Hestnes & Bakkehoi, 1995).

The most effective way to avoid any fatal consequences of a slushflow event is to limit the exposure of the hazard. The best way to do this is through spatial planning. This is efficient for constructions and housing. However, for roads and rails it always be parts of the distance that is exposed to slushflow hazard. To avoid a disaster early warning and mitigation measures area important tools to prevent fatalities and damage on infrastructure (Jaedicke et al., 2022).

3.3.1 Spatial planning

The most economical beneficially ways to secure for slushflow hazards is by spatial planning. By mapping potential effected areas and avoid establish property and infrastructure in exposed areas (Jaedicke et al., 2022). According to the Norwegian laws and regulations, specifically TEK 17 § 7-3, requirement of safety against avalanches in spatial planning. The requirement for safety regarding rapid mass movements consider rockfall, debris flows, quick clay, snow avalanche and slushflows. The requirements would limit areas based on the yearly probability of a hazard event and are divided into three different hazards zone (S1, S2 and S3) (TEK 17, § 7-3). The hazard level is given as the frequency of an event. If the return interval of slushflow events is 1000 years, the yearly probability would be 1/1000 years. The calibrated parament set is developed based on these safety return periods (Kronholm, 2021).

Numerical modelling is a common tool used in spatial planning, for both snow avalanches and debris flows (Christen, Kowalski, et al., 2010). However, since is not established an own model for slushflows today the use of these in spatial planning are limited (Jaedicke et al., 2022). Another important step in the process of spatial planning is to gather information of frequency of previous events. However, the documentation of slushflow events is limited. To improve the quality of spatial planning in the future it is important to improve the database to get a better picture of the historical events, and to gain a understanding of the occurrence of these events (Hestnes et al., 2017; Jaedicke et al., 2022).

3.3.2 Mitigation

Physical mitigation measures could be done for both possible release areas and runouts. Measures that could affect the hazard includes drainage changes, vegetation, hydrological conditions, and terrain changes (Jaedicke et al., 2022). Numerical simulation tools are used for hazard estimations and protection planning (Sampl & Zwinger, 2004). One of the main challenges for establishments of mitigation measures for slushflow is to calculate the slushflow velocity and flow height based on the data set foundation that exist today (Jaedicke et al., 2022). After a slushflow incident in Vannledningsdalen January 2012, NGI reviewed the existing mitigation measures. In this worked they used the RAMMS:debrisflow to simulate slushflow events. By using a terrain model excluding mitigation measures they calibrated the friction input parameters based on old slushflow events. The friction parameter combinations μ=0.05 and ξ=5000 [m/s^2] matched the runout to some extent. These parameters were used to simulate events with modified terrain including the revised mitigation measures. This simulation provided valuable indicators on slushflow travels in the path, the flow thickness and expected spread of the deposition. The simulations also indicated possible shortcomings in the proposed design of the mitigation measures (Jonsson & Gauer, 2014).

3.3.3 Early warning

Since it is connected a significant hazard to slushflows in Norway, hazard prediction and early warning is an important preventive measure (Sund et al., 2023). Efficient early warning requires good spatial planning in advance, to map areas exposed to slushflow hazard. When the slushflow danger reach critical condition these areas could be evacuate and roads and rails could be closed (Jaedicke et al., 2022). Regional early warning for slushflow was established in Norway in 2013/2014 and has been operational since. This assessment are based on snow cover and hydro-metrological conditions, collected from different sources, including data from automatic stations and field observations. The main factors that is the foundation of this assessment is ground conditions, snow properties, air temperature and water supply to snow (Sund et al., 2023).

3.3.4 Climate changes effect on the future risk of slushflows

One important factor to consider when determining the slushflow hazard, is the climate of the region. This factor decides both the timing and probability of slushflow initiation. Due to the changing climate the, the frequency and impact of slushflow could change (Relf et al., 2015). Warmer and wetter climates are projected for at high latitudes, which is likely to increase the frequency and occurrence of slushflow events, as snowpacks are more likely to become saturated, due to higher temperatures causing melting and precipitation falling as rain instead of snow (Hanssen-Bauer et al., 2009). Increasing global temperature and winter rain precipitation could lead to a higher frequency of slushflow events (Jaedicke et al., 2008). As climate changes continuous, the frequency and impacts of slushflows may become more intense and impacts larger areas and greater number of people (Relf et al., 2015).

The climate effects on the slushflow hazard would depend on the region. Most of the artic and part of the cold continental regions are prone to more snow and rain in the winter, and would with the prognosed climate be prone to a higher frequency of slushflow events in the further (Hestnes et al., 2017). Spitzbergen is usually related to cold climate. However, in the recent years mild weather have become more frequent. Because of the more frequent warm weather the risk of slushflow events is elevated mid-winter, and is not only occurring in May as previously recorded (Jonsson & Gauer, 2014).

4. Method

4.1 Skred AS reproducing

Skred AS worked on calibrating the friction parameters in the RAMMS:Debrisflow model to simulate the runouts of five already released slushflows. Additionally, Skred AS developed friction parameters for slushflow events using RAMMS:Debrisflow 1.7.20 in 2021. These calibrated parameters are based on the well documented events. The events are in different parts of southern of Norway.

The process of reproducing the events from Skred AS initially started with gathering the exact data they used in the simulation. The first step was to collect all the vector files used in the simulations. The polygons for all the events were sent to The Arctic University in Norway (UiT) as one shapefile from Skred AS. The Coordinate Reference System (CRS) for the events of this shapefile is “EPSG: 25833 – ETRS89/UTM zone 33N”.

4.1.1 Digital terrain model’s (DTM)

Calculations from RAMMS simulations are affected by the digital elevation model (Bühler et al., 2011). The simulation resolution in RAMMS:: Debrisflow “sim resolution” is automatically equal to the digital terrain model (Kronholm, 2021). However, this can be adjusted by the user. The used digital elevation models are based on LiDAR data, with a horizontal resolution of either 0.5 or 1 m, that represent the terrain. The calculations on the events are generated with a 2 m horizontal resolution (Kronholm, 2021). The DTM´s used in the simulations are all downloaded from hoydedata.no. The different DTM of the events are merged and resampled to 2x2 m grid size for the simulations.

Table 2: Overview of DTM's from Skred AS events.

Events	DTM	Horizontal resolution	Simulation resolution
Oppdal, Storliedalen, Landlaupet; 10.5.2018	«NDH Oppdal 2pkt 2016»	1 m	2 m
Vik, Juvik, Djupevikelvi; 29.12.2019	«NDH Høyanger-Vik Stølsheimen 2pkt 2016"	1 m	2 m
Balestrand, Ese; 21.3.2021	National terrain model UTM33N	1 m	2 m
Tinn, Stavro, Stavsrobekken; 29.4.2019	National terrain model UTM33N	1 m	2 m
Hattfjelldal, Skarsmodalen, Rapbekken; 16.5.2010	«NDH Hattfjelldal sør 2pkt 2019»	0.5 m	2 m
Source of data:	https://hoydedata.no/LaserInnsyn2/		

All these terrain models are downloaded in the same CRS as the shapefile with the release areas of the events "EPSG: 2583 – ETRS89 / UTM zone 33N". All the different DTM files from the specific area of the events are merged into one DTM in QGIS, using the raster tool "Miscellaneous". After creating one DTM covering the area of the event, the resolution for the DTM's is changed into a 2x2 m resolution for the simulations, to replicate the work Kronholm (2021) did establishing the dataset. The last step in the raster file preparation is to convert the DTM's into an ASCII format for the RAMMS simulations.

4.1.2 RAMMS set-up

The simulations made by Kronholm (2021) were simulated with RAMMS:Debrisflow 1.7.20 version. However, the simulations made in this report are simulated with the RAMMS:Debrisflow 1.8.0 version. The changes in the program versions would lead to some differences. The user manual recommends starting the simulations with standard friction values to calibrate the model. The standard values on the 1.7.20 version used were μ=0,2 and ξ = 200 m/s^2, the same values as for the 1.8.0 version.

The snow density used in all the simulations is 1000 kg/m^3 due to the high-water content in the saturated snow. Stop criteria used for all the simulations are set to 5% of the total momentum. The end time is set to 1000 sec, and the dump step 2 sec (Kronholm, 2021).

The parameters values used for the different simulations of the different replicated events are shown in the table 3 below.

Table 3: Simulation parameters for Skred AS events.

Events	**Simulation ID**	**Release area**	**Density [kg/m^3]**	**Fracture depth [m]**	**Friction parameters**		**Erosion**
					μ	ξ [m/s^2]	
Oppdal	O1	"Øverst_full"	1000	1	0.05	2000	no
	O2	"Nedre"	1000	1.5	0.15	500	no
	O3	"Nedre"	1000	2.9	0.15	500	no
	O4	"Midt"	1000	1.4	0.08	2000	no

	O7	"Nedre"	1000	1.5	0.08	2000	no
Juvik	V1	"Øvre"	1000	1.3	0.08	2000	no
Balestrand	B1	"Midt"	1000	0.7	0.05	2000	no
Tinn	T1	"Midt"	1000	10	0.08	2000	no
Hattfjeldal	H1	"Skardmodalen"	1000	1.5	0.08	2000	no

4.1.3 Comparing Skred AS's and reproduced simulations

To compare the results from the reproduced events and the original simulations, the figures from the report was reconstructed in QGIS. Where possible, the same scale is used in the figure as that used in the simulation. The low velocity or shallow depths were investigated to spot differences that could be caused by different versions of RAMMS.

Kalle Kronholm from Skred AS provided the raster files from their simulations generated in the work of establishing the friction parameter set for slushflows in RAMMS:Debrisflow. The raster files were downloaded to QGIS to visualize the result, to illustrate both the similarities and the differences between the simulations done with 1.7.20 version and 1.8.0 version of the program.

4.2 Extended dataset for validation of established friction parameters

To statistical confidently validate the calibration of friction parameters set (Kronholm, 2021), a good dataset foundation data set is necessary. The initial step in this process was to get an overview of the documented slushflow events in the national database of rapid mass movements. This was done by looking at the distribution of the location and quality of the registered slushflow events that is already documented. Graziella Devoli and Monica Sund at NVE helped with getting an understanding of the database content and the way the events have been registered based on the way they are documented.

The quality of the data in this database varied between quality-controlled events that was given a quality between A, B, C and D (Devoli et al., 2020). To simulate events the release area must be documented. To validate the friction parameters the whole extent of the run-out and release areas must also be well documented. The quality A data was mapped with outline of extent of the event. However, the run-out and release areas was generated with the same polygon layer, where the initial release areas were often not defined. The events that are used in the RAMMS simulations in this thesis are events that happened in Northern-Norway during Winter/spring 2023. Documentation of the events is done by communication with the Road Authority in Norway, “Statens Vegvesen”, and Troms- and Finnmark Fylkeskommune (TFFK).

During winter/spring 2023 there were three registered road crossing slushflow events in Troms- and Finmark, and one event in Nordland. Through communication with Trond Jøran Nilsen at TFFK (Troms- og Finnmark Fylkeskommune) and the Road Administration (Statens Vegvesen) drone videos, and photos documented events was shared.

4.2.1 Field observations

24.4.2023 a slushflow event closed Fv 7962 in Burfjord. On the day of the event Tor Ole Larsen documented the extent of the event with drone video and photos. On the day after the event, the full extent of the event was documented from a helicopter. The release areas were investigated from the air and surrounding areas with similar signs of saturated snow observed

nearby the event. After getting an overview of the event from the air, the deposits crossing the road and the debris was more closely investigated. Christopher D'Amboise from UiT was a part of the planning and investigation of the fieldwork. Trond Jøran Nilsen provided the helicopter on TFFK behalf, that was originally used for planning and safety purposes of the road cleaning work.

Figure 10: Helicopter provided by TFFK. Christopher D'Amboise from UiT to the left and Trond Jøran Nilsen from TFFK to the right.

An important part of the fieldwork was to investigate the deposit by foot, conducting a closer examination and investigation of the event than was conducted from the air. Differences in deposition composition was investigated over the road, and further up in the runout channel. The horizontal extent of the event was mapped in field as well as signs from the vertical extent (figure 9). These observations would indicate the maximum flow height of the slushflow during the event and could be observed in trees and over rocks. These observations were later compared to the to the simulation results to validate the credibility of the friction parameters.

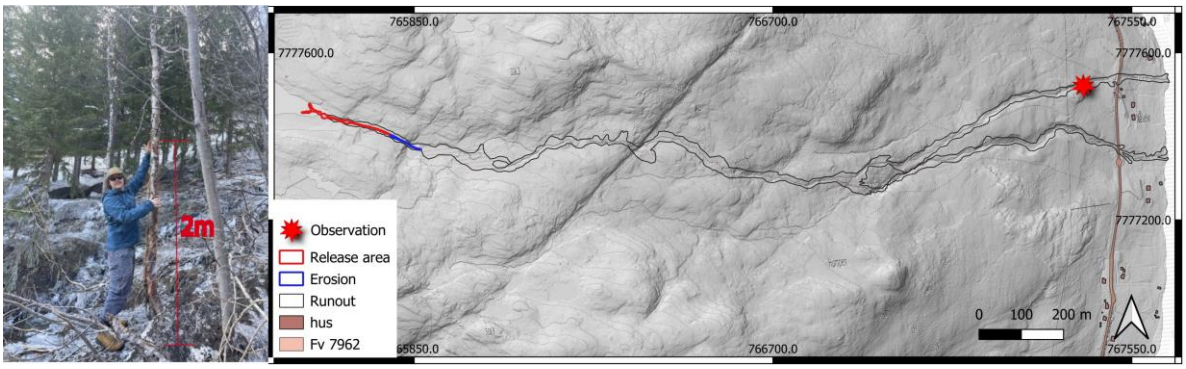

Figure 11: Observations of max flow height from 25.4.2023, the day after the Fv 7962 Nålelva event. Christopher D'Amboise from UiT as a scale. Basemap hillshade based on DTM from https://hoydedata.no/LaserInnsyn2/, overlayed "topografisk Norgeskart gåtoner» from Kartverket.

4.2.2 Digitising runout, release areas and erosion zones

All the documentation of the three field sites was used to digitise the spatial extent of the events. To find the exact location of events that were not visited in field skredregistreringer.no and recognizable terrain features in the described area was used. The digitising of event is made in QGIS Desktop 3.34.3. The base of the documentation is photos from the event, mostly from the air. Documentation from the Bakfjorddalen and Leirbotnvannet events were drone videos and photos provided by Trond Jøran Nilsen. Another valuable tool in the digitising process was a desktop terrain study using high resolution terrain models. This terrain models are downloaded as raster files from høydedata.no. The DTM's used for the events are described in Table 4. These terrain models are based on Lidar data, that gives a realistic picture of the terrain. The digital terrain models are used to create "Hillshade" that is a raster analysis tool in GIS.

Table 4: Overview of DTM's for Northern Norway events.

Events	DTM	Horizontal resolution	Simulation resolution
Fv889 Bakfjorddalen, Bakfjord, Måsøy; 17.2.2023	National terrain model UTM33	1 m	2 m
E6 Leirbotnvannet, Alta; 13.5.2023	National terrain model UTM33	1 m	5 m
Fv7962 Nålelva, Burfjord, Kvænangen; 24.4.2023	"NDH Kvænangen 2pkt 2016"	0.5 m	2 m
Source of data:	https://hoydedata.no/LaserInnsyn2/		

Photos are used, to identify and then digitise the initial release areas and the erosion zones where snow was eroded and added to the slushflow along the flowpath (Figure12). By comparing the photos with the features from the high-resolution digital terrain model it was possible to digitise the event with a reasonably high degree of accuracy. The extent of the whole run-out of the event, separated from the release area is drawn with different polygons in QGIS to create different shapefiles. The release area shapefiles are later going to be used in the RAMMS simulations. However, the runout polygon is used to validate the friction parameters by comparing the simulations with the observed runout. Mapping the infrastructure is also an important step in the digitising process, to gain an understanding of the vulnerability of the area of the event.

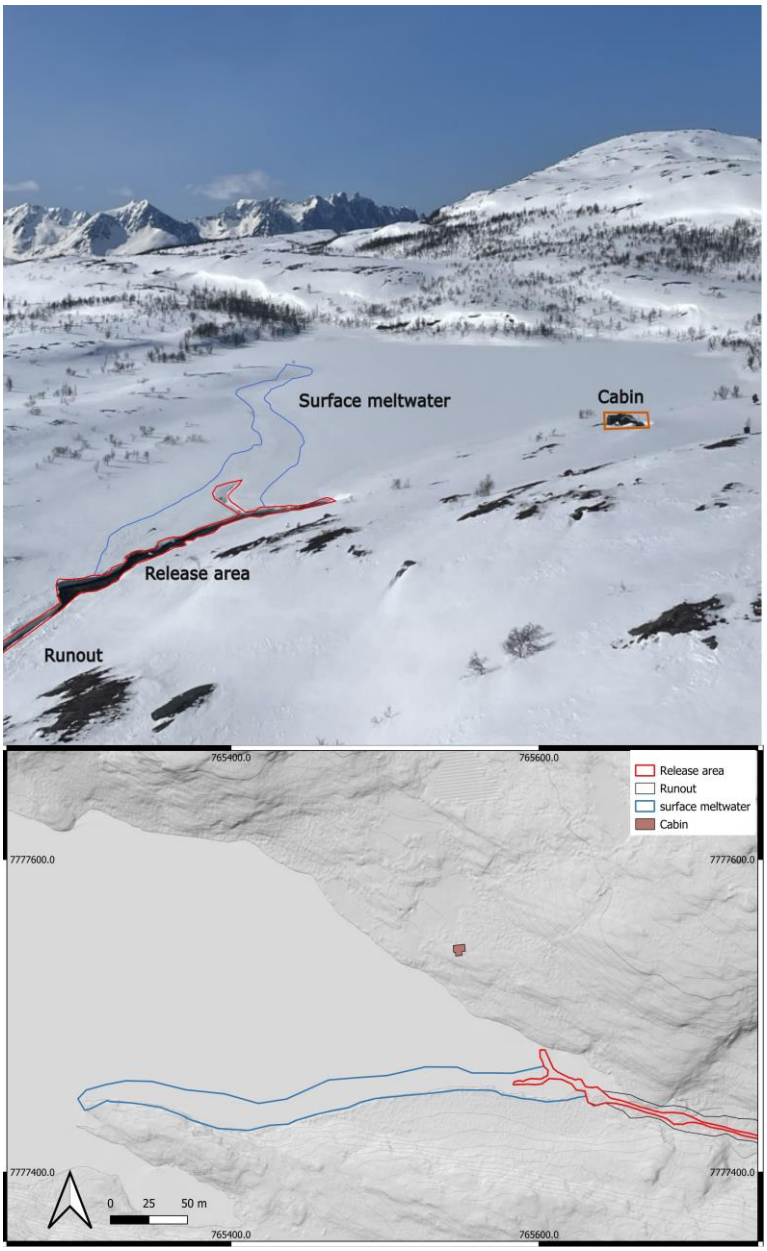

Figure 12: Example of mapping from air photo. The brown mark in the figure shows the infrastructure at risk for the slushflow hazard. The Light blue outline shows the observations of surface flow deposits on top of the snowpack. The red indicates the release area of the event. The background in the map is a hillshade model generated from DTM downloaded from høydedata. Underlying "Topografisk Norgeskart gråtoner" from Kartverket.

With the GIS plug-in tool "georeferencing" is it possible to link photos from field closely with the location in the map. To increase the quality of the event mapping, the photo foundation should be as close to the event as possible, and this requires a bird's eye view of the deposit. By using the "Hillshade" generated from the DTM, it is possible to use reference points from the terrain to correspond with the photo. In this way it is possible to outline the

deposits, an example from where this is done is shown in figure 10. This is the most accurate digitising method used in this report.

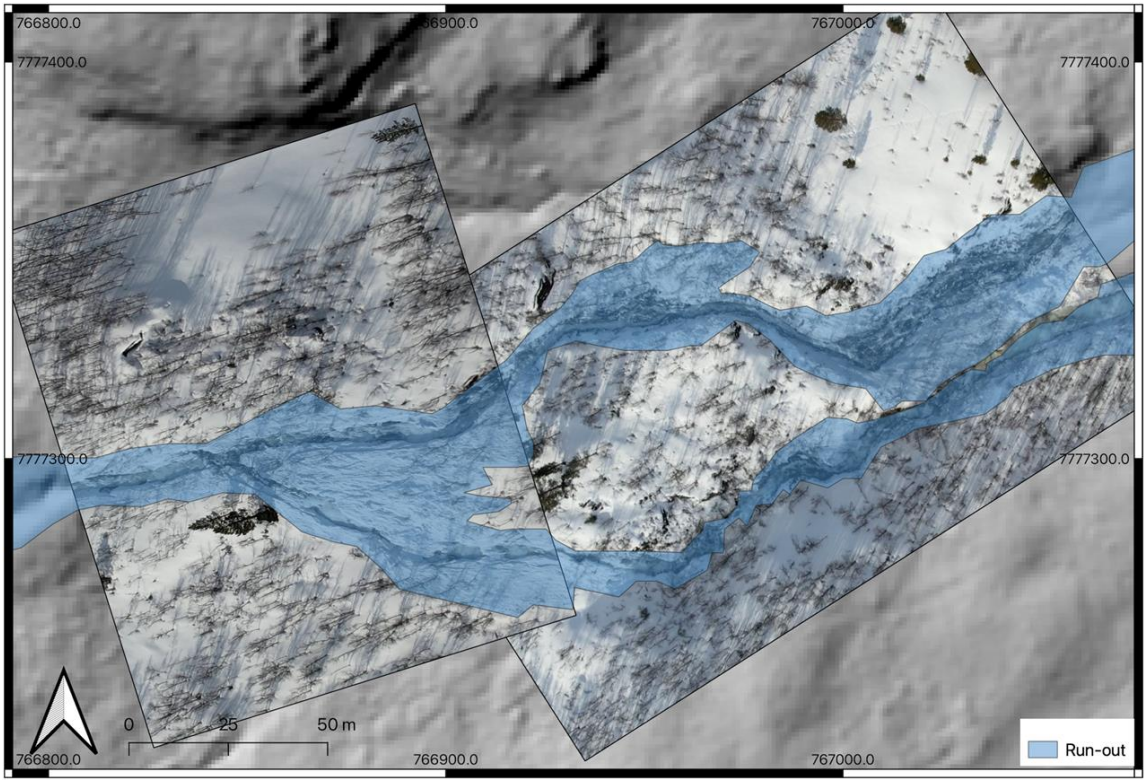

Figure 13: Example from Nålelva where georeferencing is used as a digitising tool. The runout of the event is marked with polygons. Drone photo taken of Tor Ole Larsen, is placed on over a hillshade model generated from høydedata.

One useful tool in the process of mapping the spatial extent from desktop terrain data was to create a 3D model based of the DTM in QGIS. This tool was used for identifying the location of the release areas, where air photos from different angles are provided. With this method it is possible to recreate the same angle from the drone photos, and easier identify the terrain features seen in the photo (figure 12).

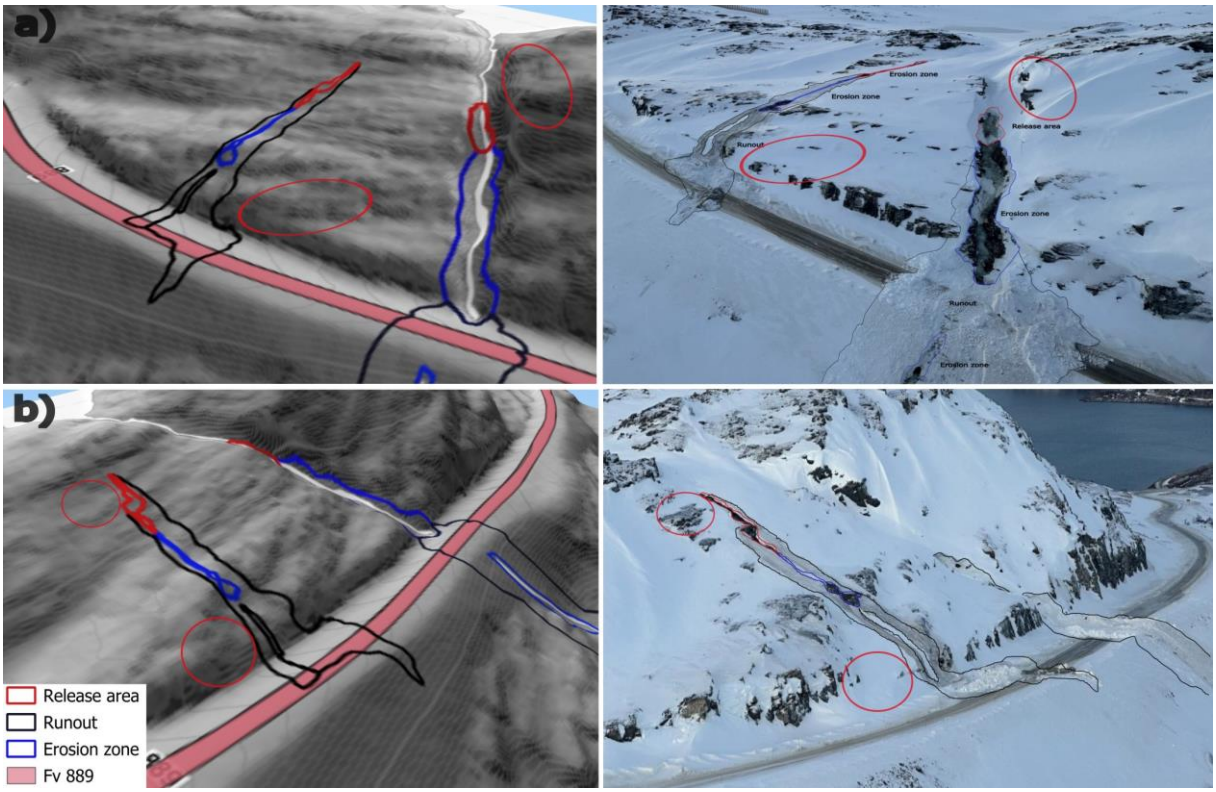

Figure 14: The elevation model from hoydedata.no can be used to create 3D terrain models of the terrain. This is used as a mapping tool to identify the location of the release areas most accurately, erosion zone and runout from drone photos taken from different angles. The red circles illustrate different terrain features that is recognizable from the terrain model and the photos. Situation a) and b) shows how the different angles are used to identify and limit the location of the event.

4.3 RAMMS set-up

The DTM used in the simulations are described in table 5. The Coordinate Reference System (CRS) used for the events is "EPSG: 25833 – ETRS89/UTM zone 33N". The resolution for the simulations is 2x2 m for Bakfjorddalen and Nålelva, and 5 m for Leirbotn due to the long runout. The stop criteria are the same as described in the process of creating the friction parameters, with a 5% percentage of the total momentum. The "End time (s)" of the simulations are set to 1000, with "Dump step (s)" 2.00. The density used in all the simulations are 1000 kg/m^3 to model the water saturated snowpack. All simulations were made with frictions parameters from table 5.

Table 5: Friction parameters for Slushflows using RAMMS:Debrisflow.

Frequency	**Erosion**	μ **(-)**	ξ **(m/s^2)**
1/100	No	0.08	2000
	Yes	0.08	3000
1/1000	No	0.05	3000
	Yes	0.05	4000
1/5000	No	0.04	4000
	Yes	0.04	5000

A part of this investigation is to test the friction parameters created for the erosion zone and see how this effects the runout for hazard planning. To investigate these parameters, the zone where erosion occurred, and masses were added to the flow needed to be identified as an erosion zone. The erosion parameters that are used for all the simulations are the same.

The parameter "Erosion density (kg/m^3)" was set to 1000, to represent water saturated snow. The "erosion rate (m/s)" was set to 0.050, that would indicate loose wet sediments. Since the observations along slushflow paths indicated erosion along the ground the "Pot. Erosion depth (per kPa)" was sat to 0.200, deep. "The critical shear stress (kPa)" would represent the amount of pressure needed for the flow to erode the snow along the path and was set to "low" 0,500 to represent the weakness of the saturated snow compared to sediments. The erosion depth was always sat to the same as the release fracture depth since it was observed erosion to the ground.

4.3.1 Release area

All the digitised release areas were tested in RAMMS, with the friction parameters describes in table 5. However, since the RAMMS model is designed for simulating debris flows, the release areas for the simulations must in some cases be adjusted compared to what is observed and mapped for the events. Even though the friction parameters are adjusted, RAMMS struggles with gentle slope releases. The trend of slushflow release areas show that these events tend to release in gentle slopes (Sund et al., 2020), compared to debris flows that normally releases in steeper slope over 20° (Imaizumi et al., 2006). If the observed release area is initiated in slope gentler than 10° is it recommended to create another release area to simulate the runout as described Skred AS (Kronholm, 2021).

This type of release area was made for the Oppdal event from (table 6). The release areas created for the simulations differ from the mapped events in this case. Here the release areas must be placed in more sensitive parts of the flow path, with a much steeper angle.

Table 6: Values from the differences of release areas between observations and calculated release used for simulations for the Oppdal event.

Oppdal	**Release area ID**	**Mean slope**	**Release depth [m]**	**Incline area [m^2]**	**Release volume [m^3]**
Observed release areas	"Øverst"	7,89	1	3987,2	3987,16
	"Øvest_full"	4,82	1	21141,36	21141,36
Simulated release areas	"Midt"	25,88	1,4/2,7	4438,6	6214,08/12872,03
	"Nedre"	47,56	1,5/2,9	4284,1	6279,21/12134

Based on the comparison of the observed release area and release areas created for simulating the runout of the event, new release areas for the Nålelva and Leirbotnvannet event was created. To create the release areas for the simulations the DTM's from table 3 is used to create a slope map in GIS, with the raster analysis tool "slope". A profile of the slope gradient

is also made for the slushflow release area to illustrate the steepness of the event. Sensitive parts of the path were tested, both the spatial extent of the release area and the location. The simulations made is described in appendix 1. This table also provide properties like “mean slope”, “Incline area”, “Release depth” and “Release volume”. To test the sensitivity of the location, simulations were generating using the same release volume (release depth and spatial extent) and parameterisation in three different locations, to compare the deposition.

4.3.2 Release depth

Since the function “block release” is used in all the simulations, the decision of the release depth is a significant part of the model input. The release depth input in the simulations is originally based on the interpolation of the snow depth for the location that is accessible in NVEs database Xgeo. The snow depth at the location in Bakfjorddalen on the day registered for the event was 43 cm. Since it is just an interpolation of the snowpack the fracture depth used is 50 cm, to be on the more conservative side, based on the typical terrain features of channels and depressions that slushflows normally releases in.

For the Nålelva event the snow depth from Xgeo, taken from the date of release, gives a snowpack depth of 94 cm. The release depth for the documented release simulations is 1 m. For simulations made with release areas created in more sensitive parts of the slushflow path some other release depths are used to compare the same volume with releases in different parts of the path. For the event in Leirbotn the snow depth for the area was registered to be 69,6 cm, and the release depth for the simulations are 0.70 m.

4.3.3 Erosion zone

When deciding the erosion zones for the simulations, signs of erosion to ground level was the main observation to decide the location for this zone. Kronholm (2021) describes that in some cases they added the masses from the erosion zone into the release areas. The difference between separating the release area and an erosion zone or add the eroded material into the initial release area are tested. In cases where the release area is defined in sensitive part of the slope, the erosion zone is defined as the areas where observations of eroded masses.

5. Results

This chapter presents the main results of this thesis. Firstly the parameter set established for use in RAMMS: Debrisflow for slushflow simulations is tested by replicating the same events (Kronholm, 2021). This data set is then extended and validated by modelling events at the three sites in this thesis: Bakfjorddalen, Nålelva and Leirbotnvannet. This includes documentation and observations from the field, as well as the digitisation of the different slushflow events as shapefiles in QGIS. For all the events the results of the digitised release areas and erosion zones are used as input in RAMMS. The output of these simulations is exported to QGIS and compared with the digitised extent of the runout. For the case of Bakfjorddalen, different methods for mapping and digitising release areas are tested. For the other two cases, where the release areas are in very gentle slopes, different release areas in the slushflow path are used to properly test the friction parameter set.

5.1 Reproduction of an established parameter set

The established parameter set (Kronholm, 2021) is based on the investigation of five different field sites. Some of the results from their simulations, presented as figures in their report, are reproduced in this project (Kronholm, 2021). The parameters that are used for the replication of the simulated events are described in table 3.

The results from this work show that it is possible to reproduce their events, using the same parameters and input files (release area and DTM's), with minor differences in the result (Figure 15 and 16). The main difference observed between the simulations is the spatial extent of the runout in the low velocity and shallow flow heights deposits. Observations from the different simulation (Table 3) indicates a smaller deviation from the steeper part of the path where the flow follows channels (Figure 16), and larger deviations in the gentle slope angles where the deposits spread out (Figure 15).

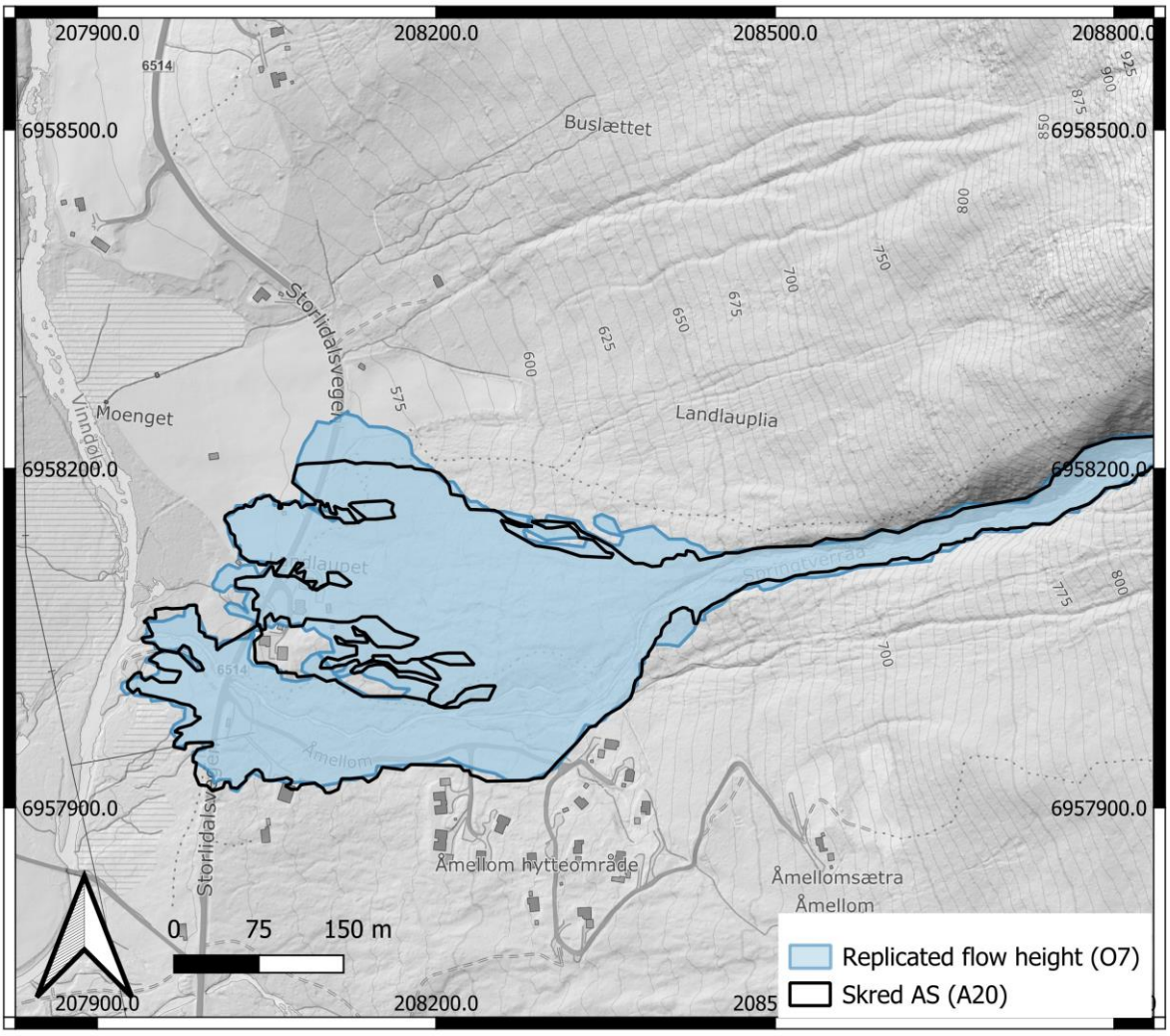

Figure 15: Comparison of the spatial deviation from the max flow height from the replicated event compared with the original event. The blue polygon is the output of simulation O7 table 3, from the Oppdal event. The black outline illustrates the original simulation of this event (Kronholm, 2021). Basemap is hillshade generated from DTM and "topografisk Norgeskart gråtone" from Kartverket.

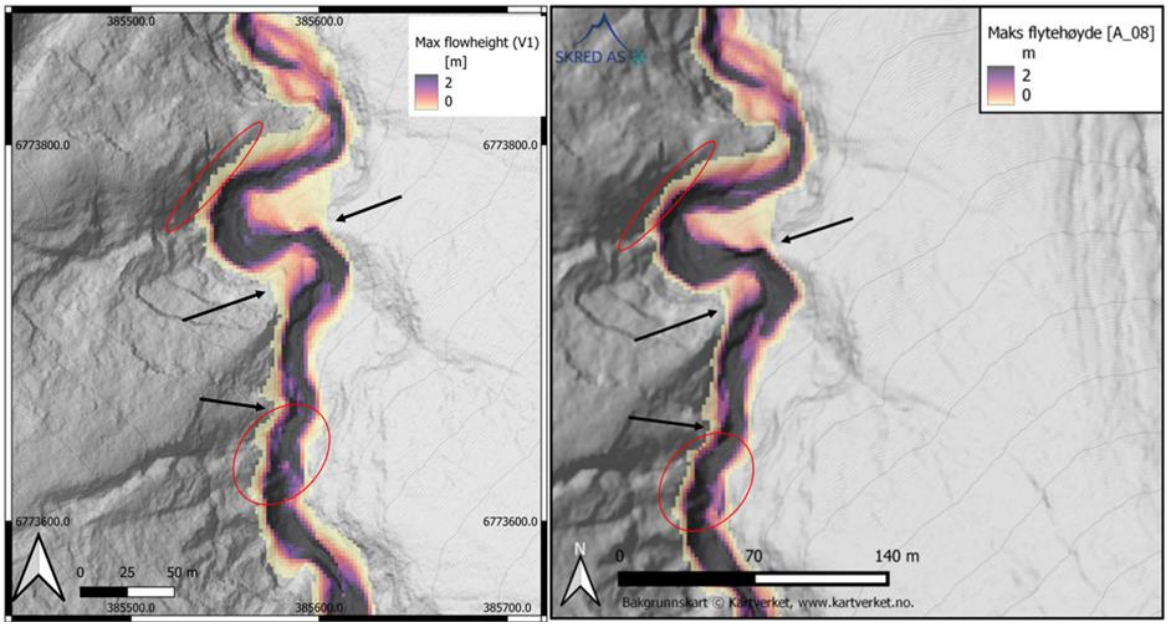

Figure 16: The figure is modified from Kronholm et. al 2021. The results from the simulations V1 (table 3) to the left, are compared to the figure from the original report. The red circles illustrate differences in the flow height for the two different models, with the same parameters and input files. Base map in the left figure, is a hillshade generated from a DTM collected from https://hoydedata.no/LaserInnsyn2/, with an overlaying map layer called "topografisk Norgeskart gåtoner» from Kartverket.

Even thought there was some differences in the spatial extent for low max flow heights, the higher impact flow values would match the original events (Figure 16 and 17). The max flow height would follow the same flow pattern, Figure 15, for the flow heights above 0,5m (yellow to red deposit) despite the differences in the spatial extent.

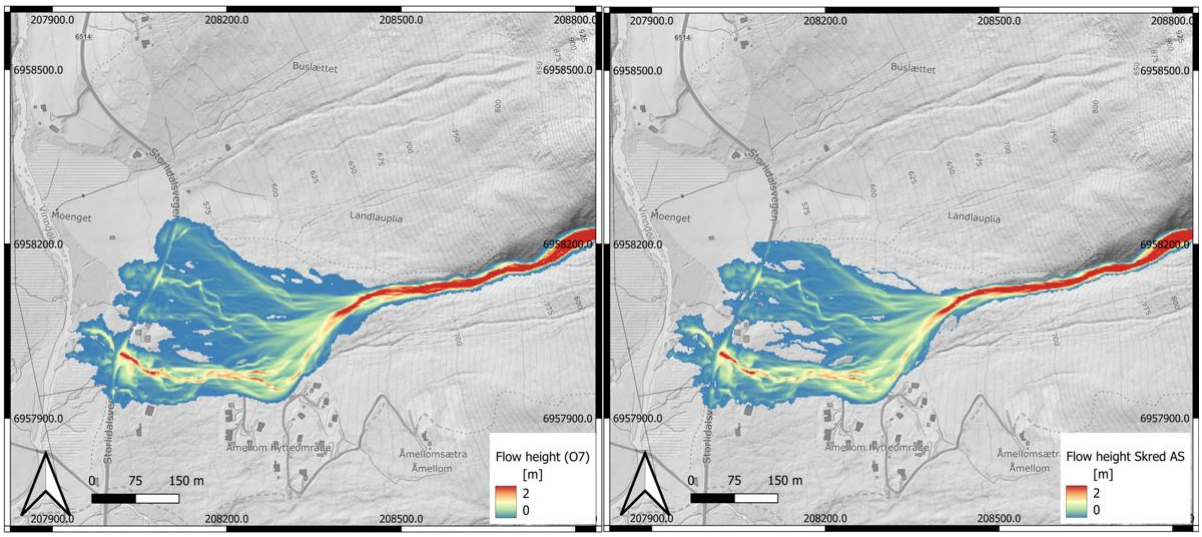

Figure 17: The figure to the left is the reproduced event of the Oppdal event. To the right hand side is the original event (Kronholm, 2021). The simulations are made with release area "nedre" with 1,5 m release depth, total volume of 6300 m^3. The parameters friction parameters used my = 0,08 and xi = 2000 m/s^2. Base map hillshade based on DTM from "Høydedata" and "Topografisk Norgeskart gråtoner" from Kartverket.

5.2 Parameter set validation

For the parameter set validation, the field sites are digitised based on the slushflow observations. The digitised release areas are simulated to validate the calibrated parameters set (Kronholm, 2021). The output of the simulations is compared with the digitised spatial extent of the event. In cases where the release areas are too gentle to simulate a realistic event, more sensitive parts of the slushflow path are used to define release areas.

5.2.1 Fv 889 Bakfjorddalen

The result from these events includes the process of defining the release and erosion area from field observation. The different input values are simulated, and spatial differences of the runout between different mapping scenarios are compared. The simulation results are also compared with observations from max pressure from the field.

5.2.2.1 Digitising

Observations of the spatial extent of the flow were made from drone documentation in the field and from desktop terrain data (Figure 18-20). The release area of the two is placed under the small lake. Observations of water saturated snow was identified on this lake (Figure 18). The largest event released and followed the channel, while the smaller event follows a less pronounces stream.

Figure 18: Documentation of Fv 889 Bakfjorddalen events. The identified release areas are outlined in red, erosion zone in blue and runout in black. On the flat area above the releases is the grey-blue area illustrating saturated snow marked with a light blue outline.

Both events were digitised outlining the runout, the release areas and erosion zone (Figure 18). Based on the field documentation the areas where the snow was removed to the bedrock, was divided into release area or erosion zone. The release area of the events was mapped initiating in the upper most part of the events. The transition over to the erosion zone was marked where signs of deposition on the channel sides is observed.

The full extent of the events shows that the slushflow deposits in the gentler part of the runout (Figure 19). The observation from this event shows that the erosion zones are more pronounced in steeper parts of the path, and that the event spreads out more in the gentler parts of the slope.

Figure 19: Overview of the total runout of the largest event, with the mapped area where erosion is observed down to the ground.

The field observations from these events are combined with terrain features from detailed DTM models and the two slushflow events in Bakfjorddalen were digitised with polygons in QGIS (Figure 20). The digitising is based mainly on drone images from different angles to analyse the full extent of the slushflow events.

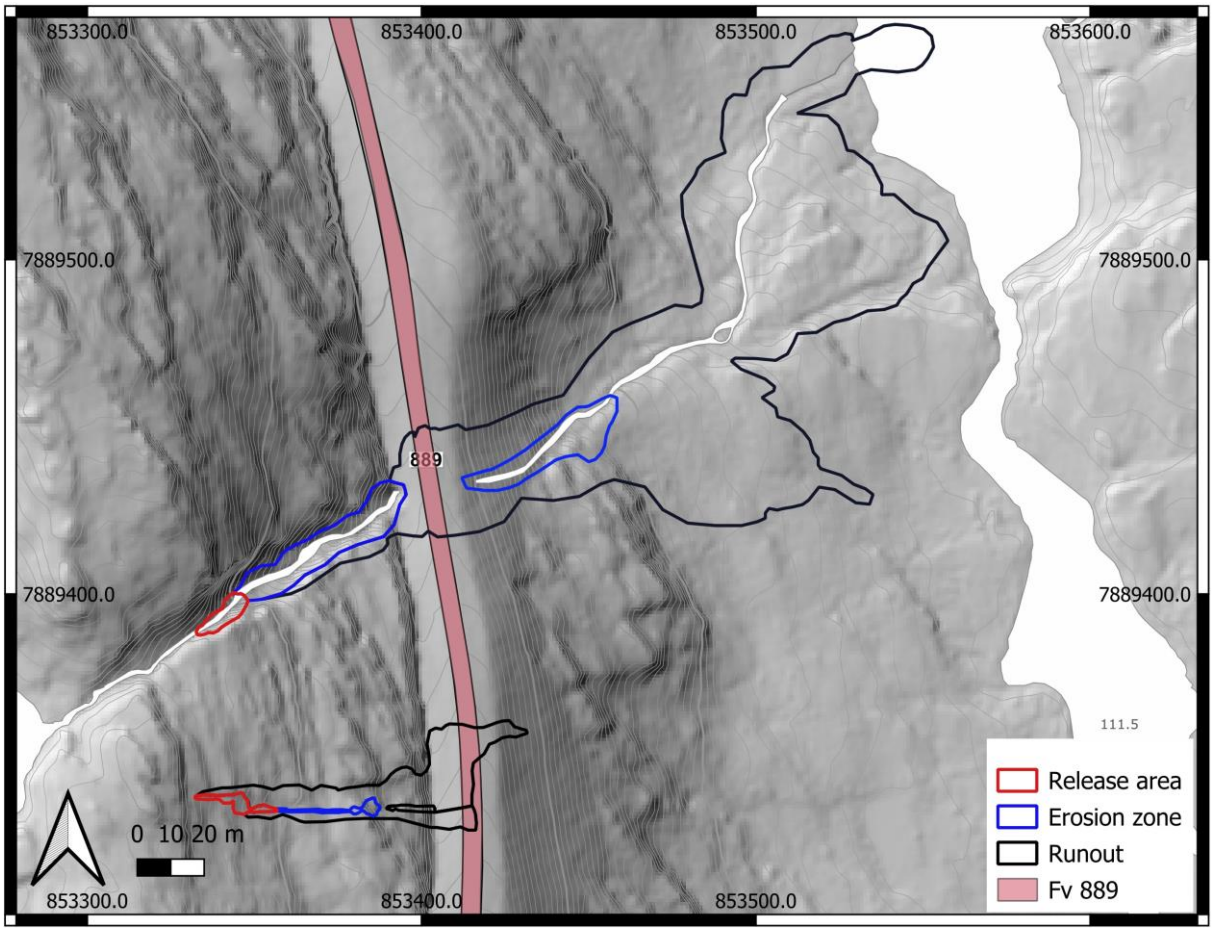

Figure 20: Digitised events crossing the road Fv 889 in Bakfjorddalen. The largest event crosses the road Fv 889 and follows the channel all the way to a flat part of the river. The red outlines the release areas, the blue outlines the erosion zones and the black outlines the runout. Basemap "Topografisk Norgeskart gråtoner" overlying hillshade generated from DTM from høydedata.

5.2.2.2 Simulation inputs

The release area input depends on the digitised spatial extent of the event. At this field site two different mapping scenarios were tested. The first scenario A (Figure 21, 22) separates the release area and erosion zones, as mapped for the documentation of the event (Figure 18). In release scenario B (Figure 21-23) the mapped release area and the erosion zone is now included as one release block. The second erosion zone for the large event (Figure 20) is still mapped as an erosion zone.

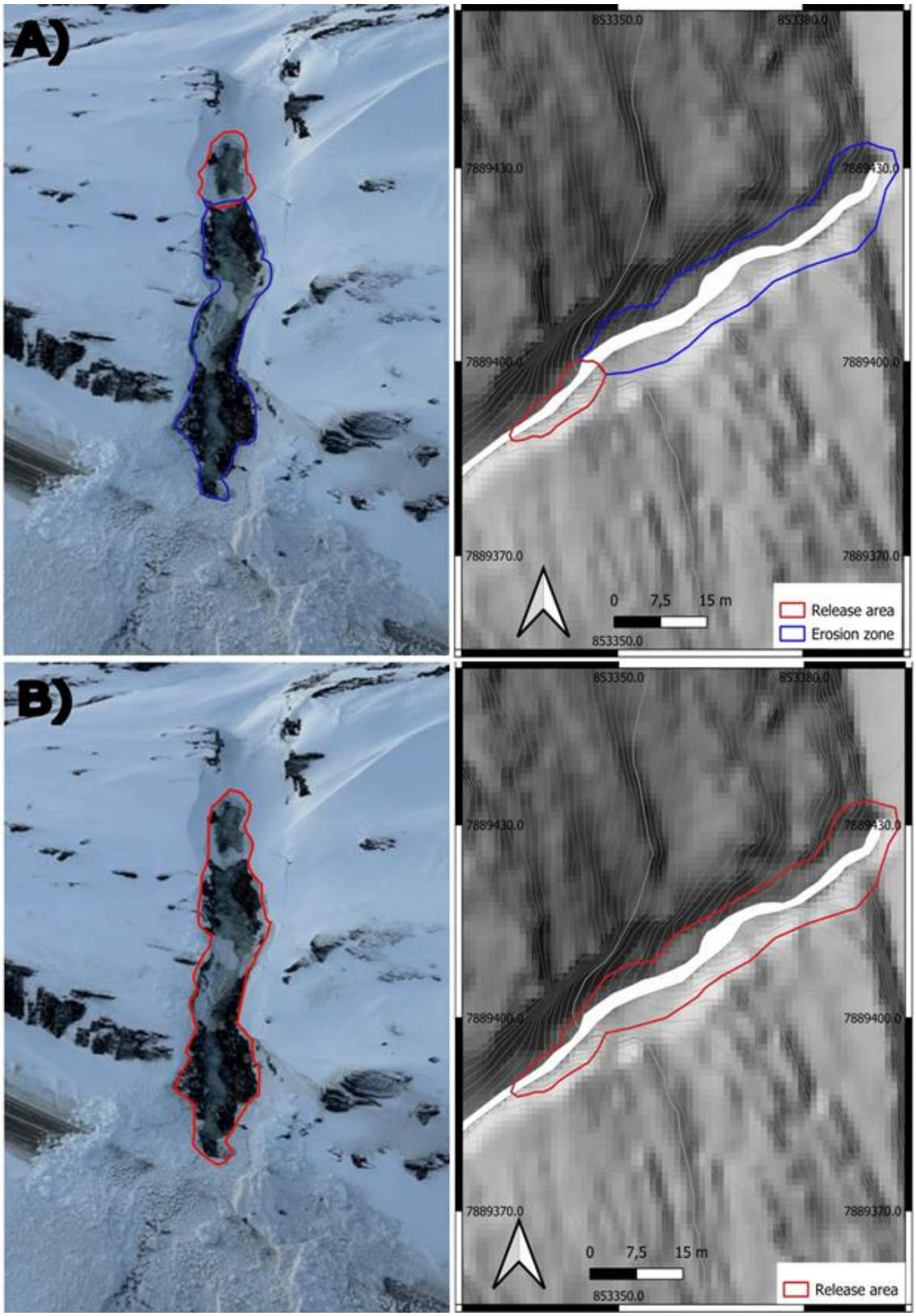

Figure 21: Mapped release areas, and erosion zone from the smallest event in Bakfjorddalen. The release conditions mapped in situation A divide the initial release of event and an erosion zone, where masses could be added at a later stage of the event.

The initial starting condition for the largest event had a mean slope angle for the release area, just above 30° (Table 7). The release depth for both release scenarios A and B was set to 0.5 m from Xgeo. However, the spatial extent of the release areas would be the largest difference between the two releasing scenarios. The total release volume for scenario A, would be 50 m^3 and scenario B would have a total release volume of 377 m^3.

Table 7: Release area properties for scenario A and B for the large event in Bakfjorddalen.

Scenario	**Mean slope angle**	**Inclined release area [m^2]**	**Release depth [m]**	**Release volume [m^3]**
A	34	103	0.5	50
B	31.8	754	0.5	377

The smaller event releases in a gentler slope (Figure 22) with a slope gradient of just above 20° (Table 8). The difference in the spatial extent for this event is not as extensive as for the larger event (Figure 21). With the same release depth of 0.5 m, the total release volume for scenario A be 43 m^3 and 90 m^3 for scenario B.

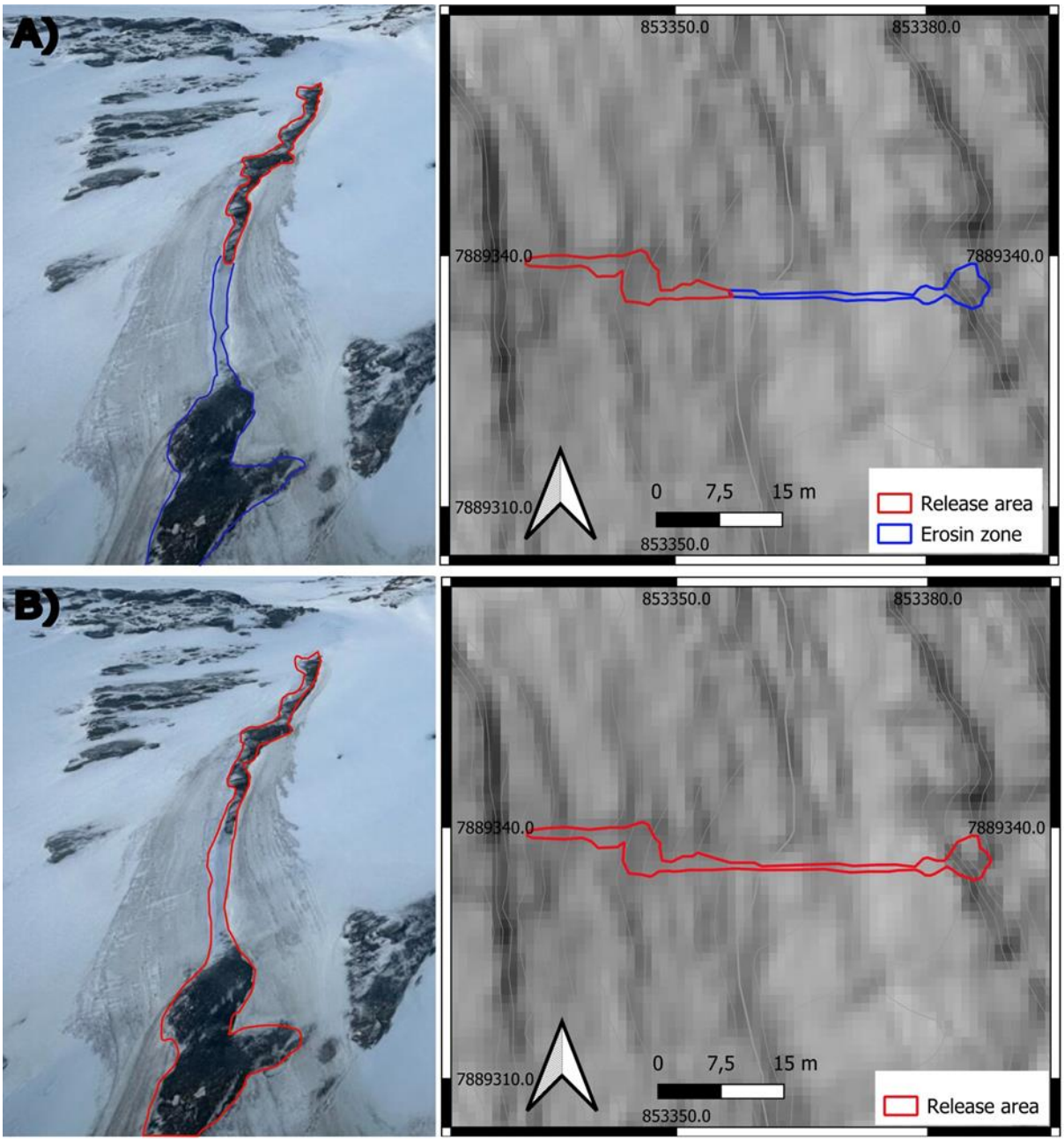

Figure 22: Mapped release areas, and erosion zone from the smallest event in Bakfjorddalen. The release conditions mapped in situation A divides the initial release of event and an erosion zone, where masses could be mapped at a later stage of the event.

Table 8: Release area properties for scenario A and B for the small event in Bakfjorddalen

Scenario	Mean slope angle	Inclined release area [m^2]	Release depth [m]	Release volume [m^3]
A	20.1	86.3	0.5	43
B	21	180.3	0.5	90

5.2.2.3 Simulation outputs

To validate the established friction parameter set described in table 1, both release scenario A and B were simulated (Figure 21, 22). All simulations were made with the release areas A and B, with a release depth of 0.5 m, to represent the average snow coverage of the area at the time of the event.

The simulations of scenario A (Figure 23), represents all simulations of the parameters representing the hazard zones according to the Norwegian regulations S1 (1/100), S2 (1/1000) and S3 (1/5000) (TEK 17, § 7-3), both including and excluding the erosion zone. Simulations made with the total release volume of the 50 m^3 for the large event, and 43 m^3 for the small event, resulted in a shorter runout length than the full extent of the event. However, the spread of the deposit would be larger, especially, for the small event (Figure 23).

The simulations made including the erosion zones, shows a longer runout than simulations without this variable. However, the simulations made with the friction parameters representing a return-period of 100 years, would in this case have a longer runout extent than the parameters used for the more vulnerable hazard zones (Figure 23). This result indicates that the combination of μ and ξ determined for 100-year return period would give the flow a higher mobility in this type of terrain than for 1000 and 5000-years events. However, results made with release scenario B follows the expectations for the total runout for the 100-year, 1000-year and 5000-year return periods (Figure 24).

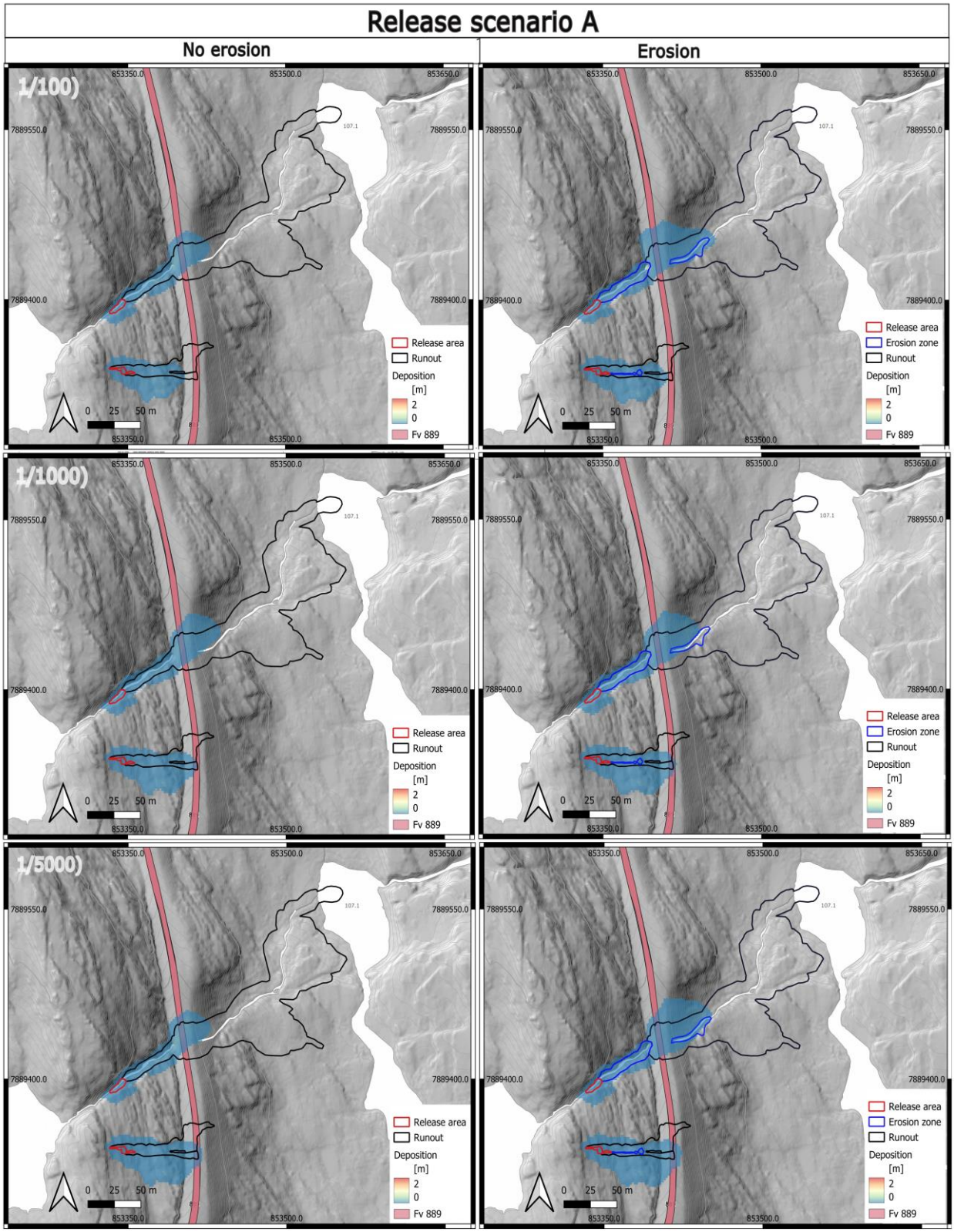

Figure 23: The friction parameter set is tested on release scenario A for the different return periods used for hazard planning according to the Norwegians laws. All event frequencies are tested with (right) and without (left) added masses in the flow path.

Simulations based on scenario B (Figure 21,22), resulted in a longer simulation runout than the observations of the event (Figure 24). The total runout length for the different hazard zones would match the observations more than with release scenario A (Figure 23). However, there are still some significant differences between the simulation outputs and the mapped event.

The mobility of the slushflow when the release is defined like scenario B allows the large slushflow event to follow in the ditch along the road, that has a gentle slope downwards toward the north. The total spread of the event is the largest deviation from the documentation of the event when the slope angle decreases, and the deposits spread out crossing the road. This spread increases when the combination of friction parameters symbolises the more vulnerable hazard requirements.

The total runout of the event with and without erosion, in all the different slushflow frequencies, would have a larger extent when reaching the flatter area and continue further when it reaches the horizontal river (Figure 24). The observations of the simulation deposits show they would accumulate at the end of this runout, with a slightly higher height of the deposit at the end of the lobe shape. This accumulation would differ from the observations (Figure 19, 25), where the deposit is at its highest in the transitions between steeper and flatter terrain (Figure 25).

The behaviour of the different friction parameters (Table 1) is as expected (Figure 24). The different friction parameter combinations result in a gradual increase of runout for the higher impact events. By adding erosion using the same release areas, the total extent of the events would also lead to a slightly longer runout for all the frequencies. The simulation results from the different hazard scenarios A and B, show a significant difference in the total runout length. By adding the erosion zone into the release area (scenario B), the runout length would significantly differ from release scenario A simulations with erosion.

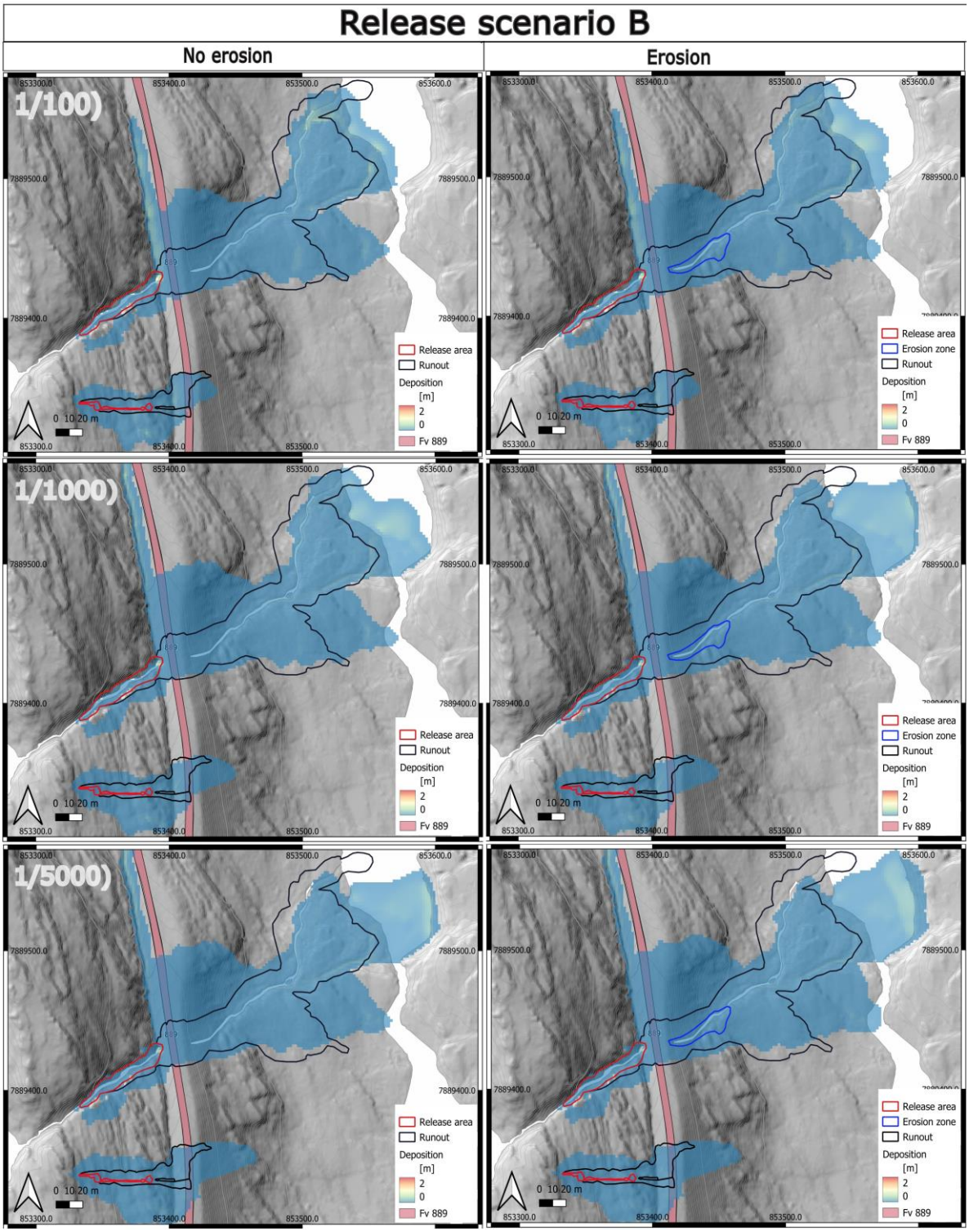

Figure 24: The friction parameter set is tested on release scenario B for the different return periods used for hazard planning according to the Norwegians laws. All event frequencies are tested with (right) and without (left) added masses in the flow path.

An important observation from the documentation of the events in the field was the displacement of three large vehicles (Figure 25). The observation of vehicles swept of the road, gives an indication of the pressure inside the dynamic process of the slushflow. The simulation output for the max pressure along the slushflow path, simulated for both release scenario A and B with (Figure 26) gives a realistic result for scenario B. The observations of the vehicles in the deposits also give a scale for the deposition height. In the transition from a steeper to a gentler slope towards the position of the third vehicle, it is possible to see signs of a levee of snow deposits, that also occur on the other northern side of the digger. These levee observations from the field are not shown in the simulation output for the deposition (Figure 24).

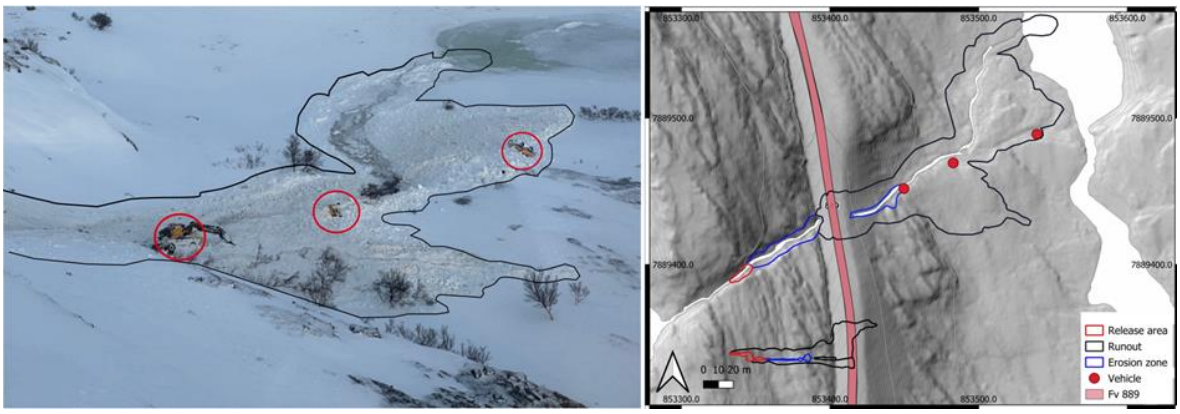

Figure 25: Transported vehicles along the slushflow path. Indicators of the max pressure of the slushflow event.

The pressure output from simulation of release scenario A and B for yearly frequency of 1/100 (Figure 26) strengthen the credibility of the input values for scenario B. The pressure output from this scenario shows a maximum pressure (250 kPa) that would be capable of displacing the vehicles.

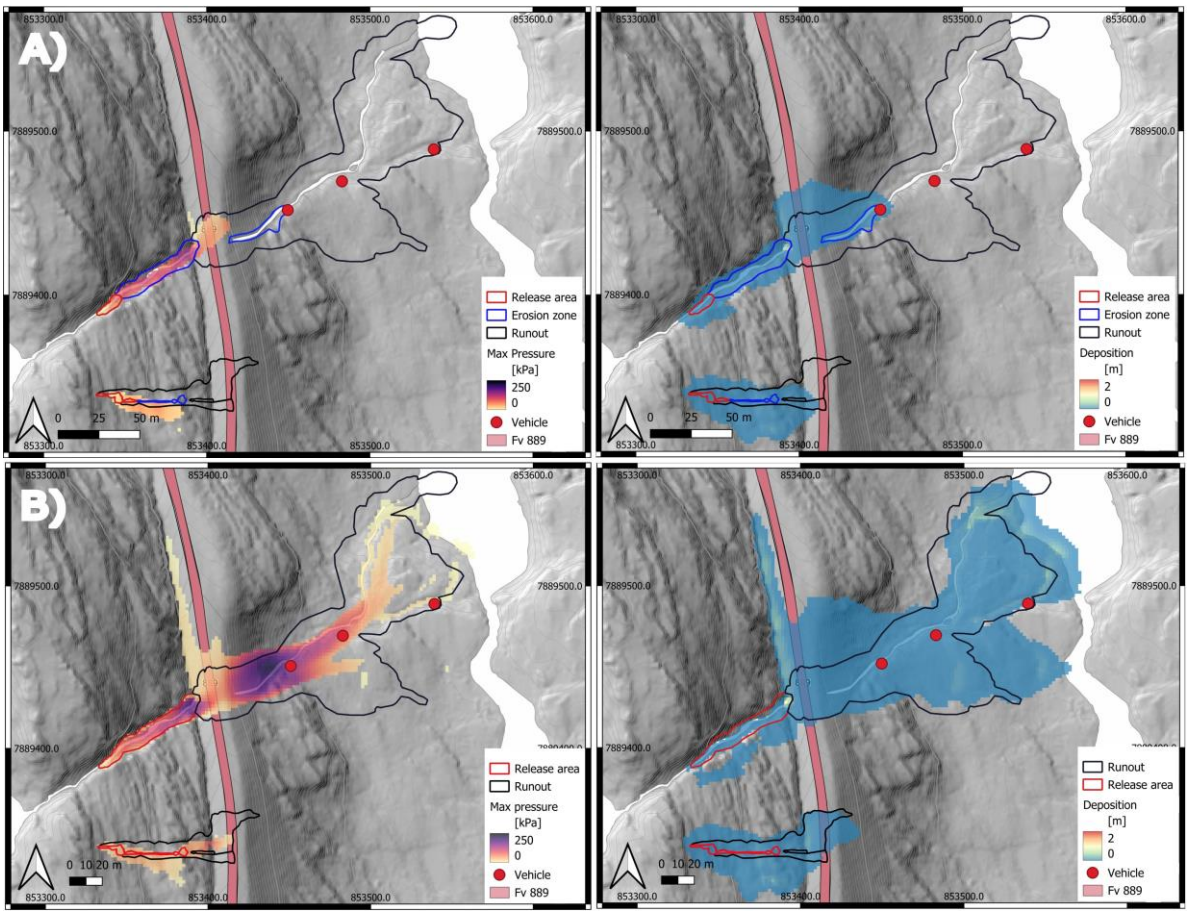

Figure 26: The simulations show the difference in release condition A (simulation B2 and B22) and B (simulation B7 and B27). Here both events from Bakfjorddalen is illustrated. The maximum pressure and deposition are illustrated for both releasing conditions. Where the red points illustrate the vehicle that was moved from the road along the slushflow path. The parameter set used in the simulations would equal a frequency of 1/100, A with erosion μ=0.08 and ξ =2000 m/s^2, B without, μ=0.08 and ξ =3000m/s^2. The snow depth used in both simulations are 0,5m.

Since the simulation output for the release scenario A, does not give a comparable runout of the actual extent of the event (Figure 23, 26), different input variables for the release depth were investigated (Figure 27). Due to the terrain features within the release area (Figure 14), the possibility of snow accumulation is high. The release depth was adjusted to 1 m. By changing the release depth for the events (Table 9) the runout changed significantly. The volume change resulted in a longer, more expansive runout. The flow pattern between scenario A and B still varies for the two scenarios.

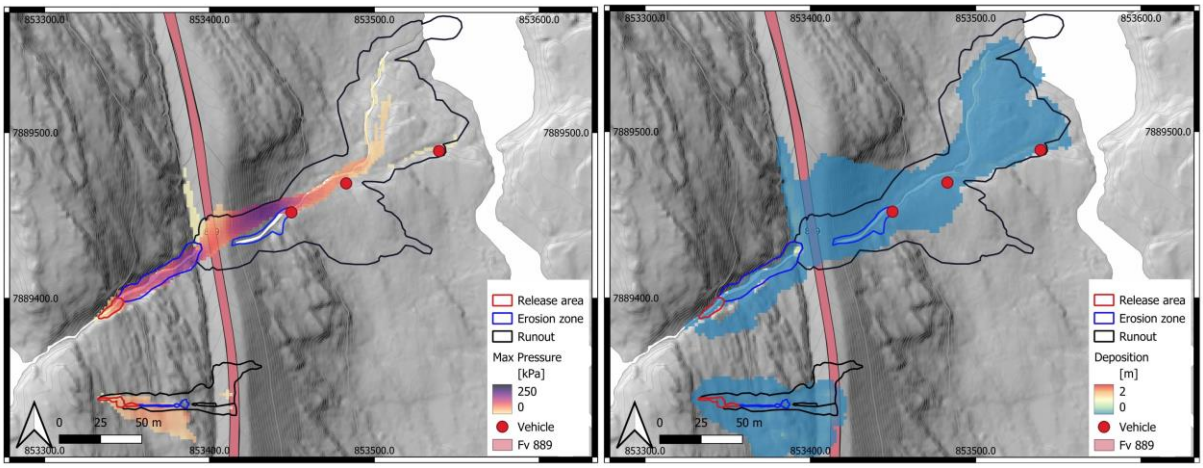

Figure 27: Release scenario A simulated with 1 m fracture depth, with μ=0,08, ξ = 3000 m/s^2.

Table 9: Simulation parameters for release scenario A for both events.

Event	Release volume [m^3]	Release slope angle [°]	Release depth [m]	Friction parameters		Erosion	Erosion depth [m]
				μ	ξ [m/s^2]		
Large	103,9	34	1	0,08	3000	yes	1
Small	86,3	20,1	1	0,08	3000	yes	1

The simulations generated by changing the location of the release area, but keeping the volume and parameter constant, gives significantly difference in the results (Figure 28). The location of the release furthers down in the channel (Figure 28a) would follow the channel terrain features more, then when the release area is located further up in the channel (Figure 28c) closer to the observations of the saturated snow.

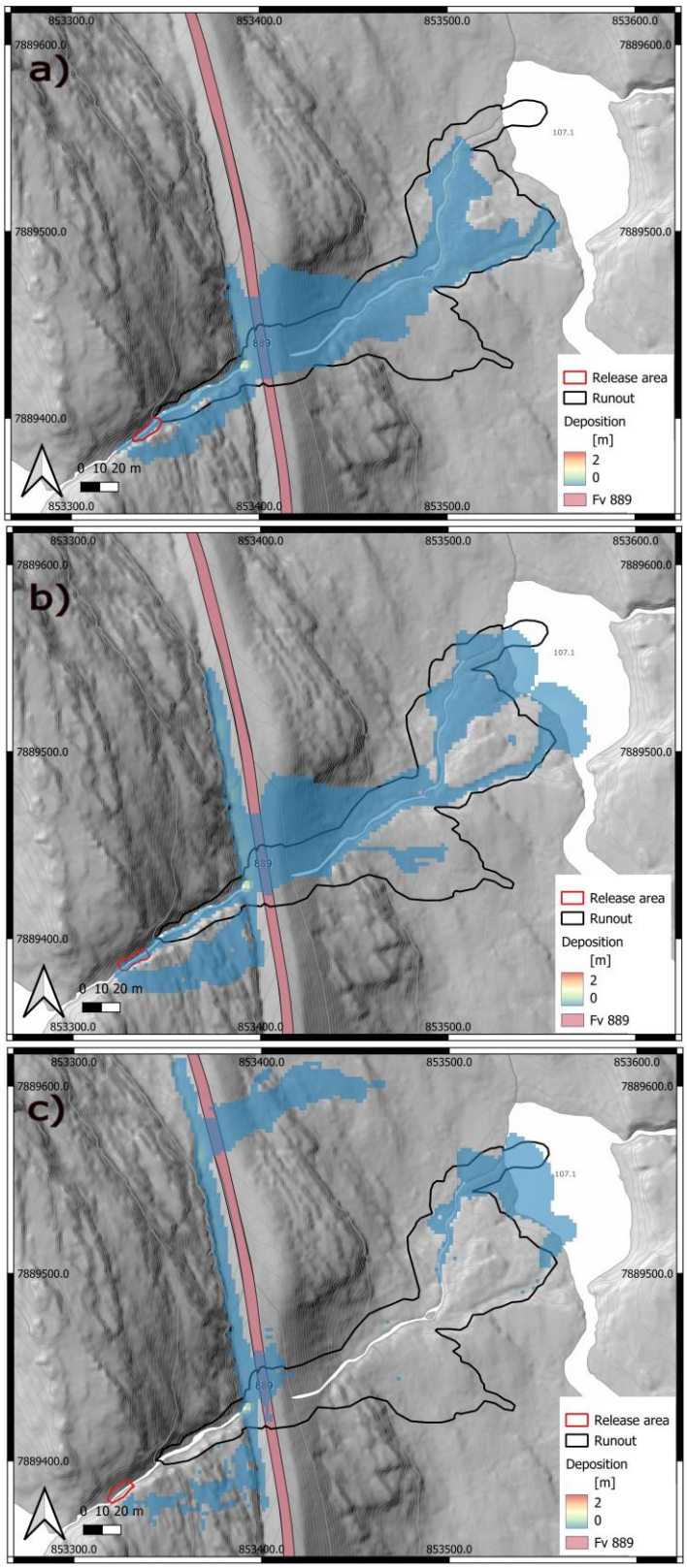

Figure 28: Different locations of the release area were tested to investigate the sensitivity of the decided location. Total release volume for all three release areas was around 100 m^3, the friction parameters used for the simulations μ=0.08 and ξ= 2000 m/s^2.

5.2.2 Fv 7962 Nålelva

The Nålelva event was visited in the field and the digitising is based on the field observations of release area, deposition, and some indications of the maximum flow height. Since this event released in a gentle slope, there have been several release areas created to simulate this event in the process of validating the friction parameters.

5.2.2.1 Digitising

A combination of high resolution DTM and drone documentation from field is used during the digitising of the event (Figure 29-31). To identify the vulnerability in the area the infrastructure and houses were identified. All the identified features are digitised into shapefiles in QGIS. One interesting observation from field, was some snow deposit from surface meltwater (Figure 29). This could potentially have been the initiation mechanism of the slushflow release. Since this snow deposit is released in a very gentle slope from a point release, is it not possible to simulate this flow in RAMMS:Debrisflow. The release area of the event was digitised where the snowpack collapsed to the ground (Figure 29).

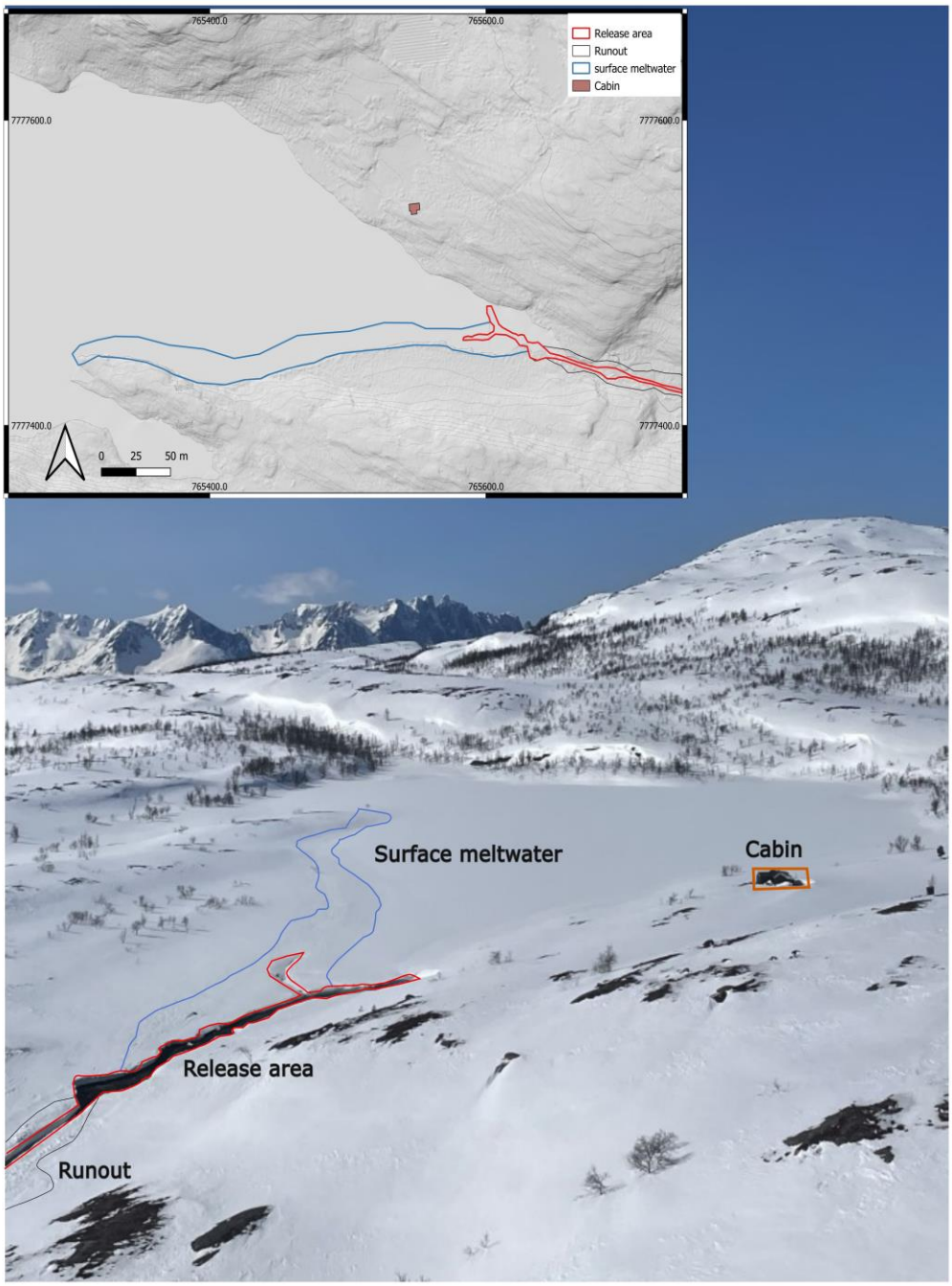

Figure 29: Documentation of the slushflow event in Nålelva. Deposit of flow on top of the snowpack was observed on the lake over the release areas for the slushflow event.

The release area transitions into an erosion zone, while deposition is observed on the sides of the eroded channel (Figure 30). Where the slushflow flows to the peat, a large area of blue-grey water saturated snow is observed. This is an indicator of high water-content in the snowpack, which implies low shear strength of the material and so the flow runs further down slope.

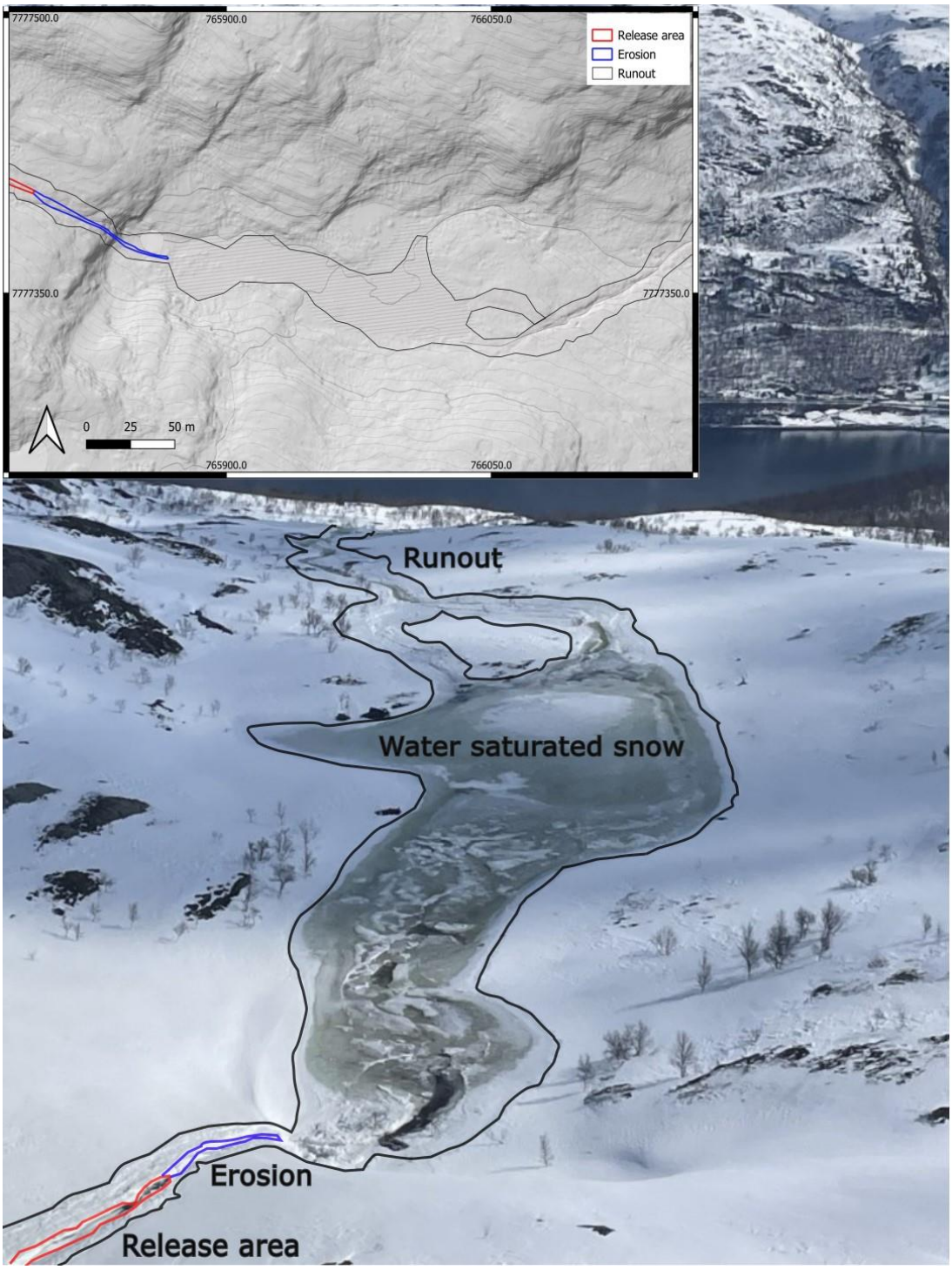

Figure 30: Overview of the water saturated snow under the release area and erosion zone of the slushflow, further down in the slushflow path.

The slushflow entrain a lot of sediments, when the slushflow crosses the Fv 7962 the deposits have turned brown (Figure 31). The shape of the deposit also changes with the deposition mixture. At the end of the runout lobe shapes are observed, with higher viscosity material. In the upper part of the path the material deposits indicate like fluid deposition (Figure 13). The runout outline from this event shows the clear pulse movement of the flow (Figure 30, 31).

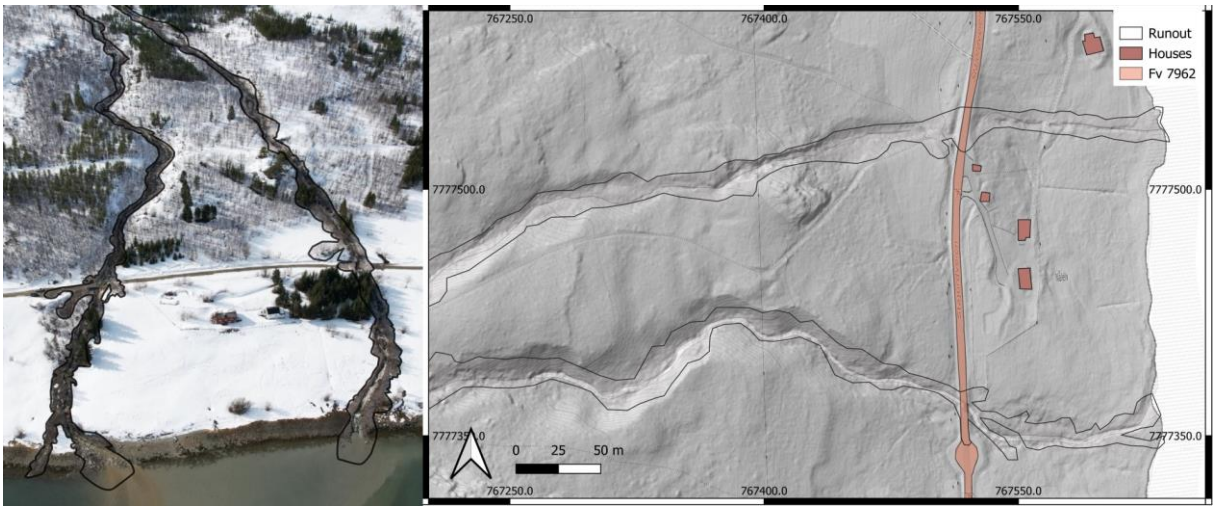

Figure 31: The deposition of the flow in the bottom part of the event. The deposition in the photo to the left contains more sediments and organic material then deposits further up in the slushflow path. On the right side the runout is mapped according to the vulnerably infrastructure and residents.

The observations of the dark sediments crossing the road (Figure 32) indicates entrainment of sediments along the slushflow path. The change in composition indicates an erosion depth deeper than the snow in the area.

Figure 32: Observations of slush-debris mixture crossing the Fv 7962. This figure shows extent of the event when crossing the

5.2.2.2 Simulation

The documented release area, with a mean slope angle of 3.5°, was simulated with the friction parameters for a 1/1000-year event (Table 10). The simulated runout for this event, is significantly shorter than the field observations (Figure 33), where the simulated runout wouldn't move past the water saturated peat (Figure 31).

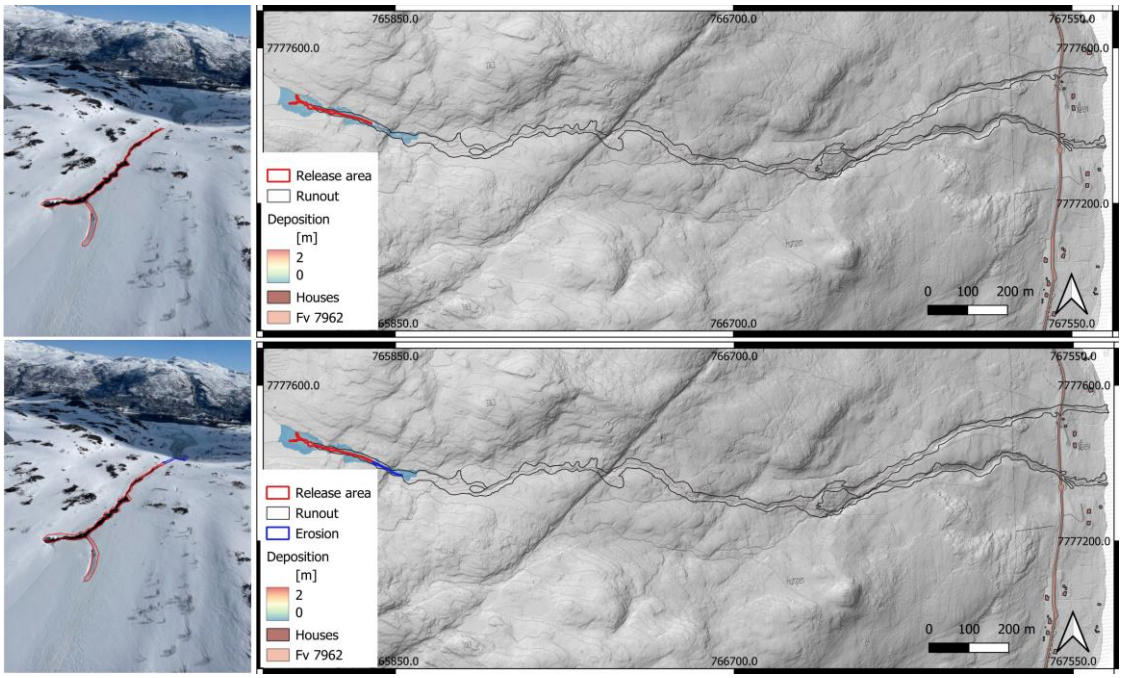

Figure 33: Documented release area and erosion zone, simulated with the friction parameters of 1000 years frequency events.

Table 10: Parameters used for simulating the documented event at Nålelva for 100-, 1000- and 5000-years events.

Type of release	Frequency	Erosion	Mean slope [°]	Incline area [m^2]	Release depth [m]	Release volume [m^3]	Friction parameters	
							μ	ξ
Observed release area	1/100	no	3.5	311	1	762	0.08	2000
	1/100	yes	3.5	311	1	762	0.08	3000
	1/1000	no	3.5	311	1	762	0.05	3000
	1/1000	yes	3.5	311	1	762	0.05	4000
	1/5000	no	3.5	311	1	762	0.04	4000
	1/5000	yes	3.5	311	1	762	0.04	5000

The simulations of the documented release area, with a total release volume of 762 m^3, gave a significantly shorter runout than the observations (Figure 34). All the simulations deviated from the observations. However, there were some differences in the runout length between the different friction parameter combinations. The simulations generated with erosion zones do not differ from the simulations generated with. This indicates that the threshold values of mass entertainment are not met and could either be caused by the total volume or the slope gradient of the path. The runout would stay the same even with a constant μ value, but a slightly different ξ value (Table 10).

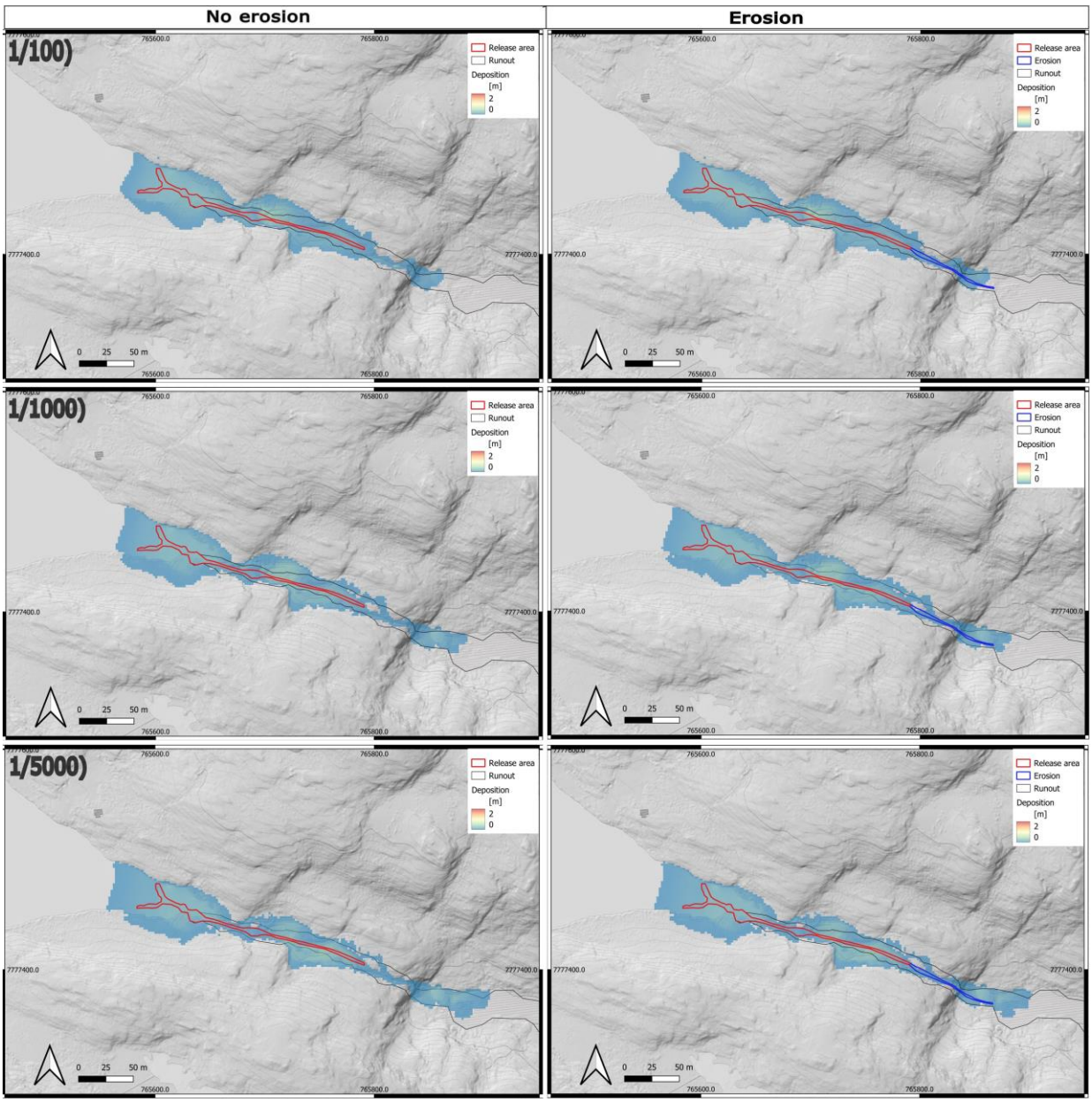

Figure 34: The friction parameters are tested on the observed release area (red outline) of the event. The observed area of the event, multiple with the interpolated snow depth would give a total release volume of 762 m^3. All friction parameters developed for slushflow modelling have been tested, both with (right) and without (left) erosion.

Since the mean slope of the documented release area only had a slope angle of 3.5 °, other release areas were tested in more sensitive parts of the slushflow path. In table 11 the two of the different release areas that are illustrated in Figure 31 is described. Both simulated events had a total release volume of around 3400 m^3 and was tested for the 1/100 and 1/1000 parameter sets without erosion. However, the difference in slope angle was almost twice between A and B, with a mean angle of 11 °, and C and D, with a mean angle of 20 °.

Table 11: The properties and friction parameters for release areas used to test the simulation sensitivity at Nålelva

Figure	Type of event	Erosion	Mean slope [°]	Incline area [m^2]	Release depth [m]	Release volume [m^3]	Friction parameters	
							μ	ξ
35 a	Simulated	no	11.3	1874	1,8	3373.2	0.08	2000
35 b	Simulated	no	11.3	311	1,8	3373.2	0.05	3000
35 c	Simulated	no	19.9	213.6	1	3412	0.08	2000
35 d	Simulated	no	19.9	213.6	1	3412	0.05	3000

The max flow height of these simulations (Figure 35) is compared with the observations of flow height from field. The upper most release area (Figure 35 a-b) has a smaller surface area than the lower release area (Figure 35 c-d). To simulate the same volume, different snow depths have been used and are 1.8 m and 1 m (Table 11). This could potentially affect the way the slushflow moves in the terrain for the uppermost event compared to the lower event, simulated with a snow depth that would match the accessible data from the area. The red point in the runout, indicates the vertical observation of the flow height of 2 m (Figure 9). The first release area would reach the road with the parameters developed for 1000-years return period events (Figure 35a-b). The runout would follow the terrain as the actual event did with a relatively high accuracy in the upper part. The lower release (Figure 35 c-d) would have a larger amount of material accumulated around the defined release area, than when the release area is localized further up in the path. This causes both the simulations of 1/100 and 1/1000, to reach the road where the vulnerable infrastructure and houses are located.

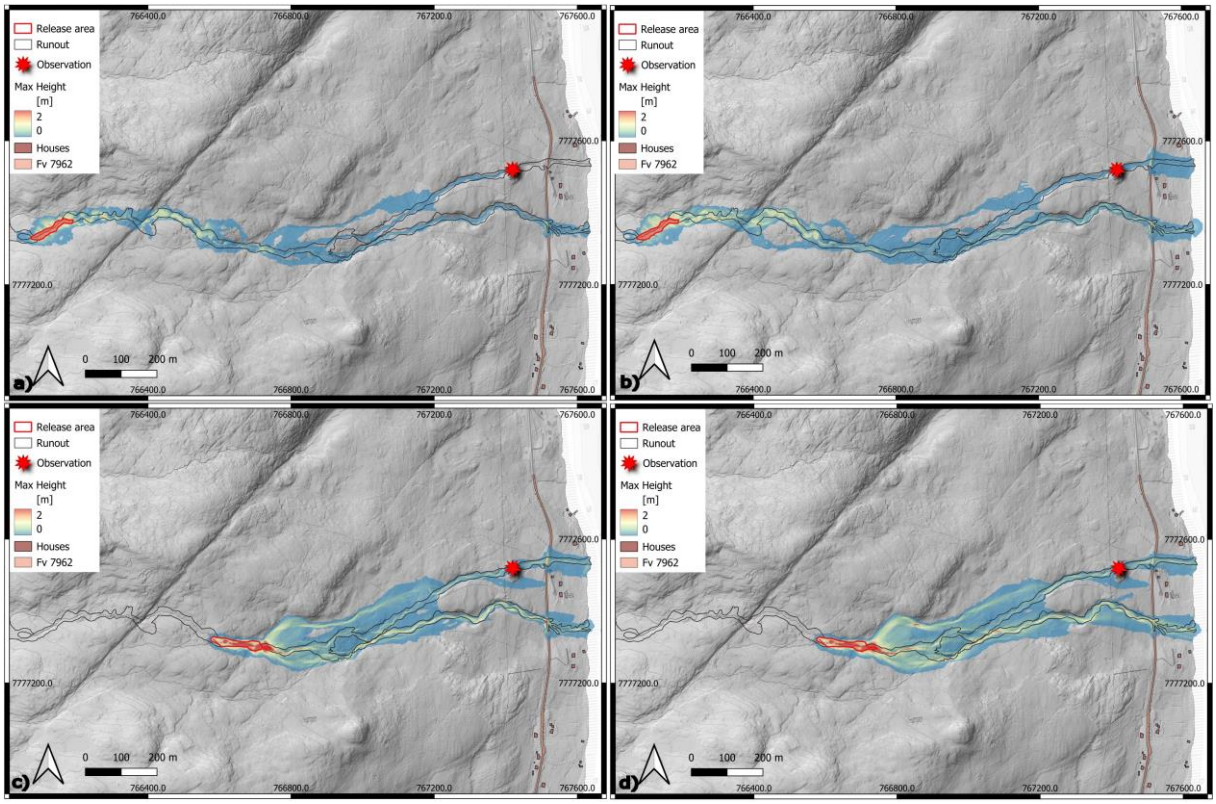

Figure 35: All four simulations are simulated with a volume around 3400m^3. The simulations show the difference of the friction parameter set for 100- and 1000-years events for different locations, slope angle and fracture depth for the initial release conditions.

Similar release scenarios as mapped in Bakfjorddalen were also tested for the Nålelva event. Since the snow was mostly eroded to the ground in the channel where the event was observed, a mapping scenario with scenario A, was to map the release area in the areas where snow was removed in the channel, and transition into erosion zone after the flatter area in the path (Figure 36). In scenario B the whole area is defined as the release area for the event. The simulation of scenario A was simulated with a release depth 1 m with a total release volume of 3038 m^3, while scenario B was simulated with release depth of 0,5 m and ended up with a total release volume of 6329 m^3 (Table 12).

Table 12: Release area properties and friction parameters for simulations of test release areas.

Figure	Type of event	Erosion	Mean slope [°]	Incline area [m²]	Release depth [m]	Release volume [m³]	Friction parameters	
							μ	ξ
A	Simulated	yes	12.2	3038	1	3038	0,08	3000
B	Simulated	no	17.9 12.2	9621.2 3037.7	0.5	6329.4	0,08	2000

The release scenario B, Figure 36, would follow the slushflow path in the upper part of the terrain slightly closer to what is observed in this event, than scenario B. However, when the slushflow crosses the road the simulated release scenario A would have a more accurate extent than scenario B, that would have deposition that would overflow in the middle part of the slushflow path and have twice as large extent crossing the road. In this simulation scenario, one of the houses would be affected by the slushflow, that was safe during the actual event.

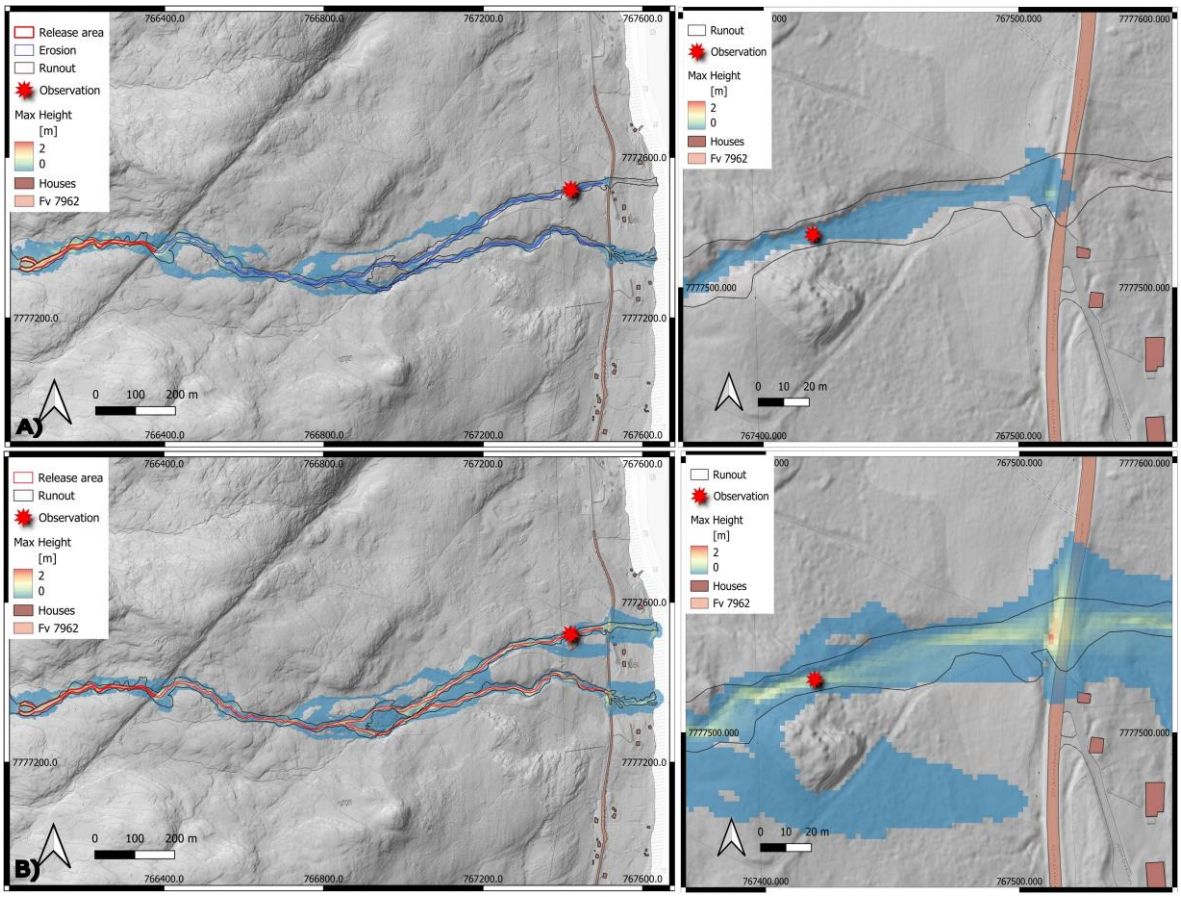

Figure 36: Shows the difference in the flow height when the release area is following the channel and developing to an erosion zone where masses are added along the flow path, compared to using the channel as a release area. Both simulations are simulated with μ=0,08 while A is simulated with ξ = 3000 m/s2, and B ξ = 2000 m/s2, both friction parameters for a 100-year return period.

5.2.3 E6 Leirbotnvannet

The Leirbotn event was the event that released in the gentlest slope of the investigated events. It was also the event with the longest observed runout, which resulted in a lower resolution simulation. Because of the continued supply of water and low gradient runout, there were some challenges generating output matching the observations of the event.

5.2.3.1 Digitising

The digitising of this event is based on drone videos, where some important features are mapped (Figures 37, 38, 39). The initiation area of the release was observed under a water-saturated bog (Figure 37). The transition from observations of the release and the wate saturated area indicated just a small change in the slope angle.

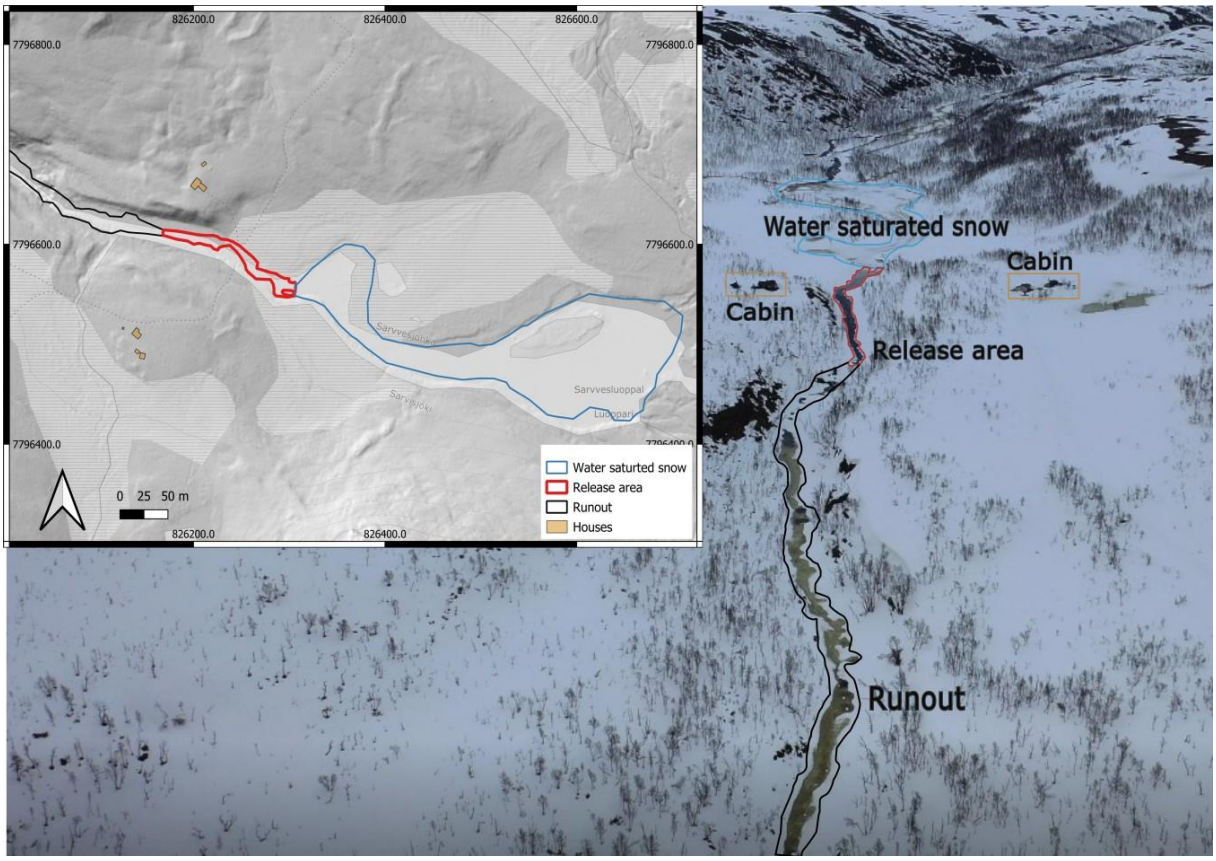

Figure 37: The observation of possible initial starting area of the slushflow event. In the photo taken by Trond Jøran Nilsen from TFFK, it is possible to see that the river has saturated the snow in the lake/bog area (blue), has initiated a slushflow release right below. The houses close to the event are mapped with yellow, release area outlined with red and the runout in black.

When the slushflow, followed the river valley it entrained masses from the slush and river ice. As the slushflow accumulated ice flowed downslope and started deposits on the trafficked road E6 (Figure 38). The bridge that was also affected by this slushflow. There were also cabins close to the event that potentially could be vulnerable to similar events in the future.

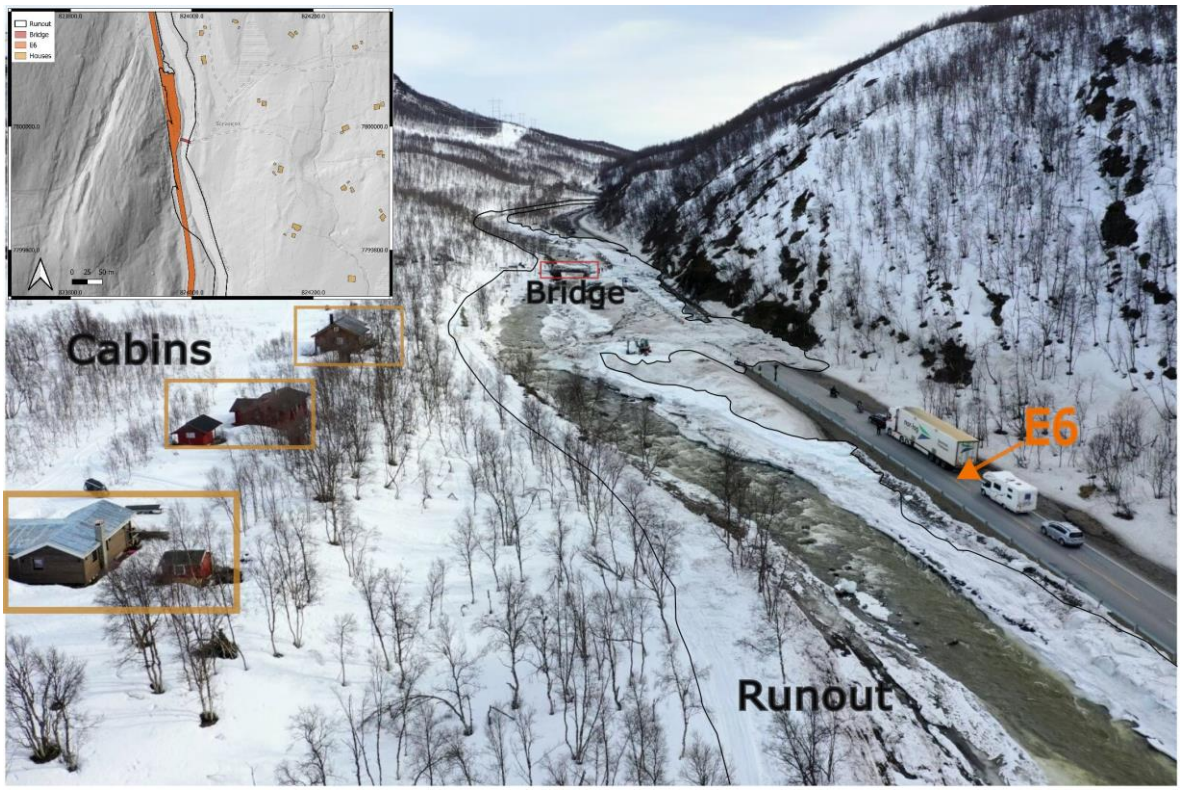

Figure 38: Photo from Trond Jøran Nilsen where the deposits flow over the marked bridge in red, and deposits on E6. Cabins close to the event is marked with yellow. The digitised event is shown in the map in the left-hand side.

The slushflow deposited as a lobe shape deposit, entrained two cars (Figure 39). These cars have been transported with the slushflow from either the parking where the deposits started to move along the road, or they have been transported from parking connected to some of the cabins along the slushflow path. Another interesting observation is how the high mobility spread threatens the house (Figure 39).

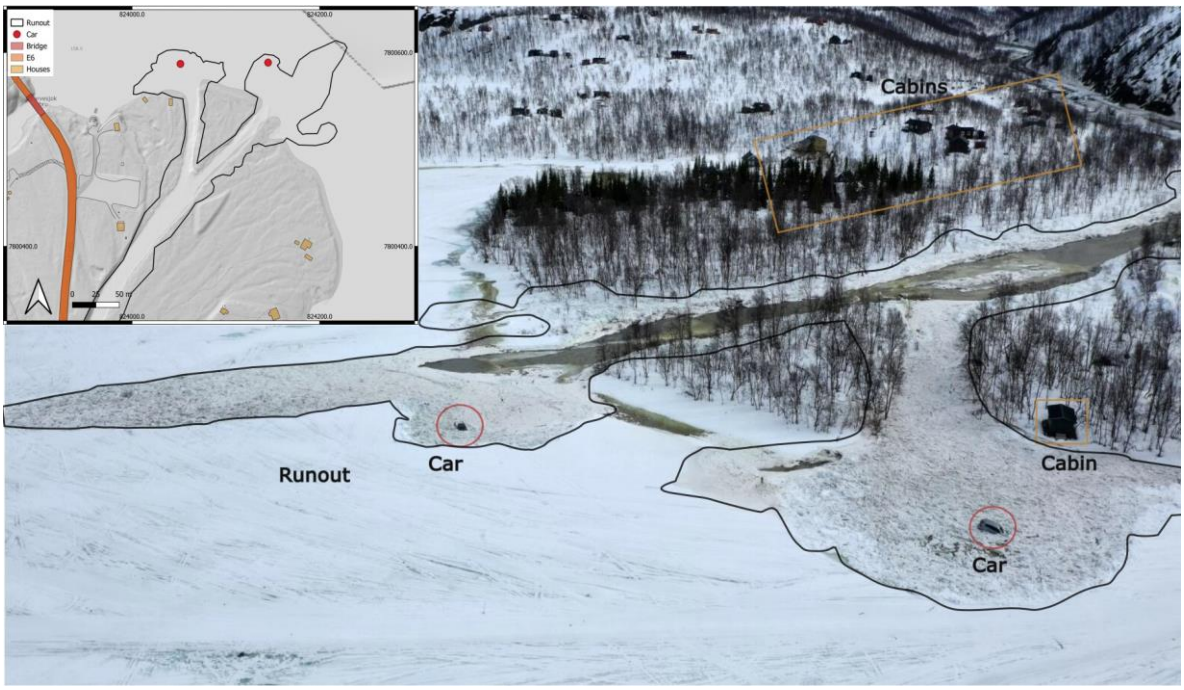

Figure 39: Photo from Trond Jøran Nilsen. The figure shows the lobe shaped deposit on Leirbotnvannet. The cabin close to the runout is marked with yellow to indicate the potential risk. The cars are marked with red circles and is probably transported from either the road or a parking lot.

The digitised event shows how the slushflow moved downslope through the terrain over a large distance, passing vulnerable areas, along a trafficked road (Figure 40). The force during this event is illustrated with the red points in the end of the runout that symbolize the displacement of the two cars.

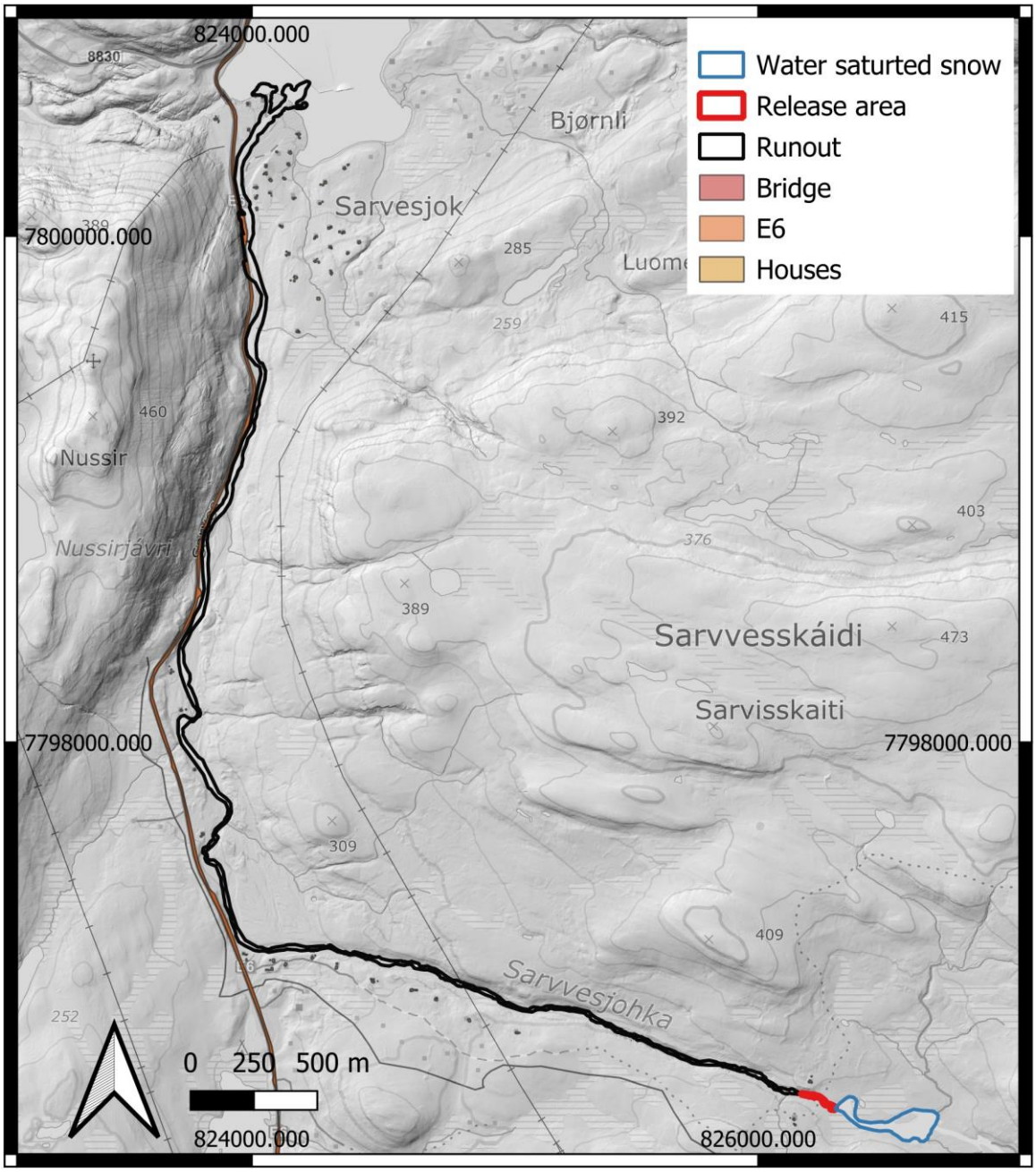

Figure 40: Digitising of the Leirbotnvannet event where signs of slushflow release are observed far up in the valley.

5.2.3.2 Simulations

Important information that was observed in field was the entrainment of masses along the slushflow path (Figure 41). The flow in the upper part of the slushflow path was mainly slush (Figure 41.1). Moving down slope large amounts of ice were added to the flow (Figure 41.2), resulting in a change of flow height, form 0.5m to above 2m crossing the bridge (Figure 41).

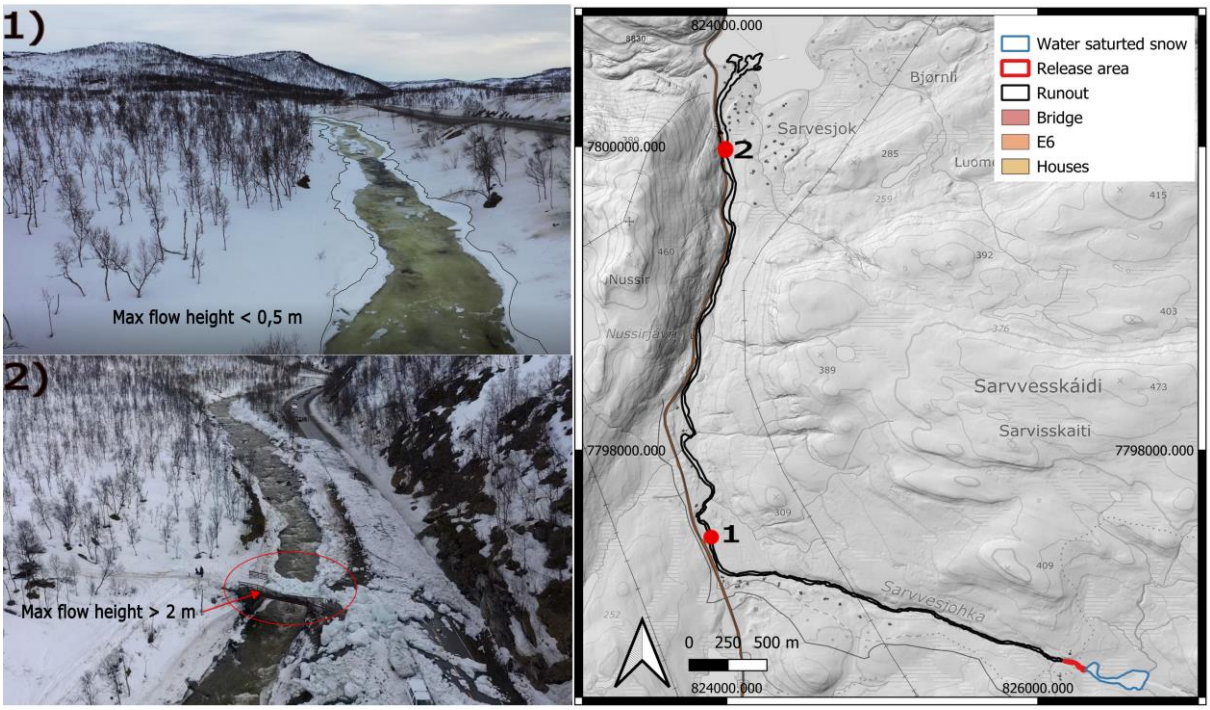

Figure 41: Observations of flow heights different parts of the slushflow path.

The simulation of the digitised release area was, as expected, challenging due to the low release angle of the event, with a mean slope angle of 1.3 °, and a total release volume of 1040 m^3 (Table 13). The initial release with the friction parameters for 1/100, 1/1000 and 1/5000 gives a small different in the runout distance (Figure 38).

Table 13: The documented release properties and friction parameters for simulation of 1/100, 1/1000 and 1/5000 years events.

Type of release	Erosion	Mean slope [°]	Incline area [m^2]	Release depth [m]	Release volume [m^3]	Friction parameters	
						μ	ξ
Documented	no	1.3	1468	0.7	1040.3	0.08	2000
Documented	no	1.3	1468	0.7	1040.3	0.05	3000
Documented	no	1.3	1468	0.7	1040.3	0.08	2000

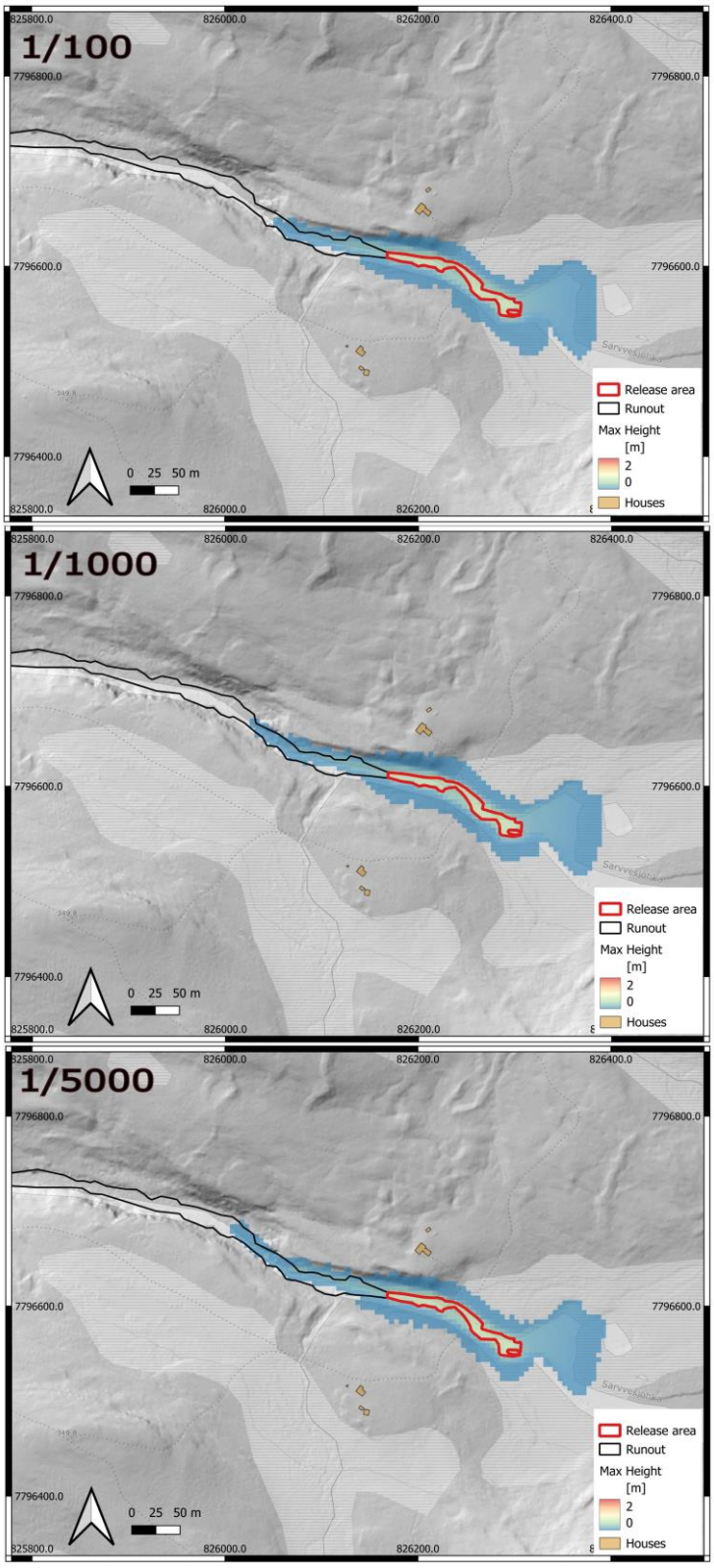

Figure 42: Simulations of documented release areas, with the different return periods for 100, 1000 and 5000 years events. The simulation shows the max flow height during the event.

Since the slushflow released and moved down a gentle slope it was almost impossible to choose a release area that would create a runout matching the observations from the field documentation. In this case different release areas were tested, and the lowest friction parameter set without including erosion was used. The simulation of the release area where it evidences of mass entrainment was observed matches the digitised runout to some extent, with a slope release of 1.9° (Figure 43). Different release depths were investigated to see how this parameter would affect the extent of the event (Table 14). The simulation generated with the accessible information about the snow depth of 0.7 m gives a more realistic result then simulation generated with a 1 m snow depth (Figure 43). By changing the input parameter of the flow height with 30 cm, the spread of the slushflow in the terrain change significantly. This would change the vulnerable areas of an event, and the hazard situation for one of the cabins would increase. None of the simulations generated of this event matched the observation of max height in Figure 41, or max pressure in Figure 39.

Table 14: The properties and friction parameters for release areas used to test the release depth for the Leirbotn event.

Erosion	Mean slope [°]	Incline area [m^2]	Release depth [m]	Release volume [m^3]	Friction parameters	
					μ	ξ
no	1.9	5120.8	0.7	3584.6	0.04	4000
no	1.9	5120.8	1	5120.8	0.04	4000

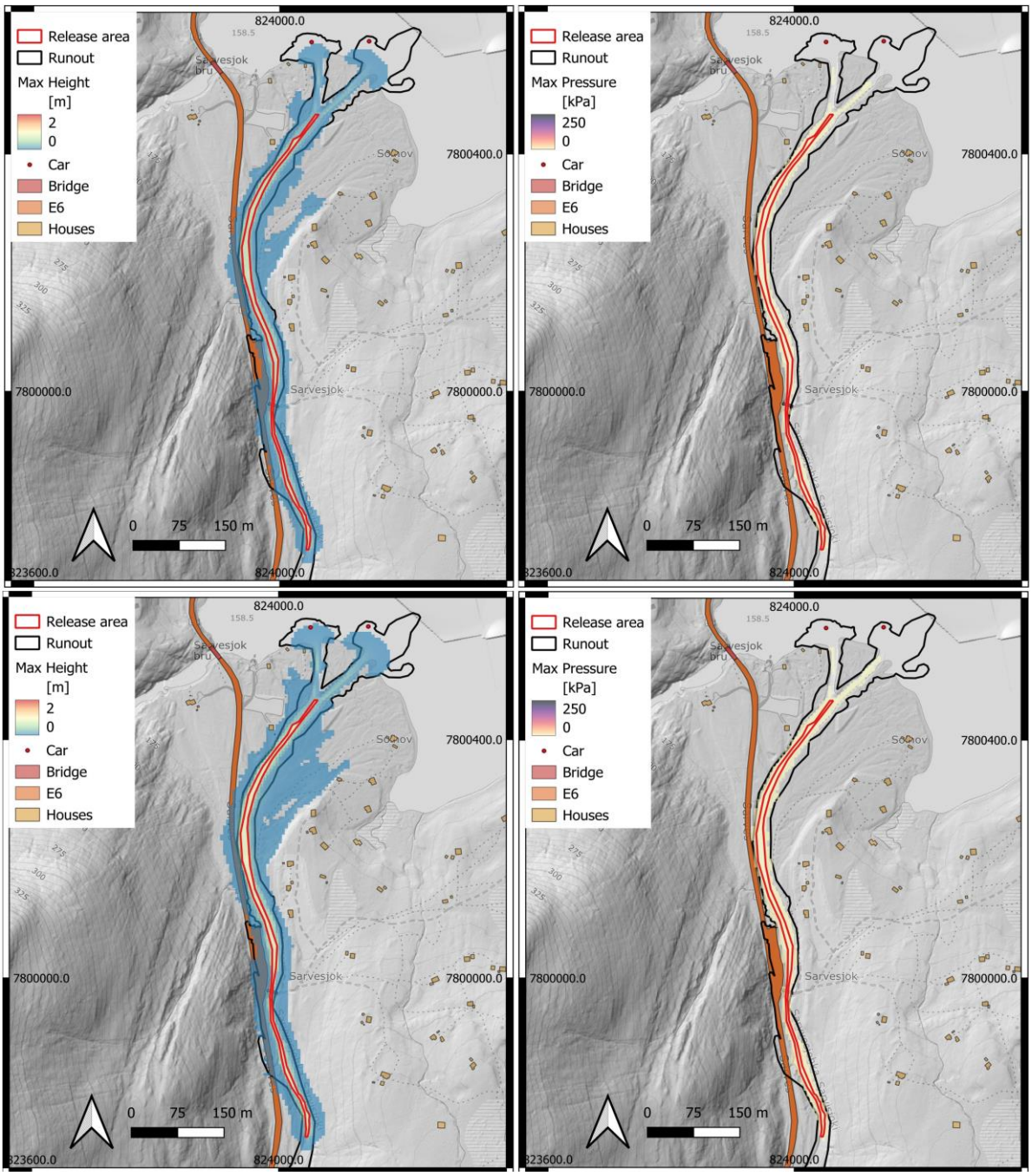

Figure 43: Simulated release area, to see how the friction parameters are affected by the slushflow dynamic. The simulations are done with the same release area and friction parameters with different release depth. The simulations on top are simulated with 0.7 m release depth, and simulations under with 1 m release depth.

6. Discussion

6.1 Limitations of RAMMS:Debrisflow to simulate slushflow runouts

To be able to predict a slushflow runout, based on simulations made with the RAMMS: Debrisflow model, the limitations and assumptions in the model needs to be understood. Graf et al. (2019) emphasized that experience in the field would be a crucial factor to generate relevant hazard scenarios. Standardized guidelines for the different input parameters would be a necessary recourse for consistent hazard assessments. Nevertheless, significant uncertainties linked to the predictability of the slushflow occurrence makes this challenging to do based of the available information today. The limitations of this method will be discussed in different subsections below, 6.1.1 Data foundation, 6.1.2 Digitising of events, 6.1.3 Defining release area, 6.1.4 Deciding release depth, 6.1.5 Digital terrain model resolution, 6.1.7 Erosion module and 6.1.7 Friction parameters.

6.1.1 Dataset foundation

The initial step of the parameter validation was to find well documented events to digitised to validate the calibrated parameter set (Kronholm, 2021). As stated in chapter “1.1 National rapid mass movement database (NSDB)” the quality of the slushflow documentation vary. The spatial extent of an event can be registered either as a point describing the position of observation or to polygons identifying the initial release, and the full runout of the events. However, the accuracy of the documentation is based on the available information about the event, and even the high quality events could have some uncertainties around the location of release area. Christen, Bartelt, et al. (2010) highlights the importance of accurate documentation for back-calculation to be able to calibrate parameterisation based on the events. Because of the large uncertainties to the quality of the dataset each event used in this work were documented and digitised in the scope of this project.

As articulated by Christen et al. (2012) there is a need of well-tested parameters to be able to use RAMMS to simulate events with a statistical confidence. To be able to do this there is a

need of a solid dataset of historical slushflow events. The parameterisation used for slushflow events is as mentioned only based on five events. In the work of validating the parametrisation by extend the dataset with four new events. The events used in the establishments of the parameterisation was replicated to validate the method. This study confirms that it is possible to follow this method with only a few minor uncertainties (Figure 15-17). The main differences in the events, were observed in areas with low velocity and shallow deposits. This main factor contributing to these differences, is likely the use of a newer version RAMMS:Debrisflow model program, as the same shapefiles, parameter set and DTMs downloaded from høydedata, were used. One clear difference observed in this work was that the original simulation used a DTM with a slightly smaller extent (Figure 15-16). This means that the full extent of the runout in their simulation, was not fully captured as it has been in this investigation. However, as these differences related to the extent of the DTM it was still possible to successfully generate similar results through following their method.

6.1.2 Digitising of events

The digitising of the event would affect the credibility of validation of the parametrisation. This makes the digitising a crucial step in the investigation of the limitations of using RAMMS:Debrisflow to simulate slushflow runouts. One of the problems concerning the digitising is that "well documented" slushflows can be digitised in a variety of ways. Since the input variables would affect the outcome of the event, correctly identify the release areas of the former event is arguably the most important part of the digitising for simulation purposes. Even with high quality documentation of events is this not always a straightforward task as will be discussed below.

Hestnes (1985) stated that the difference in release areas can vary for different types of events. Since slushflows are relatively infrequent compared to other geohazards the exact initiation and dynamic is not as well known. Which leads to large uncertainties of the initiation mechanisms observed around these events. Because of this there are some uncertainties connected to defining the release area. To be able to validate the friction parameter, through back-calculations of these events, the release area needs to be defined correctly.

The two events in Bakfjoddalen (Figure 21, 22), illustrate differences in identifying and digitising the slushflow release areas. Since the release of the event was not documented, and the mapping of the release areas is made by investigating the deposits, is there is no exact answer for what happened in the event. The different output of the simulated runout when the same snow depth is used gives differences in the result (Figure 23, 24). This leads to the problem where simulations with differences in the release areas do not give the same result, and so there is already a large uncertainty when digitising good quality events based on a well-documented field observation.

Moving forward to use this model with less uncertainties, one important step in the further work would be to standardize a way to decide the release areas for the simulation, to get a more consistent way of mapping the events and limit the uncertainties caused by the digitising. This could be done by investigating different mapping scenarios for already high-quality documented events, to see how the release areas spatial extent effects the runout.

Mapping the full extent of the event is a necessary step for the validation of the simulations. The full extent of the event provides the information about how the flow potentially moved in the terrain and presents the opportunity to further investigate the event to understand the dynamic combinations of the friction parameters. Screening of the deposits provides insight into the flow pattern and material mixture of entrained sediment. The flow shape and deposition mixture are therefore a useful observation to make during documentation of the events, as these mobility indicators will affect the parameter calibration used to simulate slushflows.

6.1.3 Defining release area

Scherer et al. (1998) highlighted the challenges around identifying slushflow release areas, which make the process of mapping the spatial extent of predicted slushflow difficult. For the simulation Kronholm (2021) made in the establishment of the friction parameter set, the release areas were estimated differently depending on each event. Since there are already uncertainties connected to digitised historical events, there should be created guidelines of deciding the spatial extent of the release area. This would increase the credibility using this

model as a tool to prediction future runout, and potentially reduce the risk connected to slushflow events.

To be able to create these guidelines the initiation mechanisms need to be understood. As Jaedicke et al. (2022) stated slushflows are complex interactions between snow, water, terrain, and the weather. All these factors would lead to a wide range of different types of slushflow. The three field sites confirm this complex variation of events. By investigating the slope gradient of the release areas, the initial release has been observed between 1.3° to 34°.

Since the slushflow initiation is connected to the loss of cohesion between the snow crystals, caused by saturated of snow that often is related to low gradient terrain. However, since the gravitational mass flows need gravity to release, they are expected to release in slopes with different angle. In most of the research about slushflows the observations of the slope angle of release are observed differently. In a study of 75 slushflow events by Nyberg (1985) found an average release of 19°. Hestnes (1996), Sund et al. (2020) and Elder and Kattelmann (1993) mentions that slushflows are expected to release angle less than 30°. However, both Jaedicke et al. (2022) and Pérez-Guillén et al. (2019) confirms observations of slushflow release above 30°. The larger event in Bakfjorddalen which released in a slope with 34° support the statement of slushflows occurring above the 30°. These starting conditions should therefore also be considered when defining potential future release areas for simulations.

Two of the events released in slopes angle of 1.3° and 3.5°. This observation is not unusual for slushflow release. As mention Elder and Kattelmann (1993) observed slushflow releasing in a slope as gentle as 6°, with a mean slope angle of 3° for the runout. This means that the occurrence of these events is common. However, to simulate these types of events using this this software could be challenging. Simulations generated based of the observation of release area in field, both in the study by Kronholm (2021) and the results of this project (Figure 33 34, 38, 42) would not give comparable simulation output with the field observations of the runout.

Although, the simulations did not reach as far as observed, they provide valuable insight of the assumptions made in the software that limits the model for simulating slushflow runouts. Even though RAMMS:Debrisflow gives the freedom to calibrate the parametrisation to

simulate slushflows to some degree, the initiation mechanisms between slush and debris would differ too much to use this model to simulate low gradient events. The challenge to this model appears to be linked to the different slope angle between debris flow and slushflow release initiation. This assumption cannot be overcome by only changing the density and friction parameters. This obstacle was solved in Kronholm (2021) study by define the slushflow release area in more sensitive parts of the slushflow path, that referred to where the path roles over into steeper terrain. In this study this was based on release area observations with slope angles gentler then 10°. For the Leirbotn event the slope gradient was relatively low the whole path, and there were no clear parts of the paths that was more sensitive to define a release area for simulations. Since these types of slushflow events are observed in other studies, is there a need to develop a way to simulate these types of events, where the slope gradient in the flow path do not exceeds 10°.

For the Nålelva event it was possible to define release areas in the more sensitive parts of the path, as Kronholm (2021) did in his study. There were observed several possible locations where the flow rolled over into steeper terrain. Since there are no existing guidelines of deciding these types of release areas, different locations were tested to see how the simulation output would differ when using the same release volume (Figure 31). There were observed significantly different runout which would result in different estimate of the vulnerability of area. The sensitivity of the location of the release area was investigated in the Bakfjorddalen event. By testing different locations release areas with same volume, with slightly different locations, the runout results change significantly. The minor differences in the location change had large impact on the flow direction, and the flow terrain interaction at the large event in Bakfjorddalen, Figure 28. The result of differences in simulations of already digitised events (Figure 23, 24, 34, 42), support the need to create guidelines of deciding release areas to be able to predict slushflow runouts with a high credibility for slushflow mitigation and spatial planning.

Since a slushflow can initiate in a gentler slope than what is expected from a debris flow initiation, there are limitations when using the model to replicate events releasing in slopes with a low slope gradient. In the case where the slushflow rolls over into steeper terrain, the release area is defined in a steeper part of the path. However, as observed in this project this is

not the case for all types of slushflow paths. The most effective way to receive a representative output of the event is to either change the location or volume of the release area. To truly test the capability of RAMMS:Debrisflow to simulate realistic runouts for spatial planning, there is the pressing need to develop a standardised method to delineate release areas.

6.1.4 Deciding release depth

By testing different release depths for the simulations, indicate a significantly impact on the simulation based of this input variable (Figure 26, 27, 42). Since there was not taken any measures of the snow depth in any of the field sites, the release depth input is in mainly based on NVE's database Xgeo, that provides interpolations of the average local snow depth on specific dates. This database would provide an estimated snow depth based on the metrological data in the area. Because this is an interpolation, this is just an estimate, and some uncertainties of the simulation result is connected to this.

At the location in Bakfjorddalen the observed snow depth for the NVE database xgeo, gave a snow depth interpolation of 43 cm in the location of the slushflow. The terrain features gave indications of a higher snow depth in the channels. The differences between the terrain model and the snow-covered terrain, indicating accumulation of snow in the channel (Figure 14). This is supported by Sund et al. (2020) observations of a snow depth of 0.5 m is needed for a slushflow to occur. This could be an indication of terrain features where slushflows typically release could have deeper snow depth then what is observed in the surrounding area. Because of the effect the release depth has on the flow interaction with the terrain this is a factor that should be heavy considered when creating possible hazard scenarios in spatial planning. A standardized method for choosing the depth based on the metrological data and terrain features available could be an important step to reduce the uncertainties using this model.

6.1.5 Digital terrain model resolution (DTM)

As mentioned, the software needs an accurate digitised representation of the terrain to simulate the terrain flow interaction. The DTM used in this project is a terrain models based on LiDAR data collection, which high gives a high resolution replication of the terrain. Majid

and MOTAMEDI (2024) investigated the results of using difference cell sizes on debris flow simulations and found significantly results of the cell size resolution. The use of to low resolution showed loss of important terrain information when simulating debris flows. Too high resolutions could also give inaccurate results of the flow process. However, for snow avalanche studies there are often used 5 m cell size to replicate the snow-covered terrain accurately. The simulations made for this thesis was used 2 m cell size, as Kronholm (2021) used in the study for the smaller events (Bakfjorddalen and Nålelva), and 5 m cell size for the Leirbotnevent, to be able to generate a result. The high simulation resolution could be a contributing effect to the short simulation runouts. Where a lower resolution DTM could potentially provide a more accurate representation of the snow-covered terrain. The comparison of the snow-covered terrain from field observations and a 3D view of the digital terrain model (Figure 14) indicates some differences between the DTM and the actual terrain surface of the event.

6.1.6 Erosion module

Jaedicke et al. (2022) states that the slushflows often grows downslope because of added masses of water and material along the way. These scenarios are often developed river valleys. The observation from the field sites supports these statements (Figure 18,19, 31, 32, 41). In the river valley along E6 in Leirbotn the flow has clearly transition from a water-snow mixture to depositing ice, by adding considerable amount of ice further down in the slushflow path (Figure 39, 41). The entrainment of ice threatens the frequently used road (Figure 38). Because of the low slope gradient of this events the simulated flow never met threshold values for erosion along the path. Since it wasn’t possible to simulate this entrainment along the path using the erosional module, the solution was to define this area as a release area in the channel. The release area was defined in the lower part of the slushflow path where most of the entrainment was observed. This method gave some results of the deposition pattern of the observations (Figure 42). However, there was not possible to recreate the pressure in the flow dynamic that displaced the two cars (Figure 39) which indicates uncertainties of the result of this model using this software and parameterisation on these types of events.

The entrainment in the Nålelva event had a different composition. In the top part of the event there was observations indicating entrainment of slush (Figure 29, 30). The deposition changes the colour in the path because of sediment entrainment. Based on the geomorphological map (Figure 5B) the transition of the flow composition is located in the area where there is mapped moraine material. The simulation including the digitised erosion zone gives no difference in the runout then simulations where these are excluded (Figure 34). These observations support the classification of rapid mass movements including slushflows developed from Hestnes et al. (2017) showing different the variation in composition of water, snow, ice and debris.

The only location where the simulations including the defined erosional zones where adding masses along the path was in Bakfjorddalen (Figure 23, 24), where the slope was steeper than in the other field sites (Figure 6). The digitised release had a significantly lower total release volume, Scenario A 50/86.3 m^2 and Scenario B 377/90 m^2 (Table 7, 8), then the Nålelva with a release area of 762 m^2 (Table 10). This indicates that the terrain profile is the limiting factor for adding masses along the path using the erosional module. Because there are clear limitations of the use of the model in low gradient events, mainly driven by water access and mass entrainments, there should in the future be created guidelines for what type of the potential slushflow terrain this model is used to predict the slushflow prone areas.

One limitation by using this method as Meyrat et al. (2022) highlighted there are challenges connected to accurately defining both initial starting zone and the area the area that potentially would be affected by mass entrainment. Because the erosional module only is active under certain conditions, the erosional zones should also be placed in the steeper part of the path. Kronholm (2021) discusses how the erosion parameters are only based of entrainment of snow, and do not account for sediment entrainment where the slushflow potentially transition into a debris flows. Future work could be to investigate different parameterisation. As Jaedicke et al. (2022) mentions the future climate would force the snow-cover to move further up in the terrain. However, since the slushflow have the potential to travel further down in the valley and transition into debris flow could be relevant to investigate more. Pérez-Guillén et al. (2019) describes the occurrence of these types of slushflow events at Mt. Fuji in Japan. On limitation that followed by defining the erosion zone as a part of the release area, would be

that the different material entrainment along the slushflow no longer can be included. A better method to include the complexity of the slushflow events needs to be investigated more.

6.1.7 Friction parameter validation

The parameterisations, including the friction parameters (Table 1), is established based on homogeneous flows (Kronholm, 2021). The observation in this study shows a diversity of flow behaviour based on composition and terrain in the three different field sites. The water assess would be one of the main driving factors for the slushflow mobility. Another variable influencing the slushflow is the composition of materials. This factor is important to considered when adapting RAMMS:Debrisflow to simulate different slushflow events. As Kronholm (2021) mentions this parameterisation do not accounting for entrainment of sediments or transferring to a debris flow. Hestnes (1996) started this work by categorizing different type of initiation mechanisms (Figure 8). The different initiation types would arguably have different mobility and material in the flow. As Jaedicke et al. (2022) describes the interaction between snow, water, terrain and weather would lead to a wide range of unique events. Hestnes et al. (2017) classified rapid mass movements including slushflows is a term covering all events with mixture at least water and snow with possible entrainment of different materials like ice, debris, or organic material (Figure 7). To find better suited friction parameters to predict the range of slushflow, there should be done more work to classify the different type of events.

Even though simulation output is affected by the other input values, the investigation of the simulations of the different combinations of the friction parameters (Table 1), gives a valuable result. All the simulation (Figure 23, 24, 34, 32), expects the yearly probability of 1/100 release scenario A in Bakfjorddalen (Figure 23), would give an increased runout extent for decreased yearly probability.

6.2 Hazard assessment for slushflow

To reduce danger slushflows poses to everything in its path, is it important to predict where slushflows may initiate and travel in the terrain. Based on the limited understanding of these mechanisms and uncertainties connected to the slushflow database, the RAMMS:Debrisflow model is a useful tool to generate simulation outputs to visualize the potential slushflow extent. This model is proven to simulate comparable results with the field observation for the slushflows located in terrain with a slope angle above 10°. If the limitation of the model is considered when it is used for hazard assessment, the output simulation could be an effective tool deciding the susceptibility areas of slushflow hazard. However, to create realistic scenarios the experience from the user, when defining the input variables, would be a determining factor of the results. Based on the result, volume and location of the release area heavily determines the simulation outputs (Figure 23, 24, 28). The main shortcoming is connected to the generalising parameterisation for RAMMS:Debrisflow to simulate the wide range of slushflow events that occur, particularly result in significant uncertainties when simulating events that occur on low slope gradients.

The combinations of low frequency of slushflow events and high variability of the initiation mechanisms makes it hard to limit the spatial extent of possible slushflow release areas. Hestnes et al. (2017) draw attention to importance of improving the slushflow database, to gain the understanding of the mechanisms causing these events. Because of the lack of documentation it is challenging to estimate the spatial footprint of the slushflow hazard. Jaedicke and Sandersen (2021) emphasised the risk of overestimate the slushflow danger, since the existing research in the field would lead to high amount of potential release areas, even though the observations of slushflow events is registered to be relatively rare. The next sections would evaluate the result with the observations from field 6.2.1 Impact pressure and 6.2.2. Indicator of slushflow release.

6.2.1 Impact pressure

From the documentation of the events, vehicles being dragged along the slushflow path gives indicators of the maximum pressure of the event. To validate the friction parameter set developed for slushflow simulations, the max pressure can be used to compare transport and

deposition of the vehicle. As Rapin (2002) describes the potential damage of an impact pressure from 100-300 kPa would be able to pull out large fir trees, and a pressure over 300 kPa would be able to move large blocks. The large's vehicle is deposited on the end of the high-pressure area with a max pressure around 250-270 kPa, and smaller vehicles have been dragged further along the path where the pressure decreases (Figure 26B). This is a good indication that the friction parameters set, and use of this model could potentially be used to estimate the damage potential of an event. Even though the impact pressure generally fits, it is some insecurities regarding the input parameters of the simulation. The difference in max pressure and the path is depending on the input volume or location (Figure 26).

6.2.2 Indicators of slushflow release

One observation that was present in all the events was the appearance of a blue-grey colour on the snow surface (Figure 18, 30 and 37). As Hestnes (1985) described this as an indication of saturated snow, which means that the bindings between the crystals are weakened. The location of the release area according to these observations, would not always be intuitive. The location of the observed water saturated snow compared with the initiation of slushflow events are different for each field site. At the Langfjordbotn event (Figure 37) the blue-grey water saturated area was linked to the initiation of the slushflow. The observations from Bakfjorddalen shows these observations do not directly connect to the location of the release areas but provides indications of high-water content of the snow in the overlying areas.

At the Nåleleva event the blue grey snow cover was observed further down in the slushflow path. The observed saturation of the peat area looked to be caused by the drainage of water from the upper release of the slushflow event (Figure 29 and 30). Onesti (1987) mentions the slushflow release is not only caused by the low shear strength in the slush, but other contributing factors like acceleration rate of free water input into the snowpack. The observations of the melt water flow on top of the slushflow surface (Figure 29) could be the releasing mechanism behind the initial release area observed at Nålelva. When the slush started propagating downslope, the water flow from the slush deposited drained into the peat that could have led to a new release of the event from where the terrain transitions from horizontal to a gentler slope angle (Figure 30).

7. Conclusion

The three field sites, represented by four slushflow events occurring over winter/spring 2023, show that the calibrated slushflow parameterisations using RAMMS:Debrisflow fit the digitised runout to some extent. However, there are arguable differences that are observed in the slushflow initiation, mass entrainment and water content. The model will generate relatively well represented simulation outputs for slushflows that either initiate in steeper slopes or ones that roll into steeper terrain in the slushflow path. Due to the assumptions in this model, it is only possible to generate realistic results for the slushflows paths with terrain profiles over 10°. As observed in this project this is not always the case for all types of slushflow paths. The observation of the occurrence of this event is highly related to the water access and material entrainment. If the water access is high, the mobility of the slushflow appears to be high, which leads to longer runouts in low gradient terrain. Generalising RAMMS:Debrisflow to simulate the wide range of slushflow events that occur, leads to large uncertainties particularly when simulating events that occur on low slope gradients. To be able to cover these types of events there is a need to classify these events to develop a method to include these in hazard assessments.

One shortcoming of using the RAMMS: Debrisflow model is that the runout is sensitive to the input data. Through analysing different simulation scenarios, it is clear that the spatial extent of the release area has a significant impact on every aspect of the simulation results. The investigation into the responsiveness of changing the release area's location, indicates that the flow pattern in the terrain varies between different locations. The pattern of the flow is also affected by the chosen release depth in the snowpack. The most effective way to receive a representative output of the event is to either change the location or volume of the release area. This project highlights that the variable of the release area is too sensitive to validate the established friction parameter set developed for slushflow modelling using this software. To truly test the capability of RAMMS:Debrisflow to simulate realistic runouts for spatial planning, there is the pressing need to develop a standardised method to delineate release areas.

8. References

Anma, S. (1988). Deforestation by Slush Avalanches and Vegetation Recovery on the Eastern Slope of Mt. Fuji. *International Symposion INTERPRAEVENT-GRAZ*, 133-156.

Armanini, A., & Michiue, M. (1997). *Recent developments on debris flows* (Vol. 64). Springer.

Bartelt, P., Bühler, Y., Buser, O., Christen, M., & Meier, L. (2012). Modeling mass‐dependent flow regime transitions to predict the stopping and depositional behavior of snow avalanches. *Journal of Geophysical Research: Earth Surface*, *117*(F1).

Bühler, Y., Christen, M., Kowalski, J., & Bartelt, P. (2011). Sensitivity of snow avalanche simulations to digital elevation model quality and resolution. *Annals of glaciology*, *52*(58), 72-80.

Christen, M., Bartelt, P., & Kowalski, J. (2010). Back calculation of the In den Arelen avalanche with RAMMS: interpretation of model results. *Annals of Glaciology*, *51*(54), 161-168.

Christen, M., Bühler, Y., Bartelt, P., Leine, R., Glover, J., Schweizer, A., Graf, C., McArdell, B. W., Gerber, W., & Deubelbeiss, Y. (2012). Integral hazard management using a unified software environment. 12th Congress Interpraevent,

Christen, M., Kowalski, J., & Bartelt, P. (2010). RAMMS: Numerical simulation of dense snow avalanches in three-dimensional terrain. *Cold Regions Science and Technology*, *63*(1-2), 1-14.

Devoli, G., Jarsve, K., Mongstad, H., Sandboe, K., & Jensen, O. (2020). *Kontroll av registrerte skredhendelser og tildeling av kvalitetsnivå for utglidning, jordskred, flomskred og sørpeskred* (NVE rapport, Issue.

Elder, K., & Kattelmann, R. (1993). A low‐angle slushflow in the Kirgiz Range, Kirgizstan. *Permafrost and Periglacial Processes*, *4*(4), 301-310.

Fierz, C., Armstrong, R. L., Durand, Y., Etchevers, P., Greene, E., McClung, D. M., Nishimura, K., Satyawali, P. K., & Sokratov, S. A. (2009). The international classification for seasonal snow on the ground.

Graf, C., Christen, M., McArdell, B. W., & Bartelt, P. (2019). Overview of a decade of applied debris-flow runout modeling in Switzerland, An: challenges and recommendations. *Association of Environmental and Engineering Geologists; special publication 28*.

Gude, M., & Scherer, D. (1998). Snowmelt and slushflows: hydrological and hazard implications. *Annals of glaciology*, *26*, 381-384.

Hanssen-Bauer, I., Drange, H., Førland, E., Roald, L., Børsheim, K., Hisdal, H., Lawrence, D., Nesje, A., Sandven, S., & Sorteberg, A. (2009). Climate in Norway 2100. *Background information to NOU Climate adaptation (In Norwegian: Klima i Norge 2100. Bakgrunnsmateriale til NOU Klimatilplassing), Oslo: Norsk klimasenter*.

Hestnes, E. (1985). A contribution to the prediction of slush avalanches. *Annals of glaciology*, *6*, 1-4.

Hestnes, E. (1996). Slushflow hazard—where, why and when? 25 years of experience with slushflow consulting and research. , *26*, 370-376.

Hestnes, E., & Bakkehoi, S. (1995). Prediction of slushflow hazard. Objectives and procedures of an ongoing research project in Rana, North Norway. Les apports de la recherche scientifique à la sécurité neige glace et avalanche,

Hestnes, E., Bakkehøi, S., & Jaedicke, C. (2017). GLOBAL WARMING REDUCES THE CONSEQUENCES OF SLUSHFLOWS. Физика, химия и механика снега,

Hestnes, E., Bakkehøi, S., & Kristensen, K. (2012). Slushflows-A challenging problem to authorities and experts. *Data of Glaciological Studies, Moscow. Publication*(1), 74-87.

Hestnes, E., Bakkehøi, S., Sandersen, F., & Andresen, L. (1994). *Weather and snowpack conditions essential to slushflow release and downslope propagation*. Norges Geotekniske Institutt.

Hestnes, E., & Jaedicke, C. (2018). Global warning reduces the consequences of snow-related hazards.

Hestnes, E., & Lied, K. (1980). Natural-hazard maps for land-use planning in Norway. *Journal of Glaciology*, *26*(94), 331-343.

Hestnes, E., & Sandersen, F. (1987). Slushflow activity in the Rana district, North Norway. Proceedings of the Davos Symposium, IAHS Publication,

Hungr, O., Leroueil, S., & Picarelli, L. (2014). The Varnes classification of landslide types, an update. *Landslides*, *11*, 167-194.

Imaizumi, F., Sidle, R. C., Tsuchiya, S., & Ohsaka, O. (2006). Hydrogeomorphic processes in a steep debris flow initiation zone. *Geophysical Research Letters*, *33*(10).

Jaedicke, C., Kalsnes, B., & Solheim, A. (2022). Sørpeskred. Egenskaper, historikk og sikringsløsninger.

Jaedicke, C., Kern, M., Gauer, P., Baillifard, M.-A., & Platzer, K. (2008). Chute experiments on slushflow dynamics. *Cold Regions Science and Technology*, *51*(2-3), 156-167.

Jaedicke, C., & Sandersen, F. (2021). FOU 80606-Identifisering av løsneområder for sørpeskred.

Jonsson, A., & Gauer, P. (2014). Optimizing mitigation measures against slush flows by means of numerical modelling–a case study Longyearbyen, Svalbard. *Proceedings of INTERPRAEVENT-2014 in the Pacific Rim–Natural Disaster Mitigation to Establish Society with the Resilience*, 25-28.

Kobayashi, S., Izumi, K., & Kamiishi, I. (1994). Slushflow disasters in Japan and its characteristics. International Snow Science Workshop,

Kronholm, K. (2021). *Bruk av RAMMS:: DEBRISFLOW på kjente sørpeskredhendelser* (8241021313).

Majid, G., & MOTAMEDI, A. (2024). Evaluation of Errors and Uncertainties in Debris Flow Modeling with RAMMS.

Meyrat, G., McArdell, B., Ivanova, K., Müller, C., & Bartelt, P. (2022). A dilatant, two-layer debris flow model validated by flow density measurements at the Swiss illgraben test site. *Landslides*, *19*(2), 265-276.

Nobles, L. H. (1966). *Slush avalanches in northern Greenland and the classification of rapid mass movements*. na.

Nyberg, R. (1985). *Debris flows and slush avalanches in northern Swedish Lappland: distribution and geomorphological significance*

Onesti, L. (1987). Slushflow release mechanism: A first approximation. *IAHS Publ*, *162*, 331-336.

Onesti, L. J., & Hestnes, E. (1989). Slush-flow questionnaire. *Annals of glaciology*, *13*, 226-230.

Pérez-Guillén, C., Tsunematsu, K., Nishimura, K., & Issler, D. (2019). Seismic location and tracking of snow avalanches and slush flows on Mt. Fuji, Japan. *Earth Surface Dynamics*, *7*(4), 989-1007.

Rapp, A. (1960). Recent development of mountain slopes in Kärkevagge and surroundings, northern Scandinavia. *Geografiska Annaler*, *42*(2-3), 65-200.

Relf, G., Kendra, J. M., Schwartz, R. M., Leathers, D. J., & Levia, D. F. (2015). Slushflows: science and planning considerations for an expanding hazard. *Natural Hazards*, *78*, 333-354.

Salm, B. (1993). Flow, flow transition and runout distances of flowing avalanches. *Annals of glaciology*, *18*, 221-226.

Sampl, P., & Zwinger, T. (2004). Avalanche simulation with SAMOS. *Annals of Glaciology*, *38*, 393-398.

Scherer, D., Gude, M., Gempeler, M., & Parlow, E. (1998). Atmospheric and hydrological boundary conditions for slushflow initiation due to snowmelt. *Annals of Glaciology*, *26*, 377-380.

Shieh, C.-L., Jan, C.-D., & Tsai, Y.-F. (1996). A numerical simulation of debris flow and its application. *Natural Hazards*, *13*, 39-54.

Simoni, A., Mammoliti, M., & Graf, C. (2012). Performance Of 2D debris flow simulation model RAMMS. annual international conference on geological and earth sciences GEOS,

Stimberis, J., & Rubin, C. M. (2011). Glide avalanche response to an extreme rain-on-snow event, Snoqualmie Pass, Washington, USA. *Journal of Glaciology*, *57*(203), 468-474.

Sund, M., Grønsten, H. A., & Seljesæter, S. Å. (2023). Operational regional slushflow early warning. *Natural Hazards and Earth System Sciences Discussions*, *2023*, 1-31.

Sund, M., Grønsten, H. A., & Skuset, S. (2020). Varsling av regional sørpeskredfare. *NVE Rapport*.

Vegvesen, S. (2014). Flom og Sørpeskred. *Håndbok v139, Statens vegvesen håndbokserie*.

Washburn, A., & Goldthwait, R. (1958). Slushflows. *Geological Society of America Bulletin*, *69*, 1657-1658.

Zhang, Y. (2019). Numerical simulation of debris flow runout using Ramms: a case study of Luzhuang Gully in China. *Computer Modeling in Engineering & Sciences*, *121*(3), 981-1009.

9. Appendix

Event	Simulation ID	Release area	Release area		Density [kg/m^3]	Block release		Release volume [m^3]	Friction		Erosion	Erosion zone	Erosion depth	**Figure**
			Mean slope release area	Mean altitude [m]		Incline area [m^2]	Release depth [m]		My	Ksi [m/s^2]				
Nålelva	N1	"Nålelva_nedre"	22,79	217,55	1000	1820,6	2	3641,11	0,08	2000	no			
	N2	"Nålelva_nedre"	22,79	217,55	1000	1850,6	1	1820,56	0,08	2000	no			
	N3	"Nålelva_midt"	13,77	292,96	1000	1020,7	1	1020,66	0,08	2000	no			
	N4	"Nålelva_midt"	13,77	292,96	1000	1020,7	2	2042,32	0,05	3000	no			
	N5	"Nålelva_midt_stor"	8,52	294,78	1000	2874,2	1	2874,19	0,05	3000	no			

	N6	"Nålelva_midt_stor2"	9,16	293,32	1000	3312,9	0,868	2875,57	0,08	2000	no			
	N7	"Nålelva_midt_lang"	11,81	289,03	1000	2320,4	1,24	2877,27	0,08	2000	no			
	N9	"Nålelva_low"	21,19	169,6	1000	5597,8	1	5597,82	0,08	2000	no			
	N10	"Nålelva_low2.0"	20,67	214,73	1000	3075,3	1	3075,27	0,08	3000	yes	"Nålelva_low"	1	
	N11	"Nålelva_low2.0"	20,67	214,73	1000	3075,3	1	3075,27	0,08	2000	no			
	N12	"Nålelva_low_steep_short"	23,86	220,9	1000		1,5	3064	0,08	2000	no			
	N13	"Nålelva_low__short"	14,83	203,53	1000	1033,1	3	3099,28	0,08	2000	no			
	N14	"Nålelva_low_long"	19,94	213,59	1000	3412	1	3412	0,08	2000	no			35
	N15	"Nålelva_low_long"	19,94	213,59	1000	342	1	3412	0,08	3000	yes	"Nålelva_erosion_low"	1	

	N16	"Nålelva_low_lower"	14,72	203,66	1000	1389,8	2,5	3474,4	0,08	2000	no			
	N17	"Nålelva_mid"	29,65	258,57	1000	585,6	6	3513,8	0,08	2000	no			
	N18	"Nålelva_mid_large"	19,75	266,45	1000	1311,2	2,7	3540,24	0,08	2000	no			
	N19	"Nålelva_mid_larger"	18,12	268,56	1000	1636,7	2,1	3437,15	0,08	2000	no			
	N20	"Nålelva_upper"	11,33	291,41	1000	1874	1,8	3373,23	0,08	2000	no			
	N21	"Nålelva_upper"	11,33	291,41	1000	1874	1,8	3373,23	0,08	3000	yes		1	35
	N22	"Nålelva_upper"	11,33	291,41	1000	1874	1,8	3373,23	0,05	3000	no			35
	N23	"Nålelva_top"	14	309,34	1000	1614,7	2,1	3390	0,08	2000	no			
	N24	"Nålelva_top"	14	309,34	1000	1614,7	2,1	3390	0,05	3000	no			
	N25	"Nålelva_top_large"	7,18	310,63	1000	4292,5	0,8	3434	0,08	2000	no			

	N26	"Nålelva_top_large"	7,18	310,63	1000	4292,55	1	4292,55	0,05	3000	no			
	N27	"Nålelva_event"	6,82	309,57	1000	1387,7	1	1387,68	0,08	2000	no			
	N28	"Nålelva_low_realistic"	12,23	286,43	1000	3037,66	1	3037,66	0,08	2000	no			
	N29	"Nålelva_event"	6,82	309,57	1000	1387,7	1	1387,68	0,05	3000	no			
	N30	"Nålelva_low_realistic"	12,23	286,43	1000	3037,7	1	3037,66	0,05	4000	no			
	N32	"Nålelva_low_realistic"	12,23	286,43	1000	3038,7	1	3037,7	0,08	3000	yes	"Nålelva_erosion_zone"	1	36
	N33	"Nålelva_low_realistic"	12,23	286,43	1000	3038,7	1	3037,7	0,08	3000	yes	"Nålelva_erosion_zone"	1	
	N34	"Nålelva_low_realistic"	12,23	286,43	1000	3038,7	1	3037,7	0,05	4000	yes	"Nålelva_erosion_zone"	1	

	N35	"Release_event_nålelva"	6,82	309,57	1000	1387,7	1	1387,68	0,05	4000	yes	"erosion_Nålelva_top"	1	
	N36	"Release_event_nålelva"	6,82	309,57	1000	1387,7	1	1387,68	0,08	3000	yes	"erosion_Nålelva_top"	1	
	N37	"Release_area_Nålelva_hele"	7,76	294,42	1000	6678,4	1	6678,39	0,08	2000	no			
	N38	"Release_area_Nålelva_hele"	7,76	294,42	1000	6678,4	1	6678,39	0,08	3000	yes	"Nålelva_erosion_zone"	1	
	N39	"Release_area_Nålelva_hele"	7,76	294,42	1000	6678,4	1	6678,39	0,05	3000	no			
	N40	"Release_area_Nålelva_hele"	7,76	294,42	1000	6678,4	1	6678,39	0,05	4000	yes	"Nålelva_erosion_zone"	1	
	N41	"Release_area_Nålelva_hele"	7,76	294,42	1000	6678,4	1	6678,39	0,04	4000	no			

	N42	"Release_area_Nålelva_hele"	7,76	294,42	1000	6678,4	1	6678,39	0,04	5000	yes	"Nålelva_erosion_zone"	1	
	N43	"Release_area_Nålelva_hele"	7,76	294,42	1000	6678,4			0,05					
	N44	"Release_area_Nålelva_hele"	7,76	294,42	1000	6678,4			0,05					
	Na1	"release_area_NålelvaA"	3,46	311,23	1000	761,9	1	761,9	0,08	2000	no			34
	Na2	"release_area_NålelvaA"	3,46	311,23	1000	761,9	1	761,9	0,08	3000	yes	"erosionA_Nålelva"	0,7	34
	Na3	"release_area_NålelvaA"	3,46	311,23	1000	761,9	1	761,9	0,05	3000	no			33/34
	Na4	"release_area_NålelvaA"	3,46	311,23	1000	761,9	1	761,9	0,05	4000	yes	"erosionA_Nålelva"	0,7	33/34
	Na5	"release_area_NålelvaA"	3,46	311,23	1000	761,9	1	761,9	0,04	4000	no			34

	Na6	"release_area_NålelvaA"	3,46	311,23	1000	761,9	1	761,9	0,04	5000	yes	"erosion A_Nålelva"	0,7	34
	Na8	"Nålelva_long_low"	19,94	213,59	1000	3412	1	3412	0,05	3000	no			35
	Na10	"erosion_Nålelva_halve" "low_realistic_nålelva"	17,86 12,23	210	1000	9621,2 3037,7	0,5	6329,42	0,08	2000	no			36
Bakfjord dalen	B1	"Bakfjorddalen_large"	33,96	177,19	1000	103,9	0,5	49,9	0,08	2000	no			23
	B2	"Bakfjorddalen_large"	33,96	177,19	1000	103,9	0,5	49,9	0,08	3000	yes	"Bakfjorddalen_erosion" "Bakfjorddalen_erosion2"	0,5	23/26
	B3	"Bakfjorddalen_large"	33,96	177,19	1000	103,9	0,5	49,9	0,05	3000	no			23
	B4	"Bakfjorddalen_large"	33,96	177,19	1000	103,9	0,5	49,9	0,05	4000	yes	"Bakfjorddalen_erosion"	0,5	23

												"Bakfjorddalen_erosion2"		
	B5	"Bakfjorddalen_large"	33,96	177,19	1000	103,9	0,5	49,9	0,04	4000	no			23
	B6	"Bakfjorddalen_large"	33,96	177,19	1000	103,9	0,5	49,9	0,04	5000	yes	"Bakfjorddalen_erosion" "Bakfjorddalen_erosion2"	0,5	23
	B7	"Release_erosion_bakfjorddalen_large"	31,84	164,51	1000	753,6	0,5	376,8	0,08	2000	no			24/26
	B8	"Release_erosion_bakfjorddalen_large"	31,84	164,51	1000	753,6	0,5	376,8	0,08	3000	yes	"Bakfjorddalen_erosion2"	0,5	24
	B9	"Release_erosion_bakfjorddalen_large"	31,84	164,51	1000	753,6	0,5	376,8	0,05	3000	no			24

	B10	"Release_erosion_bakfjorddalen_large"	31,84	164,51	1000	753,6	0,5	376,8	0,05	4000	yes	"Bakfjorddalen_erosion2"	0,5	24
	B11	"Release_erosion_bakfjorddalen_large"	31,84	164,51	1000	753,6	0,5	376,8	0,04	4000	no			24
	B12	"Release_erosion_bakfjorddalen_large"	31,84	164,51	1000	753,6	0,5	376,8	0,04	5000	yes	"Bakfjorddalen_erosion2"	0,5	24
	B13	"Bakfjorddalen_large"	33,96	177,19	1000	103,9	3,5	363,61	0,08	2000	no			
	B14	"Bakfjorddalen_large"	33,96	177,19	1000	103,9	1,5	155,83	0,08	2000	no			
	B15	"Bakfjorddalen_large"	33,96	177,19	1000	103,9	1	103,89	0,08	2000	no			28
	B16	"Bakfjorddalen_large"	33,96	177,19	1000	103,9	0,75	77,92	0,08	2000	no			
	B17	"test1_bakfjorddalen"	23,22	182,19	1000	137,6	0,4	55,05	0,08	2000	no			

	B18	"test1_bakfjorddalen"	23,22	182,19	1000	137,6	2,7	371,62	0,08	2000	no			
	B19	"test2_bakfjorddalen"	23,1	172,48	1000	439,2	0,85	37,35	0,08	2000	no			
	B20	"test3_bakfjorddalen"	25,92	168,3	1000	286,3	1,3	372,23	0,08	2000	no			
	B21	"Bakfjordalen_small1"	20,12	179,84	1000	86,3	0,5	43,16	0,08	2000	no			23
	B22	"Bakfjordalen_small1"	20,12	179,84	1000	86,3	0,5	43,16	0,08	3000	no			23/26
	B23	"Bakfjordalen_small1"	20,12	179,84	1000	86,3	0,5	43,16	0,05	3000	yes		0,5	23
	B24	"Bakfjordalen_small1"	20,12	179,84	1000	86,3	0,5	43,16	0,05	4000	no			23
	B25	"Bakfjordalen_small1"	20,12	179,84	1000	86,3	0,5	43,16	0,04	4000	yes		0,5	23
	B26	"Bakfjordalen_small1"	20,12	179,84	1000	86,3	0,5	43,16	0,04	5000	no			23
	B27	"Bakfjorddalen_erosion_small"	20,99	176,06	1000	180,3	0,5	90,13	0,08	2000	no			24/26

	B28	"Bakfjorddalen_erosion_small"	20,99	176,06	1000	180,3	0,5	90,13	0,05	3000	no			24
	B29	"Bakfjorddalen_erosion_small"	20,99	176,06	1000	180,3	0,5	90,13	0,04	4000	no			24
	B30	"Bakfjorddalen_small1"	20,12	179,84	1000	86,3	1	86,3	0,08	2000	no			
	B31	"test_bakfjorddalen_small"	20,87	174,15	1000	167,3	0,55	83,67	0,08	2000	no			
	B32	"Bakfjorddalen_large"	33,96	177,19	1000	103,9	3,5	363,61	0,08	3000	yes	"Bakfjorddalen_erosion" "Bakfjorddalen_erosion2"	1	
	B33	"Bakfjorddalen_large"	33,96	177,19	1000	103,9	1	103,9	0,08	3000	yes	"Bakfjorddalen_erosion" "Bakfjorddalen_erosion2"	1	

	B34	"Bakfjordalen_small1"	20,12	179,84	1000	86,3	1	86,3	0,08	3000	yes	"Bakfjorddalen_small"	1	
	B35	"Bakfjorddalen_large"	33,96	177,19	1000	103,9	1	103,9	0,08	3000	yes	"Bakfjorddalen_erosion" "Bakfjorddalen_erosion2"	1	
	B36	"Release_erosion_bakfjorddalen_large"	31,84	164,5	1000	753,6	0,14	105,5	0,08	2000				
Leirbotn vannet	L1	"Leirbotn_top"	1,3	312,26	1000	1468,2	0,7	40,34	0,08	2000	no			42
	L2	"Leirbotn_top"	1,3	312,26	1000	1468,2	0,7	40,34	0,05	3000	no			42
	L3	"Leirbotn_top"	1,3	312,26	1000	1468,2	0,7	40,34	0,04	4000	no			42
	L4	"release_leirbotn_end"	3,93	161,21	1000	4001,3	0,7	2800,91	0,08	2000	no			

	L5	"release_leirbotn_end"	3,93	161,21	1000	4001,3	0,7	2800,91	0,08	2000	no			
	L6	"Leirbotnvannet_release_bottom"	2,01	160,5	1000	1777,9	0,7	1244,52	0,08	2000	no			
	L7	"Release_area_leirbotn_lower"	1,85	167,28	1000	4455,4	0,7	3118,78	0,08	2000	no			
	L8	"Release_area_E6Leirbotn"	1,9	167,4	1000	5120,8	0,7	3584,6	0,08	2000	no			
	L9	"Release_area_E6Leirbotn"	1,9	167,4	1000	5120,8	0,7	3584,6	0,05	3000	no			43
	L10	"Release_area_E6Leirbotn"	1,9	167,4	1000	5120,8	0,7	3584,6	0,04	4000	no			43